

Review

# A Review of Nanocomposite-Modified Electrochemical Sensors for Water Quality Monitoring

Olfa Kanoun <sup>1,\*</sup> , Tamara Lazarević-Pašti <sup>2</sup> , Igor Pašti <sup>3</sup> , Salem Nasraoui <sup>1,4,5</sup> , Malak Talbi <sup>1,4,5</sup>, Amina Brahem <sup>1,4,5</sup>, Anurag Adiraju <sup>1</sup>, Evgeniya Sheremet <sup>6</sup> , Raul D. Rodriguez <sup>7</sup> , Mounir Ben Ali <sup>4,5</sup> and Ammar Al-Hamry <sup>1</sup> 

- <sup>1</sup> Professorship Measurement and Sensor Technology, Chemnitz University of Technology, 09111 Chemnitz, Germany; salem.nasraoui@etit.tu-chemnitz.de (S.N.); malak.talbi@etit.tu-chemnitz.de (M.T.); amina.brahem@etit.tu-chemnitz.de (A.B.); Adiraju.Anurag@etit.tu-chemnitz.de (A.A.); ammar.al-hamry@etit.tu-chemnitz.de (A.A.-H.)
  - <sup>2</sup> Department of Physical Chemistry, “VINČA” Institute of Nuclear Sciences—National Institute of the Republic of Serbia, University of Belgrade, 11000 Belgrade, Serbia; tamara@vinca.rs
  - <sup>3</sup> Faculty of Physical Chemistry, University of Belgrade, 11000 Belgrade, Serbia; igor@ffh.bg.ac.rs
  - <sup>4</sup> NANOMISENE Lab, LR16CRMN01, Centre for Research on Microelectronics and Nanotechnology of Sousse, Technopole of Sousse B.P. 334, Sahloul, Sousse 4034, Tunisia; mounir.benali@issatso.rnu.tn
  - <sup>5</sup> Higher Institute of Applied Sciences and Technology of Sousse, University of Sousse, 4003 Tunisia of Sousse, GREENS-ISSAT, Cité Ettafala, Ibn Khaldoun, Sousse 4003, Tunisia; mounir.benali@issatso.rnu.tn
  - <sup>6</sup> Research School of Physics, Tomsk Polytechnic University, Tomsk 634050, Russia; esheremet@tpu.ru
  - <sup>7</sup> Research School of Chemical and Biomedical Technologies, Tomsk Polytechnic University, Tomsk 634050, Russia; rodriguez@tpu.ru
- \* Correspondence: olfa.kanoun@etit.tu-chemnitz.de



**Citation:** Kanoun, O.; Lazarević-Pašti, T.; Pašti, I.; Nasraoui, S.; Talbi, M.; Brahem, A.; Adiraju, A.; Sheremet, E.; Rodriguez, R.D.; Ben Ali, M.; et al. A Review of Nanocomposite-Modified Electrochemical Sensors for Water Quality Monitoring. *Sensors* **2021**, *21*, 4131. <https://doi.org/10.3390/s21124131>

Academic Editors: Najla Fourati and Mohamed M. Chehimi

Received: 6 April 2021  
Accepted: 2 June 2021  
Published: 16 June 2021

**Publisher’s Note:** MDPI stays neutral with regard to jurisdictional claims in published maps and institutional affiliations.



**Copyright:** © 2021 by the authors. Licensee MDPI, Basel, Switzerland. This article is an open access article distributed under the terms and conditions of the Creative Commons Attribution (CC BY) license (<https://creativecommons.org/licenses/by/4.0/>).

**Abstract:** Electrochemical sensors play a significant role in detecting chemical ions, molecules, and pathogens in water and other applications. These sensors are sensitive, portable, fast, inexpensive, and suitable for online and in-situ measurements compared to other methods. They can provide the detection for any compound that can undergo certain transformations within a potential window. It enables applications in multiple ion detection, mainly since these sensors are primarily non-specific. In this paper, we provide a survey of electrochemical sensors for the detection of water contaminants, i.e., pesticides, nitrate, nitrite, phosphorus, water hardeners, disinfectant, and other emergent contaminants (phenol, estrogen, gallic acid etc.). We focus on the influence of surface modification of the working electrodes by carbon nanomaterials, metallic nanostructures, imprinted polymers and evaluate the corresponding sensing performance. Especially for pesticides, which are challenging and need special care, we highlight biosensors, such as enzymatic sensors, immunobiosensor, aptasensors, and biomimetic sensors. We discuss the sensors’ overall performance, especially concerning real-sample performance and the capability for actual field application.

**Keywords:** electrochemical sensor; water contaminants; pesticides; inorganic compounds; emergent contaminants; in-situ applications; impedance spectroscopy; square wave voltammetry

## 1. Introduction

The modern chemical industry is essential for providing sufficient goods and nourishment to the world’s population, but their excess may involve danger to humans, animals, and oceans, as highlighted by the European Environment Agency. More action is needed to tackle the mixtures of chemicals found in Europe’s waters [1]. According to [2], 38% of monitored lakes and 74% of the groundwater area achieved good chemical statistics, with pollutant concentrations not exceeding EU standards. Although 89 % of the sites has good qualitative status, 11% of waters are polluted, mainly due to contamination by nitrates from agricultural run-off, salt intrusion, and other hazardous chemicals from sources such as industrial sites, mining, or waste storage.

Rapid population growth, the uncontrolled application of chemical fertilizers, the heavy use of pesticides in agriculture and industry and domestic waste have resulted in an elevated level of pollutants in the environment. The continuously increasing rate of pollution affects the quality of drinking water, depleting aquatic systems and affecting the ecological cycle. The excessive use of fertilizers/pesticides in agriculture to balance the demand and use and discharge of plastics to water resources, hospitals industries effluents lead to water contamination and water-borne diseases. In this context, water quality monitoring is essential for detecting pollution and releasing toxic substances [3]. Hence, in 2020, the previous European Drinking Water Directive will be refreshed to incorporate new drinking-water safety criteria [4].

Electroanalytical chemistry has the potential to contribute significantly to the protection of the environment [5]. Recently, there has been an increasing interest in using electrochemical processes for water treatments [6]. Electrochemical sensors and detectors are suitable for on-site surveillance of critical contaminants. Electrochemical sensors are used in water quality monitoring of conductivity, dissolved oxygen, or pH. Their use has extended over the years to a broader range of environmental applications, notably detecting trace metals, carcinogens such as nitrogen and phosphorus compounds, and organic pollutants like phenols and pesticides [7].

An electrochemical sensor aims to deliver accurate and real-time information about a specific chemical composition in a particular environment and should be capable of responding continuously and reversibly without perturbing the sample. These devices consist of two key elements: a transducer covered with a chemical or biological recognition layer. For electrochemical sensors, the interaction between the target analyte and the sensitive recognition layer gives the analytical information. In the last years, new modified electrodes have been developed based on nanocomposites and highly selective biological or chemical detection layers. Several electrochemical sensors can be designed for environmental monitoring purposes depending on the chemical nature of the analyte to detect, the sample matrix and the requirement of sensitivity and selectivity. Lastly, the challenges of achieving repeatable and cost-effective methodologies and simple-to-use equipment for everyday analysis are pertinent. Such a wide range of possible applications proves the significance of electrochemical sensors in the evolution of environmental contamination detection.

Several reviews report on electrochemical sensing for water quality analysis [8,9]. Some of them focus on one type or a group of contaminants, such as the advances in nitrate monitoring in the environment and food products [10], the detection of phosphate -based on cobalt by potentiometric method and the progress of the development of electrochemical sensors for heavy metal ions [11–13]. Other reviews have combined several types of analytes, such as biomolecules (glucose, uric acid, dopamine, and ascorbic acid), pollutants (nitrobenzene, hydrazine, pesticides and nitrophenols), and heavy metal ions [13]. Also, some reviews focused on the materials used for sensing, such as carbon nanotubes [14], graphene [15], and polymers [16].

In this contribution, we provide an overview of the electrochemical detection of contaminants from the application of specific nanomaterials and technological points of view. This review focuses on electrochemical sensors used in field measurements or that have the potential for practical in-field water monitoring, including electrodes such as glassy carbon fabricated by microtechnology and printing technology. The review covers recent advances of stable, reproducible, and cost-effective electrochemical sensors towards water contaminant detection in the environmental and drinking water quality samples, focusing on in-situ, online and on-site measurements. The primary ecological contaminants are classified into various groups such as biological and chemical. These categories included a variety of subcategories that have a significant impact on the quality of the environment. In this review, the investigated targets are mainly pesticides, water hardness, disinfectants, nitrogen, phosphorus, and other emerging contaminants.

## 2. Water Contaminants

Pesticides, nitrate, nitrite, phosphorus, water disinfectant, phenolic compounds are the most notorious pollutants found in water. The quantity of these chemicals in surface water must be below the environmental quality standards defined by these directives to be considered in good chemical condition. The European Environment Agency European waters [17] measures to restrict the release of some of these compounds, such as  $\text{NO}_2^-$ ,  $\text{NO}_3^-$ , gallic acid, 4-AP, Pb, and Ni, have been in place for many decades, but challenges remain in preventing the release of these contaminants in the environment and avoiding pollution from atmospheric compounds that are proven to be abundant, permanent, bioaccumulative, and poisonous continues to be a problem [17].

The European Commission has also released a watchlist of possible contaminants tracked in surface waters. An updated surface water watch list was adopted by the Commission [18]. Several drugs, hormones, and pesticides are currently on the list. The Drinking Water Directive strictly controls the amounts of pesticides in European drinking water. It contains the permitted quantities of pesticides, with a single pesticide limit of 0.1  $\mu\text{g/L}$  and an actual number of pesticides quantified during the detection process of 0.5  $\mu\text{g/L}$ . In addition to old mines and polluted industrial/waste sites resulting in contamination by As, Pb, Cu, and phenolic compounds, diffuse sources of emissions from agriculture (nitrates and pesticides) threaten groundwater. Table 1 summarizes some water contaminants and the corresponding guideline limit values.

**Table 1.** Maximum allowable concentration for water quality assessment for EU [19], WHO [20] and USA-EPA [21].

Analyte	EU (mg/L)	WHO (mg/L)	USA-EPA [mg/L]
Nitrate	50	50	10
Nitrite	0.50	3	1
Phosphate	-	5	-
Ammonium	0.2	1.5 at Alkaline pH	-
Chlorate	0.250	0.7	-
1,2-dichloroethane	0.003	0.03	0.04
Epichlorohydrin	0.00010	0.0004	0.3
Trihalomethanes (total)	0.1	0.1	0.08
Haloacetic acids (HAA5)	0.06	-	0.06
Halogenated acetonitriles	-	0.02	-
Trichloroacetaldehyde	-	0.1	-
2,4,6-Trichlorophenols	-	0.2	0.3
Bisphenol A	0.0025		2.5
Pesticides	0.0001	0.00003–0.2 *	
Total pesticides	0.0005		
Calcium	-	10–500	-
Magnesium	-	52.1	-

\* According to the type.

Water contamination by emerging contaminants, such as pharmaceuticals, hormones, agrochemicals, and metallic and carbon nanomaterials, is a global issue. Their harmful effects on the environment and human health have already been proven [22,23].

### 2.1. Pesticides

Pesticides are substances designed and applied to repel, kill, or regulate harmful or interfering pests during the manufacture, processing, transport or marketing of foodstuffs, agricultural commodities, animal feed, or products that may be administered to animals to control insects, bacteria or other pests [24]. Pesticides play, therefore, an essential role in agriculture, enabling a significant increase in yields thanks to the eradication and control of pests. With the growing population, the use of pesticides has increased tremendously

worldwide, with 45% of the usage coming from Europe itself, 25% from the USA, and the rest from the remaining countries [7].

Most pesticides accumulate in food, water, and the environment rather than directly reaching the target species. This unintended accumulation presents a severe threat to human health [3,25]. The active compounds present in the pesticide formulations are harmful to human health as they can cause anxiety, depression, convulsions, severe neurological disorders and cancer [26,27]. In addition, it disturbs the balance in the environment since the concentration of these toxic compounds is increasing exponentially [6]. For these reasons, there is a continuous drive for monitoring and quantification pesticides in the environment.

Pesticides can be classified according to their chemical structure as organophosphates, neonicotinoids, pyrethroids, carbamates, organochlorines [28], substituted phenols and triazines [29]. They can also be classified as herbicides, fungicides, insecticides and bactericides according to their targeted use [30]. Organophosphates and carbamates are the two main groups of pesticides mostly in use nowadays. Their toxic effects are attributed to the enzyme acetylcholinesterase inhibition [31]. Acetylcholinesterase (AChE) is an essential enzyme present in synaptic clefts of the central nervous system. The primary role of this enzyme is to hydrolyze acetylcholine, which is responsible for the proper functioning of the nervous system. AChE inhibition leads to acetylcholine accumulation and, consequently, hyperstimulation of nicotinic and muscarinic receptors and disrupted neurotransmission. [32]. Pesticide preparations available on the market nowadays contain different organophosphates and carbamates. Organophosphate preparations include, e.g., dimethoate, chlorpyrifos, and malathion. Carbamate compounds (carbaryl, carbofuran, carbosulfan) are the most widely used pesticides due to their high insecticidal activity and relatively low persistence.

## 2.2. Nitrogen

The nitrification process of the nitrogen cycle, carried out by microorganisms, produces nitrate and nitrite, which are among the naturally occurring chemical sources of nitrogen in ecosystems. Nitrate and nitrite are essential components of synthetic fertilizers, which aid plant growth to provide food for humans and animals. Via the conversion of dietary nitrates to nitric oxide, dietary nitrates have several beneficial effects on the human body, such as increasing blood flow, lowering blood pressure, and preventing cardiovascular diseases [33]. In addition, nitrite and nitrate are added during the production of foods to preserve them [34].

When nitrates reach the food chain from groundwater, surface water, and other sources, they can negatively affect the human body. If infants consume too much nitrate via their drinking water, they may develop “blue baby” disease or methemoglobinemia, which is caused by the endogenous conversion of nitrate to nitrite [10,35].

Water analysis shows nitrate concentrations in ground water are relatively low. In contrast, in agriculture and farming areas, nitrate-nitrogen concentrations are at the higher end and can exceed the 179.06  $\mu\text{M}$  limit for drinking water. In some cases, nitrate-nitrogen concentrations exceed this limit, e.g., in wastewater sewage and landfills. Nitrite can react and be converted to nitrosamines that are carcinogenic in food and the human digestive system [36]. Nitrate is less toxic and more stable, but it can be converted to nitrite by chemical reduction in water [37], so there is a great need for detection and also continuous monitoring of these species because of their toxicity. For the electrochemical methods, the suitable modification of the electrode surface can improve the sensor response signals of nitrate and nitrite and extend the dynamic range in analytical determinations. Different materials have been reported to improve the sensor characteristics including carbon nanomaterials such as graphene [38] and carbon nanotubes [39], and metallic nanoparticles [40].

### 2.3. Phosphorus

Phosphorus control is considered to be a significant public issue to date due to its substantial industrial, environmental, health, and economic impact. Phosphorus (P) is present in the environment in either an inorganic or organic state. This nutrient is a life-giving element for the growth of flora and fauna, and lake ecosystems [41]. However, excessive amounts of inorganic phosphate ( $\text{I-PO}_4$ ) are among the main causes of growth and propagation of harmful algae known as eutrophication [42] of surface waters. Most inorganic phosphate is used as fertilizer for crop production and is thus released into the environment. Overall phosphorus levels ( $\text{P-PO}_4$ ) between  $0.17\ \mu\text{M}$  and  $0.53\ \mu\text{M}$  are assumed to be the limit values for eutrophication of surface water supplies [43]. In addition,  $\text{I-PO}_4$  is widely used in food processing (meat, seafood, beverage, bakery, vegetables) for many purposes such as humidity retention, pH regulation, protein dispersion, etc. Either a surplus or a deficiency of  $\text{I-PO}_4$  can lead to severe diseases affecting human health. A lack of  $\text{I-PO}_4$  ( $\text{P-PO}_4 < 444.08\ \mu\text{M}$  in adult serum), termed hypophosphatemia, indicates malnutrition. An excess of phosphate can lead to hyperphosphatemia ( $\text{P-PO}_4 > 798.63\ \mu\text{M}$  in adult serum), considered a risk indicator for chronic cardiovascular and renal disease mortality [44]. Reliable and inexpensive detection technology is of great interest for continuous monitoring to address these environmental, economic and health issues regarding the treatment and control of phosphates [45].

### 2.4. Water Hardeners

Water hardness mainly refers to the amount of dissolved minerals, especially calcium ( $\text{Ca}^{2+}$ ) and magnesium ( $\text{Mg}^{2+}$ ) in water, two divalent cations yielding insoluble carbonates, while their bicarbonates are soluble. Besides calcium and magnesium, some other divalent cations may also contribute to the total water hardness, such as manganese ( $\text{Mn}^{2+}$ ), iron (II) or strontium ( $\text{Sr}^{2+}$ ). However, in the majority of cases, the level of these cations is significantly lower than that of magnesium and calcium, so, in practical terms, they are typically neglected [46]. For example, in the case of calcium, general guidelines for classification certify that calcium carbonate is classified more than  $180\ \text{mg/L}$  as very hard [47].

Water hardness affects water consumption by populations for personal hygiene, food preparation and laundry (with an impact on soap consumption), especially in regions rich in carbonate minerals and therefore “hard” water.

### 2.5. Water Disinfectant Byproducts

Disinfection of water is a standard procedure in municipal water to control waterborne pathogens [48]. It is an essential step for the purification of water and to prevent waterborne diseases. The commonly used disinfectants for water purification are ozone, chlorine, chloramines and chlorine oxide [49]. However, the unavoidable reaction of disinfectants with natural organic matter and anthropogenic pollutants produces numerous byproducts, also termed disinfectant by-products (DBPs). These byproducts are responsible for adverse health effects on humans, such as cancer, reproductive and developmental effects [49]. Nevertheless, with the ever-increasing demand for purified water, the use of disinfectants has increased manifold leading to as many as 700 variants of by-products in drinking water [50].

The three main DBPs of the most significant health concerns are trihalomethanes, haloacetic acids and nitrosamines [48]. Trihalomethanes are four DBPs, namely trichloromethane, bromodichloromethane, dibromochloromethane and tribromomethane [48]. Haloacetic acids are classified into nine different types and termed HAA9 based on their reaction with the pollutants [51]. The disinfection by chloramines leads to the production of nitrosamines, which have four different types [48,52]. All these compounds are carcinogenic, highly toxic and cause irreversible damage to human bodies [53].

Apart from the DBPs mentioned above, which are strictly monitored, there are several other unregulated and newly emerging DBPs like halonitromethanes, iodo-acids and iodo-



THMs, halonitriles, haloamides, halofuranones and haloaldehydes, to name a few [49]. Table 1 provides the maximum concentration limit of disinfectant by-products in drinking water according to United States Environmental Protection Agency (U.S-EPA), World Health Organization (WHO) and European Union (EU) guidelines.

## 2.6. Emergent Contaminants

Recently discovered groups of uncontrolled pollutants in surface water and ground-water commonly include daily use substances and various industrial additives. These substances are referred to as emerging contaminants (ECs). That raises a global environmental concern for water quality, posing severe potential threats to human health, wildlife, aquaculture life and ecosystems [54]. Such pollutants are usually bioactive and bio-accumulative and may have extensive occurrence and persistence. Global production of these contaminants is estimated to have been increasing from 1 million to 500 million tons per year [55]. The term of ECs could be referred to three main categories [56]. Firstly, substances recently released into the environment like industrial additives such as bisphenol A [57,58]. Secondly, chemical agents that could already have existed in the environment for several years, and only recently, their significance has begun to attract public attention, which is the case with pharmaceuticals [59], personal care products, etc. The third category concerns compounds already known for more extended periods, but whose potential harmful effects on public health and the environment have only recently been identified, for example hormones [60], steroids, surfactants etc. ECs sources are divided between specific point sources and diffuse sources [61]. Primary sources are households, industrial, hospital effluents and urban runoff.

Polyphenolic compounds (PCs) have received exceptional attention due to their harmful effect on the human body and the environment. Polyphenols are omnipresent secondary metabolites in foods [62]. They consist of phenolic hydroxyl group(s)-containing molecules, which are the basis of their antioxidant activity. In general, the reaction of this antioxidant action takes place with the loss of one electron to give a nontoxic, stable composition unable to propagate the response [63]. Antioxidants have many interactions in the food matrix, like preventing fat necrosis and reducing the harmful effects of nitrogen and active oxygen [63]. Several studies have been made to introduce sensitive and straightforward methods to evaluate antioxidant capacity (AOC) and quantify polyphenols in food. Figure 1 shows possible sources for emergent contaminants.

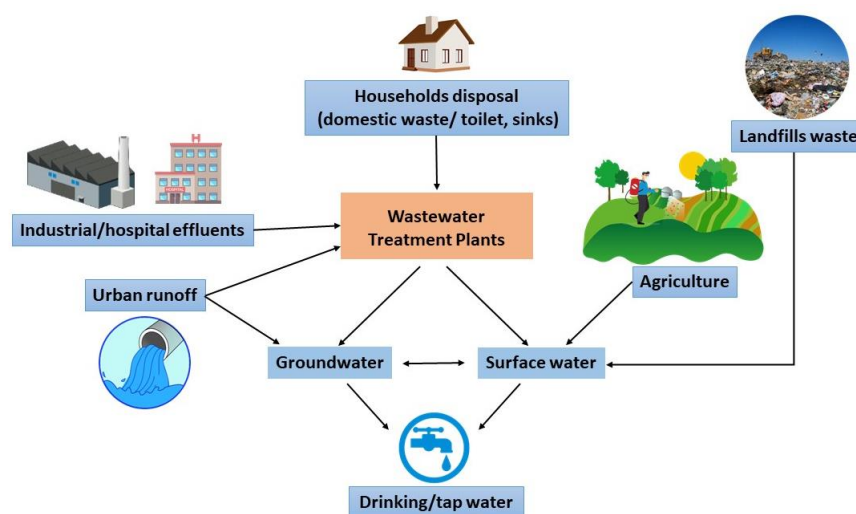


Figure 1. Primary sources of water contaminants in the environment.

### 3. Electrochemical Sensor for Water Contaminants

#### 3.1. Pesticide Sensors

Presently, high-performance liquid chromatography (HPLC) [64] and gas chromatography (GC) [28] coupled with mass spectroscopy (MS) are used to quantify various types of contaminants in the environment and food. These conventional measurement procedures are time-consuming, laborious, and typically require complex sample preparation and analyze the samples by comparing the obtained spectra with reference spectra [12,13]. Hence, there is a significant need for developing a fast, robust, low-cost, accurate and portable analytical system for the detection of pesticides.

The following text provides an overview of the electrochemical sensors for pesticide detection/quantification reported. We provide the analysis by dividing registered sensing platforms based on the receptor or active material at the working electrode.

Bio-components warrant specific interactions of pesticides with sensors and have a relatively high selectivity. Electrochemical sensors rely on direct electrochemistry of pesticides and are connected with the electrocatalytic reaction of active electrode material(s) towards electrochemical transformations of analytes. For this reason, metallic materials are not something that is traditionally found in the field of pesticide detection and have appeared only recently. As a rule, the analyte must be electrochemically active on the electrode material so that the detection becomes possible. We also note that electrochemical sensors are not famous for their selectivity as any compound which can undergo an electrochemical transformation in the potential window where the analysis is done, can interfere with the analyte. Some of the first reports indicate differential pulse voltammetry to detect neonicotinoid pesticides (clothianidin, imidacloprid, thiamethoxam, nitenpyram and dinotefuran) using disposable screen-printed sensors with a sputtered bismuth film working electrode [65]. Limits of quantification (LOQ) were found to be in the range of 0.16 to 0.30  $\mu\text{M}$ . In this work, significant efforts were made to reduce the matrix effect, and for this purpose, solid-phase extraction was employed. The use of silver amalgam electrodes was also demonstrated. Mercury meniscus modified Ag amalgam electrode was used to detect tetrachlorvinphos with LODs amounting to 0.06  $\mu\text{M}$  when differential pulse voltammetry is used and slightly better 0.04  $\mu\text{M}$  when square wave voltammetry is employed [66]. Recently, an electrochemical microcell with Ag solid amalgam was employed for difenzoquat detection using differential pulse voltammetry. This approach enables the analysis of tens of microliter volumes with LOQ for difenzoquat below 0.45  $\mu\text{M L}^{-1}$  [67]. Gold is irreplaceable in electrochemical laboratories for years, so it was also used for electrochemical detection of pesticides. Amperometric detection of the herbicide glyphosate with a LOD of 2  $\mu\text{M}$  was demonstrated using gold electrodes [68]. According to US regulations this LOD is low enough to allow detection below the maximum permitted concentration in drinking water. Still, we note that glyphosate is not considered a very toxic compound for humans. More advanced approaches include the use of colloid gold for methyl parathion detection (LOD  $10.5 \times 10^{-3} \mu\text{M}$ ) [69] and nanoporous gold for simultaneous detection of carbendazim (LOD 0.24  $\mu\text{M}$ ) and methyl parathion (LOD 0.02  $\mu\text{M}$ ) [70]. Simultaneous detection was possible due to a significant oxidation peak potential separation of the investigated pesticides (see Figure 2).

Other examples of the use of gold-based electrodes, primarily nanosized gold on different supports, can be found, for example, gold nanoparticles/ethylenediamine-reduced graphene oxide for fenitrothion (LOD  $6 \times 10^{-3} \mu\text{M}$ ) [71]; Au nanoparticles supported by reduced graphene oxide for diuron detection (2.23  $\mu\text{M}$ ) [72]; 3D graphene-Au composite for detection of 1-naphthyl methylcarbamate (LOD 0.0012  $\mu\text{M}$ ) [73]; methyl parathion detection using pillar[5]arene@AuNPs@reduced graphene oxide hybrids (LOD 0.001  $\mu\text{M}$ ) [74]; Au-Pd/reduced graphene oxide nanocomposite for parathion detection (LOD 0.008  $\mu\text{M}$ ) [75].

There are examples of ultrasensitive detection of pesticides using Au-based materials. Dong et al. [76] reported a methyl parathion LOD of only  $3.02 \times 10^{-5} \mu\text{M}$  using a multi-walled carbon nanotubes-CeO<sub>2</sub>-Au nanocomposite in combination with stripping voltammetry.

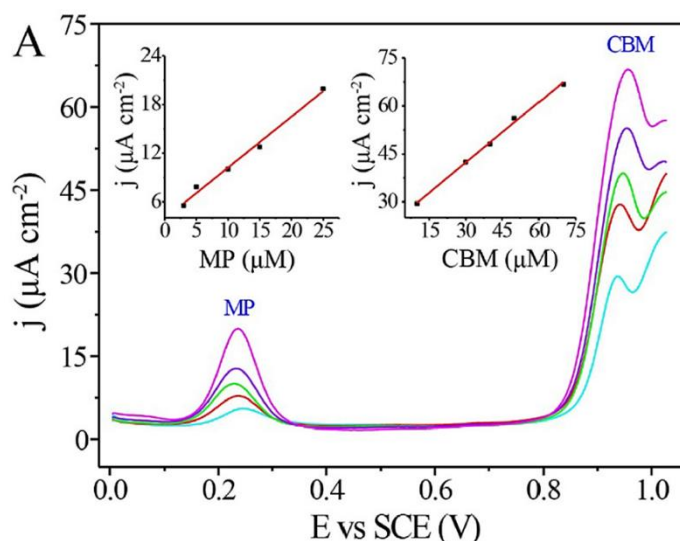


**Figure 2.** Simultaneous detection of the mixture of methyl parathion (MP) and carbendazim (CBM). The concentration ranges are  $(3\text{--}25) \times 10^3 \mu\text{M}$  for MP and  $(10\text{--}70) \times 10^3 \mu\text{M}$  for CBM. The insert profiles show the calibration curves between the peak current density and the target pesticide concentration. Reprinted from [70].

According to the investigation, such a low LOD was due to the unique combination of high electrical conductivity and adsorption properties of multi-walled carbon nanotubes and high surface area and specific catalytic activity of Au and  $\text{CeO}_2$  nanoparticles. Appreciable performance was demonstrated also for gold nanoparticles/single-walled carbon nanotubes/glassy carbon electrode containing mono-6-thio- $\beta$ -cyclodextrin (SH- $\beta$ -CD) self-assembled monolayer [77]. With the use of square wave voltammetry LOD for methyl parathion was  $10^{-4} \mu\text{M}$  with a linear response range from  $2.0\text{--}80.0 \times 10^{-3} \mu\text{M}$ . Interestingly, other frequently used pesticides like chlorpyrifos, 2,4-dichlorophenoxy acetic acid, methamidophos, triazophos, parathion showed very small effect on the analytical signal of methyl parathion.

Electrochemistry of pesticides using oxide-based electrodes is also a relatively new approach for pesticide detection. Methomyl detection using copper-oxide modified carbon paste electrode was demonstrated by Abbaci et al. [78] with a LOD of  $0.02 \mu\text{M}$ . At the same time, CuO microspheres were employed for the detection of  $\alpha$ -endosulfan using differential pulse voltammetry [79]. Very sensitive detection of diazinon, based on its direct reduction, enabling a LOD of  $3 \times 10^{-3} \mu\text{M}$  is possible using multi-walled carbon nanotubes covered by  $\text{TiO}_2$  nanoparticles [80]. In contrast, CuO- $\text{TiO}_2$  hybrid nanocomposites were used to detect methyl-parathion with differential pulse voltammetry [81]. The LOD was, in this case, 1.21 ppb with basically no interference. Other oxide materials were also used, including NiO, to detect parathion with LOD of  $0.024 \mu\text{M}$  [82].  $\text{CeO}_2$ -decorated reduced graphene oxide for determination of fenitrothion (LOD  $3.0 \times 10^{-3} \mu\text{M}$  [83]) and ZnO quantum dots for impedimetric detection of aldrin, tetradifon, glyphosate, and atrazine [84]. This platform was proposed for dual (tandem) measurements using the optical and electrochemical approaches. Some recorded low LODs were demonstrated using oxide materials for electrochemical detection of pesticides. The use of electrospun  $\text{SnO}_2$  for detection of atrazine enabled LOD of  $0.9 \text{ zM}$  [82]. Lately, several sensors for determination of methyl parathion were also reported, but with typical LODs for electrochemical detection in the submicro to the nanomolar range: 3D flower-like praseodymium molybdate-decorated reduced graphene oxide (LOD  $1.8 \times 10^{-3} \mu\text{M}$ ),  $\text{MnO}_2/\text{PANI}/\text{rGO-A}$  (LOD  $7.4 \times 10^{-3} \mu\text{M}$ ) [85] and a monolayer of zirconium (IV) phosphonate on glassy carbon electrode (LOD  $0.0045 \mu\text{M}$ ) [86]. Also, the chitosan/magnetic  $\text{Fe}_3\text{O}_4$  nanocomposite-modified glassy carbon electrode in combination with square wave voltammetry was used for bendiocarb determination, but the LOD was  $2.09 \mu\text{M}$  with a LOQ of  $6.97 \mu\text{M}$  [87].



Apparently, the selectivity was rather good, compensating for the relatively high LOD, and enabling bendiocarb detection in complex matrices.

### 3.1.1. Sensors Based on Carbon Materials

Carbon materials are irreplaceable in electrochemical laboratories for many reasons. In principle, carbon materials are good electronic conductors, cheap, abundant, easy to work with, chemically inert and suitable for making composites, as can be already concluded from the previous discussion [88]. Generally, they are however rather bad electrocatalysts for water decomposition [89]. Many electrochemical reactions can be performed on carbon materials, while other materials would suffer from electrochemical transformations or cause electrolyte decomposition. However, their chemical inertness is a problem for electrochemistry. It is necessary to have an interaction between the electrode material and the analyte to perform electrocatalytic conversion and subsequent detection/quantification. Defects and functional groups in carbon materials, which are inherently present or intentionally introduced in the material, can be beneficial for the detection. Moreover, carbon with  $sp^2$  hybridized domains can interact with pesticides which have aromatic rings via  $\pi$ - $\pi$  stacking interactions, enabling the necessary interaction with the analyte before the charge transfer step. Materials, which are traditionally used in electrochemical laboratories, are glassy carbon (GC), boron-doped diamond (BDD), and graphite materials from the carbon black (CB) family. Recently many carbon-based nanomaterials like carbon nanotubes (CNT) and graphene-based materials have been introduced. Some review papers on this topic are available in the literature [87]. While there are many cases where carbon materials are used as a support for different metallic or oxide nanostructures or scaffolds for biologically active compounds, several reports consider “only-carbon” electrodes for pesticide detection via their direct electrochemistry. In this case, similarly to the case when metallic and oxide materials are employed, typically more advanced electrochemical techniques are used to improve the detection capabilities of sensing platforms. So, instead of the standard cyclic voltammetry, differential pulse voltammetry or square wave voltammetry is employed. Typical detection limits and performances fall in the range of other electrochemical sensors for pesticides, while no record-breaking cases can be identified in this class of sensors.

Nevertheless, carbon-based materials are the most suitable for on-field use. These systems are generally very robust and rarely require special care due to the attractive properties of carbon materials. A selection of available literature reports and some of the characteristics of proposed sensing materials are summarized in Table 2.

### 3.1.2. Sensors Using Molecularly Imprinted Polymers and Their Composites

Molecular imprinted polymer technology has attracted a lot of attention as it enables specific interactions of molecules with MIP structures. This section addresses MIP as a particular matrix for recognizing pesticides and does not consider their possible bio-like functions. The molecular imprinting technique relies on the formation of specially designed cavities within a cross-linked polymeric matrix (see Figure 3). Thus, particular guest-host interactions are operative and unique recognition of the analyte is possible. This means that selectivity increases while further electrochemical transformations of recognized analytes allow for high sensitivity and low detection limits. In electrochemistry, conductivity is essential so that many conductive polymers, like polypyrrole, are used in MIP technology. It is not surprising that conductive polymers are applied in this area, as they have been in use in electrochemistry labs for more than three decades. The knowledge accumulated on the electrochemistry of conductive polymers is used in this technology. The lessons learned from electrochemical polymerization studies are used to prepare specific MIP sensing platforms in the presence of an analyte template. While selectivity and sensitivity of sensors based on the MIPs approach that of immuno-based and aptasensors, we note that MIP technology is much more affordable and could resolve many of the problems associated with sensitivity and selectivity issues.

**Table 2.** Overview of electrochemical sensors for pesticides, based on (modified) carbon materials at the working electrode.

Detection Method	Materials	Analyte	LOD ( $\mu\text{M}$ )	Dynamic Range ( $\mu\text{M}$ )	Comments	Reference
SWV *	BDD	Parathion	0.043	-	Low interference with organic pollutants compared to HMDE *	[90]
SWV	BDD	Atrazine	0.01	0.05–40	Good selectivity and repeatability	[91]
SWV DPV *	BDD	Methomyl	19 1.2	66–420 5.0–410.0	Good recovery with real samples	[92]
adsorptive stripping SWV	Sol-gel carbon ceramic electrode	Fenitrothion	0.0016	5000–1,000,000.1–50	Demonstrated on-site monitoring	[93]
SWV	Graphite-modified basal plane pyrolytic graphite electrode	Methyl parathion	3	79.0–263.3	Applied for drinking water	[94]
adsorptive stripping SWV	Poly(4-amino-3-hydroxynaphthalene Sulfonic acid) modified GCE	Fenitrothion	$0.7 \times 10^{-3}$	0.001–6.6	Good recovery in spiked water samples	[95]
SWV	Sarbone black modified GCE	Mesotrione	0.026	0.040–7.2	Applied for real water samples and juice	[96]
cyclic voltammetry and SWV	Peptide nanotubes on modified pencil graphite electrode	Fenitrothion	0.0196	0.114–1.712	Good recovery in spiked water samples	[97]
DP adsorptive cathodic stripping voltammetric	Single-walled carbon nanohorns and zein modified GCE	Fenitrothion	0.012	0.99–12	Good repeatability and reproducibility applied for real water samples and juice	[98]
SWV	Screen-printed carbon electrode	Bentazone	0.034	-	Analysis time 10 s, reusable at least 15 times, sensitivity of $0.0987 \times 10^6 \mu\text{A}/\text{M}$	[99]
adsorptive stripping voltammetry	Nano poly(3-methyl thiophene)/multiwalled carbon nanotubes	Isoproturon, Voltage cypermethrin Deltamethrin fenvalerate Dicofol	26–100	1.43–4.47 1.45–4.47 0.26–4.47 0.34–4.47 1.09–4.47 0.967–4.47	Good recovery in spiked water samples	[100]
DPV	Multiwalled carbon nanotubes-poly(acrylamide) nanocomposite	Methyl parathion	0.002	0.005–10	Demonstrated for environmental water samples	[101]

Table 2. Cont.

Detection Method	Materials	Analyte	LOD ( $\mu\text{M}$ )	Dynamic Range ( $\mu\text{M}$ )	Comments	Reference
SWV	Graphene-based electrochemical sensor	Isoproturon:	20	20–1000	Demonstrated for water, soil and vegetable samples	[102]
DPV	Graphene quantum dots with oxime as electroactive probe	Fenthion	$6.8 \times 10^{-6}$	$1.0 \times 10^{-5}$ – $5.0 \times 10^{-2}$	Performance demonstrated for water and soil samples	[103]
DPV	Ionic liquid–graphene nanosheets	Methyl parathion	$1.9 \times 10^{-5}$	0.09–0.04	Satisfactory stability and reproducibility demonstrated for spiked water samples	[104]
DPV	N-methyl-2-pyrrolidone exfoliated graphene	Carbendazim	0.78 M	$0.005$ – $1.57 \times 10^{-6}$ M	Demonstrated for ground water, soil, and cucumber samples	[105]
DPV	Pillar[5]arene/reduced graphene nanocomposite	Methyl parathion	$3 \times 10^{-10}$ M	$0.001$ – $150 \times 10^{-6}$ M	Demonstrated for soil and waste water samples	[106]
DPV	Cellulose microfiber entrapped reduced graphene oxide	Fenitrothion	0.008	Linear range up to 1134	Demonstrated for different water samples	[107]

\* SWV: Square wave voltammetry, DPV: Differential pulse voltammetry, HMDE: Hanging mercury drop electrode.

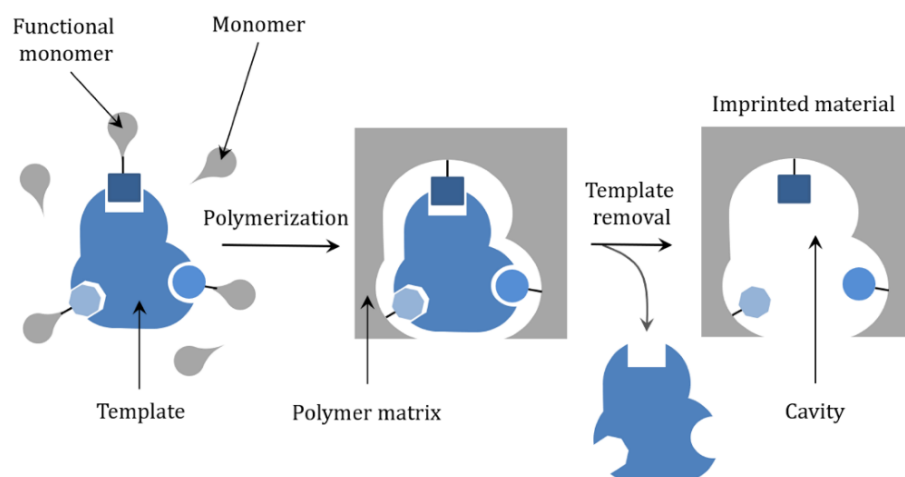


**Figure 3.** Preparation of molecularly imprinted materials.

While specifically formed MIP structures are used to recognize target analytes, electrochemical methods used to generate the analytical signal are selected to improve sensitivity. One of the possible limitations of MIPs for electrochemical detection is that polymers are sometimes also electrochemically active. Their signal might be such a high that it masks the analyte's signal, so this is something that must be considered when designing a sensing platform.

Other important issues are the possibility of irreversible electrochemical transformations of polymers and the pH sensitivity of polymers. Both issues might lead to irreversible losses of electroactivity, losses of conductivity, or conformational changes, which might disrupt recognition moieties of MIPs, compromising the sensor's overall performance [108]. We summarize existing reports on MIPs for electrochemical pesticide detection in Table 3.

**Table 3.** Overview of electrochemical sensors for pesticides, based on molecularly imprinted polymers.

Detection Method	Materials	Analyte	LOD ( $\mu\text{M}$ )	Dynamic Range ( $\mu\text{M}$ )	Comments	Reference
CV	Molecularly imprinted polypyrrole membrane	2,4-Dichloro-phenoxy acetic acid	0.83	1.0–10	Successful determination in real samples	[109]
photoelectrochemical technique	Polypyrrole-based MIP composite with $\text{TiO}_2$ *	2,4-Dichloro-phenoxyacetic acid	0.01	-	Demonstrated for spiked water samples	[110]
capacitive sensor	Polyquercetin-polyresorcinol-Gold nanoparticles by MIP technique	Methyl parathion	$3.4 \times 10^{-4}$	0.07–1	Good recovery and low interference in water samples	[111]
impedimetric	MIP/sol-gel, different monomers	Methidathion			Proof-of-concept experiments	[112]
cyclic voltammetry and SWV	MIP suspension polymerization, modification of carbon paste electrode	Diazinon	$7.9 \times 10^{-5}$	$2.5 \times 10^{-3}$ –0.10.1–2.0	Good recovery in water and apple samples	[113]
potentiometric	Methacrylic acid (functional monomer), ethylene glycol dimethyl acrylate (cross-linker)	Endosulfan	20	20 to $12 \times 10^{-3}$	Nernstian response, good stability	[114]
DPV	Methacrylic acid, ethylene glycol dimethacrylate and carbon nanotubes	Diazinon	$1.3 \times 10^{-4}$	$5 \times 10^{-4}$ –1	No sample preparation for human urine, tap, and river water samples	[115]
SWV	MIP with carbon nanotubes	Dicloran	$4.8 \times 10^{-4}$	$1 \times 10^{-3}$ –1	No interference	[116]
cyclic voltammetry	MIP from methacrylic acid, ethylene glycol dimethacrylate	Atrazine	716.26		Proof-of-concept, effects of ethanol solution analyzed	[117]
cyclic voltammetry	MIP/graphene oxide modified glassy carbon electrode	Profenofos	$5 \times 10^{-3}$	0.05–3500	Stable; enhanced selectivity vs. other structurally similar pesticides	[118]
DPV and EIS *	Acrylamide based MIP on gold electrode	Malathion	$1.79 \times 10^{-7}$	$1 \times 10^{-7}$ –0.017	Good recovery in olive oil and fruit samples	[119]

\* EIS: Electrochemical impedance spectroscopy.



### 3.1.3. Biosensors

#### (a) Enzymatic biosensors

Electrochemical biosensors are, historically, one of the first types of sensors employed for pesticide detection. Their action primarily relies on the inhibition of enzymatic components by the pesticide analyte and reduction of the electrochemical responses in the presence of analyzed pesticide. So, the indirect detection is so that the response in the presence of an analyte is compared to the response in the absence of an analyte. This is how an analytical curve is generated. Some of the first reports on this technique date back 35 years. Glass electrodes were modified with an enzymatic layer, enabling detection of carbaryl and azinphosethyl upon incubation of electrode with pesticide and enzyme-substrate [120]. Some of the first studies also used amperometric detection [121]. Several pesticides, including paraoxon, parathion, methyl paraoxon and methyl parathion, were coupled with acetylcholine and butyrylcholine esterases. Upon the contact of a pesticide with the enzyme, the activity was reduced. The detection principle involves observing the loss of enzyme activity in terms of choline production upon the exposure of inhibited enzymes to their substrates. Over the years, the research was directed either to demonstrate described detection principle for several pesticides or to improve detection limits by combining enzymatic components with different electrode materials, which show better electrocatalytic performance for detection of the products of enzymatic reactions. Using AChE detection, the detection limits for parathion and dichlorvos were  $0.021\ \mu\text{M}$  and  $10^{-4}\ \mu\text{M}$ , respectively [122]. At the same time, the use of AChE immobilized on iron oxide ( $\text{Fe}_3\text{O}_4$ )/c-MWCNT/Au electrode enabled amperometric detection of malathion, chlorpyrifos, monocrotophos and endosulfan in the concentration ranges  $0.1\text{--}40 \times 10^{-3}\ \mu\text{M}$ ,  $0.1\text{--}50 \times 10^{-3}\ \mu\text{M}$ ,  $1\text{--}50 \times 10^{-3}\ \mu\text{M}$ , and  $10\text{--}100 \times 10^{-3}\ \mu\text{M}$ , respectively [123]. Other substrates for immobilization of AChE include nanocrystalline titanasilicate and ZSM-5 [124], iron oxide nanoparticles and poly(indole-5-carboxylic acid) for the detection of malathion and chlorpyrifos at nanomolar range [125] and gold nanoparticles obtained by electroless plating on three-dimensional graphene for detection of malathion and methyl parathion in water [126].

Another interesting example is the use of inhibitory action of chlorfenvinphos and malathion on lipase enzyme, whose substrate is *p*-nitrophenol acetate [127], and the product of the enzymatic reaction is *p*-nitrophenol. The product is detected using voltammetry, so the concentration of pesticides is linked to the reduction of *p*-nitrophenol production in the presence of pesticides. Detection limits were rather high,  $84.45\ \mu\text{M}$  and  $253.03 \times 10^3\ \mu\text{M}$ , for chlorfenvinphos and malathion, respectively, but this approach is rather new and amenable to further improvements. The same inhibition principle was used for fenitrothion using tyrosinase/poly(2-hydroxybenzamide)-modified graphite electrode [128], with catechol as the substrate. In this case, the detection limit was rather low, amounting to  $4.70 \times 10^{-3}\ \mu\text{M}$ . It is important to note that, traditionally, pesticide sensors based on enzyme inhibition (mostly AChE) relied on amperometric detection. However, recently, Malvano et al. [129] compared the performance of impedimetric affinity AChE-based biosensors to “standard” amperometric ones. While impedimetric detection gave ppb detection limits, the most interesting result is that the required analysis time is significantly reduced, from 20 min for amperometric to only 4 min for impedimetric detection. The principle of impedimetric detection relies on the impedance change upon the formation complex of pesticide with AChE, and it was demonstrated for water samples spiked with carbaryl and dichlorvos.

Another possibility is to employ enzymes whose substrates are organophosphates so that the products of the enzymatic reaction are detected using electrochemical methods. An old example by Mulchandani [130] demonstrated the use of organophosphate hydrolase (OPH) immobilized onto screen-printed carbon electrodes for ultra-sensitive detection of paraoxon and methyl parathion with detection limits of  $0.09$  and  $0.07\ \mu\text{M}$ , respectively. In this approach, organophosphate hydrolase produces *p*-nitrophenol during hydrolysis of OPs, which is easily detected by amperometry. The same principles were used for the development of biosensor arrays for micro- to nanomolar detection of OPs [131] and screen-

printed, amperometric biosensor arrays for automated detection of several pesticides at  $10^{-3}$  to  $10\ \mu\text{M}$  concentration range [131].

Further work showed that the use of cross-linked enzyme crystals of organophosphate hydrolase improves sensitivity and operational stability (particularly thermal) for detection of paraoxon compared to the use of enzyme in the non-crystalline form [132]. As in the case of cholinesterase-based biosensors, the catalytic action of the substrate for enzyme immobilization plays an essential role in the detection of p-nitrophenol as the product of OPs decomposition. A bionanocomposite sensing platform was recently demonstrated, consisting of chitosan-entrapped carbon nanotubes (CS-CNTs),  $\text{ZrO}_2$  nanoparticles, and OPH [133] was used for detection of paraoxon with a detection limit of  $20\ 10^{-3}\ \mu\text{M}$ .

#### (b) Immunobiosensors

The application of immune-based components for pesticide detection is not as old an approach as the use of enzymatic biosensors but the first reports still date back 25 years. One of the first reports describes the development of a multichannel sensor for the detection of 2,4-dichlorophenoxyacetic acid with LOD of  $0.0018\ \mu\text{M}$  [134]. The same LOD was reported for the flow injection approach [135], while a LOD of  $0.089\ \mu\text{M}$  was reported for both 2,4-dichlorophenoxyacetic acid and 2,4,5-trichlorophenoxyacetic acid using potentiometric enzymatic immunoassay [136]. Other pesticides were also detected using immunobiosensors, including atrazine with biotinylated-Fab fragment K47 antibody [137] and glycine-doped polyaniline nanofilms on silicon with anti-atrazine antibodies [138]. LOD was of the order of  $\mu\text{g}$  per liter. Recently, parathion was also detected using electrochemical immunobiosensors. Impedimetric measurements by graphene-modified screen-printed immunosensor led to one LOD of  $9.31\ 10^{-8}\ \mu\text{M}$  [139]. In contrast, the use of graphene quantum dots led to further improvements of LOD and its reduction to  $8.23\ 10^{-8}\ \mu\text{M}$  [140]. However, the most astonishing is LOD of atrazine using electrospun  $\text{Mn}_2\text{O}_3$  nanofibers modified with atrazine antibodies. The LOD amounted to only  $3.93 \times 10^{-15}\ \mu\text{M}$  with impedimetric detection [141].

Microorganisms are also used as platforms for electrochemical pesticide detection. This strategy is also relatively new. The general principle relies on the toxic effects of pesticides on living cells and measuring the products of their metabolism. These systems seem particularly suitable for monitoring overall contamination as the complexity of living cells, and their responses to particular compounds seem like a big challenge for obtaining high selectivity. Amperometric detection was combined with a platform formed of *Saccharomyces cerevisiae* cells on a combination of polyvinyl alcohol hydrogel and sodium alginate as a matrix at the electrode surface for measuring toxicity of acephate, ametryn and thiram [142]. Also, *Escherichia coli*, *Shewanella oneidensis* and *Methylosinus trichosporium OB3b* immobilized on screen-printed gold electrode surface were used for monitoring water pollution. At the same time, the possibility to integrate sensors in sensor arrays was outlined in Abu-Ali et al. [143]. Recently, the use of an artificial neural network approach for identifying pollutants using bacteria immobilized on gold screen printed electrodes was demonstrated, including detection of pesticides (atrazine), heavy metal ions, and petrochemicals [144].

#### (c) Aptasensors

Aptamer technology is relatively new, so the first reports date back to only four years ago. However, superior performance is demonstrated. An impedimetric aptasensor using gold nanoparticles decorated multiwalled carbon nanotube-reduced graphene oxide nanoribbon as a platform for immobilizing aptamer (see Figure 4) demonstrated an ultra-low LOD for acetamiprid of only  $1.7\ 10^{-8}\ \mu\text{M}$  [145]. Using Pt nanowires as the platform for aptamers, in combination with impedimetric measurements, the same pesticide could be detected with a LOD of  $10^{-6}\ \mu\text{M}$ , while atrazine was detected with a LOD of  $10^{-5}\ \mu\text{M}$  [146]. These detection limits are much lower compared to the ones obtained using enzyme-based biosensors. Reusable screen-printed carbon electrodes were recently developed to detect organophosphate pesticides based on graphene oxide-ferroferric oxide combined with

Aptamer. Polydimethylsiloxane was used to avoid the adsorption of molecules on the surface of the working electrode. It was concluded that the aptasensor could be used twice without signal loss and effect of interferences [147].

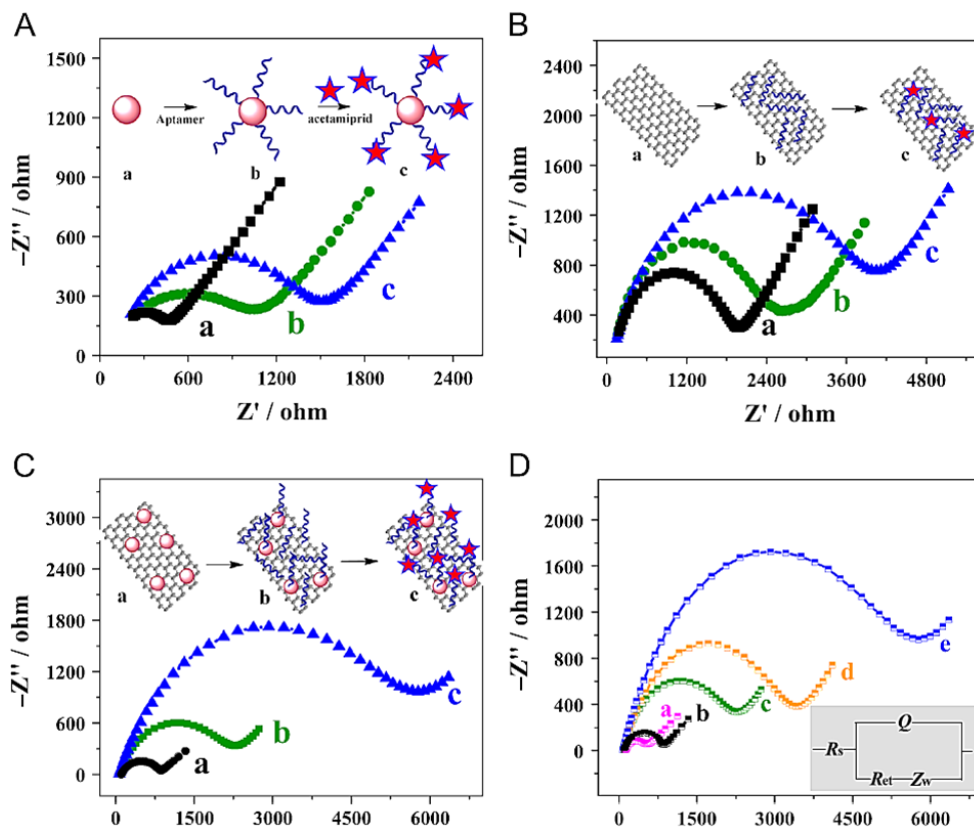


**Figure 4.** Comparison of the EIS responses for the GCE modified with different nanomaterials before and after aptamer immobilization and acetamiprid detection: (A) AuNPs/GCE, (B) MWCNT-rGONR/GCE, (C) Au/MWCNT-rGONR/GCE; (D) EIS responses of bare GCE (a), Au/MWCNT-rGONR/GCE (b), aptamer/Au/MWCNT-rGONR/GCE (c), MCH/aptamer/Au/MWCNT-rGONR/GCE (d) in 0.1 M PBS (pH 7.0) containing 5 mM  $[\text{Fe}(\text{CN})_6]^{3-/4-}$  and 0.1 M  $\text{KNO}_3$ , and EIS responses of MCH/aptamer/Au/MWCNT-rGONR/GCE (e) after 100 nM acetamiprid captured on the modified electrode in 0.1 M PBS (pH 7.0) containing 5 mM  $[\text{Fe}(\text{CN})_6]^{3-/4-}$  and 0.1 M  $\text{KNO}_3$ . Reprinted from [145].

#### (d) Biomimetic sensors

This is one of the newest sensor technologies, and only a couple of reports can be found. An astonishing performance of electrochemical biomimetic sensor based on functionalized gold nanoparticles with an oxime group and nitrogen-doped graphene composites which detects dimethoate with LOD of only  $8.7 \times 10^{-13} \text{ M}$ , was demonstrated by Zhang et al. [145], indicating performance close to that of aptasensors. Another example is the use of functionalized polyacrylamide, polyhydroxamicalkanoate, which mimics AChE. Using this platform for amperometric detection of pesticides paraoxon-ethyl (LOD  $0.36 \mu\text{M}$ ), fenitrothion (LOD  $0.61 \mu\text{M}$ ), and chlorpyrifos (LOD  $0.83 \mu\text{M}$ ) were effectively detected [148]. A bifunctional nanoenzyme, cerium oxide, mimicking organophosphate hydrolase behavior, was used to decompose methyl parathion to *p*-nitrophenol, and the same nanoenzyme coated on the surface. The obtained LOD for methyl parathion was  $0.06 \mu\text{M}$ . As one can see, the LODs are close to those of enzymatic biosensors, but, importantly, species that usually interfere with enzymatic sensors do not affect the performance of biomimetic systems.

As a conclusion on electrochemical biosensors for pesticide detection, we note that special molecules require special care, so it is hard to imagine a non-properly educated person working with bio-based sensors in the field. New technologies that appeared

some 5 years ago in this field such as aptamers and biomimetic systems offer more robust solutions. These also hold the record, as we see, in terms of sensitivity. While any compound, which inhibits the enzymes, could interfere with enzymatic biosensors relying on enzyme inhibition, this problem is resolved using specific interactions with immuno-based components. One of the best examples is the detection of atrazine using immuno-based impedimetric detection, realizing a low LOD [141]. However, this solution comes with a great price, and these sensors cannot be considered very affordable. An overview of the performance and maturity of available technologies related to bio-based sensors for pesticide detection is given in Figure 5.

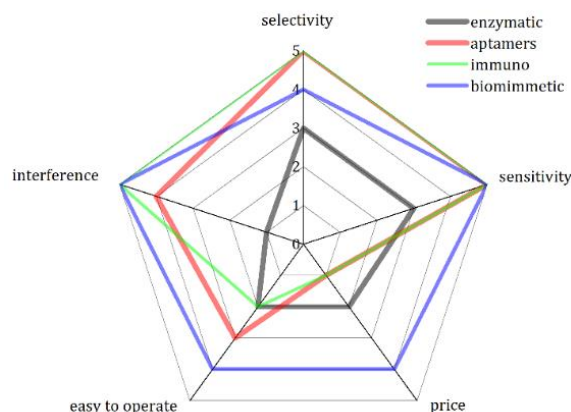


**Figure 5.** Spider diagram for the overall performance of different electrochemical biosensors for pesticide detection (1—bad, 5—very good). Remark: We do not consider sensors based on living cells.

### 3.1.4. Sensors Based on Other Materials

Besides the main classes of materials and recognition components described above, there are examples of some atypical materials or atypical combinations of materials applied for building electrochemical sensing platforms for pesticides. For example, metal-organic frameworks (MOFs) have received a lot of attention in many different fields, including analytics, so it is not surprising that MOFs were also investigated for pesticide quantification. Karimian et al. [149] applied TiO<sub>2</sub>-functionalized graphene oxide to modify MOF UiO-66 for the simultaneous determination of paraoxon and chlorpyrifos. Appreciable performances were observed, with LODs of  $0.2 \cdot 10^{-3} \mu\text{M}$  (paraoxon) and  $1.0 \cdot 10^{-3} \mu\text{M}$  (chlorpyrifos), and the corresponding linear ranges of  $1.0\text{--}100.0 \cdot 10^{-3} \mu\text{M}$  and  $5.0\text{--}300.0 \cdot 10^{-3} \mu\text{M}$ , respectively, with the use of square wave voltammetry.

MOFs might be new hot materials in this field as they combine precise and open pore structure and a possibility for functionalization in order to improve catalytic (charge transfer) properties and electrical conductivity, which must not be disregarded when talking about electrochemical sensors. Some other examples of rarely investigated classes of materials are well known in other fields of electrochemistry. One example builds metallic phosphosulfides, resulting from electrocatalysis of hydrogen production. Paraoxon ethyl was detected and quantified using graphene-based NiFe bimetallic phosphosulfide nanocomposite with a rather low LOD of  $3.7 \cdot 10^{-3} \mu\text{M}$  [150]. The synergistic effect of  $\pi$ - $\pi$  stacking interactions has been emphasized between the aromatic moiety of paraoxon ethyl and graphene and the strong catalytic effect of NiFe phosphosulfide. Another example is a carbon black-cobalt phthalocyanine (CoPc) nanocomposite. CoPc and other transition metal phthalocyanine are intensively investigated for oxygen reduction reaction as an alternative to Pt, while Cinti et al. [151] demonstrated low LOD of paraoxon (18 nM) using the mentioned composite at screen-printed electrodes. Even lower LODs were found for methyl parathion ( $3.1 \cdot 10^{-7} \mu\text{M}$ ), diazinon ( $6.7 \cdot 10^{-8} \mu\text{M}$ ) and chlorpyrifos ( $3.3 \cdot 10^{-8} \mu\text{M}$ ) in water samples using graphene oxide decorated with monodisperse boron nitride quantum dots [152]. Further examples can be found in [153–155].

### 3.2. Water Hardness Ions

Water hardness describes the total concentration of alkaline earth ions in water [156]. In real water samples the concentrations of calcium and magnesium are usually much higher than other ions, so commonly, hardness often refers to the sum of the calcium and magnesium ion concentrations. The detection of other ions like magnesium ( $Mg^{2+}$ ) is more challenging since they are present in small amounts.

Titration is nowadays the standard method for the determination of water hardness. Fluorimetry and capillary electrophoresis are also used for the determination of water hardness [155]. However, these methods have problems with complex operation procedures and expensive instruments. Ion-selective electrodes (ISEs) can provide inexpensive, simple and continuous measurements of water hardness [157,158].

Recently, screen-printed ISEs have attracted significant attention to detect several ions such as  $Pb^{2+}$ ,  $K^+$  and  $Ca^{2+}$  [159]. Due to their high cost-effectiveness and simple manufacturing processes, screen-printed electrodes (SPEs) offer unique advantages for real-time monitoring for industrial, clinical, and environmental analysis. There are many types of SPEs, one of them is potentiometric.

Electro-active materials are therefore sought and implemented as solid contacts like graphene and carbon nanotubes during the manufacturing of all-solid-state ISEs, to enhance the stability of electrode potential. An example is an integrated  $Ca^{2+}$  potentiometric strip for which electrochemical and physical techniques previously treat the conductive carbon ink-based ceramic substrate. Potentiometric and electrochemical performances strip have been investigated in seawater [160]. Potentiometric  $Ca^{2+}$  determination using screen-printed ASS sensors can be an advantageous alternative with interesting accuracy and precision compared to conventional chromatography and photometric techniques. Herein, an example of electrochemical performance of planar miniaturized all-solid-state (ASS) screen-printed potentiometric sensor to detect  $Ca^{2+}$  ions in real water samples [161]. In the same context, another potentiometric solid-contact ion-selective electrode (SC-ISEs) has been developed for the detection of  $Ca^{2+}$  using the nanocomposite of ordered bimetallic AuCu NPs coupled with multi-walled carbon nanotubes (oAuCuNPs-MWCNTs) as a transducer [162]. This investigation demonstrates a general and facile approach to develop robust and durable solid-contact ion-selective electrodes based on nanocomposite as transducing layers to meet the requirements for the clinical and environmental “in-situ” potentiometric detection.

The electrochemical methods for magnesium ( $Mg^{2+}$ ) detection are still under investigation and need more research effort since very low concentrations need to be detected.

Most electrochemical sensors for calcium and magnesium are generally ISEs. Also some research succeeded in investigating both analytes simultaneously, as mentioned in Table 4.

### 3.3. Nitrogen Sensors

The transducer functionalization and modification affect the sensor surface response by improving the output signal, reducing the overpotential of nitrite, enlarging the linear range, and enhancing the sensor characteristics such as the limit of detection and sensitivity and selectivity. Carbon nanomaterials, metal nanoparticles, and conducting polymers have promising physical and chemical characteristics improving the working electrode surface conductivity and the electrocatalytic activity toward the target. Besides, integrating two nanomaterials or more to obtain a hybridized composite can be an alternative sensitive layer for the sensor modification. As a result, the catalytic performance of the composite material is further enhanced because of the synergistic effect. Table 5 shows selected developments in the field of sensitive materials for the functionalization of working electrodes toward the detection of nitrate and nitrite published during the last five years.



**Table 4.** Overview of electrochemical sensors for water hardness ions in water.

Detection Technique	Electrode/Materials	Analyte	LOD ( $\mu\text{M}$ )	Detection Range ( $\mu\text{M}$ )	Comments	Reference
CV, EIS	Screen-printed SPEs/carbon ink	$\text{Ca}^{2+}$	1.0	$10\text{--}10 \times 10^4$	Detection in seawater	[160]
Potentiometric, EIS	Solid-contact ISE (SC-ISEs)	$\text{Ca}^{2+}$	0.6	$1\text{--}10 \times 10^4$	Mineral water and tap water	[162]
Potentiometric	Glassy Carbon Electrode/ $\text{Ca}^{2+}$ -ISM	$\text{Ca}^{2+}$	0.16	0.3–1000	Diluted artificial seawater	[163]
EIS	MWCNTs/PDMS	$\text{Ca}^{2+}$ and $\text{Mg}^{2+}$	-	29.41–5882.35	In water bodies	[164]
EIS Potentiometric	Ionophores ISEs	$\text{Ca}^{2+}$ $\text{Mg}^{2+}$	100 100		In artificial fish-breeding water	[165]
SWASV *	MEMS-Based sensor on top of a silicon wafer	$\text{Ca}^{2+}$ and $\text{Mg}^{2+}$	29.41	294.1–1470.59	-	[166]
Amperometric	On-chip amperometric sensor with ion exchange membrane	$\text{Mg}^{2+}$	5	-	-	[167]

\* SWASV: Square wave anodic stripping voltammetry.

**Table 5.** Sensor for nitrogen ions ( $\text{NO}_3$ ,  $\text{NO}_2$ ).

Detection Principle	Electrode/Materials	Analytes	LOD ( $\mu\text{M}$ )	Dynamic Range ( $\mu\text{M}$ )	Comments	Reference
Chronoamperometry	$\text{Co}_3\text{O}_4/\text{RGO}^*/\text{GCE}^+$	Nitrite	0.14	1–380	Tap water. Recovery: 99.3–101.5%.	[168]
DPV	PEDOT-Gr*/Ta	Nitrite	7	20–2000 M	PBS. (RSD) 50 continuous CV cycles 4.5%.	[169]
DPV	GNPs/graphene/MCE	Nitrite	0.1	0.3–720	Lake water, river water, industrial sewage, and milk. Recovery: 96.0–103%.	[170]
CV *	Nafion/Hb *-Pd-GR */CILE	Nitrite	0.2	40–500	Tap water and Medical facial peel. Recovery: 96.17–101.24%	[171]
SWV	Cu/MWCNT */rGO/GCE	Nitrate Nitrite	0.02 0.03	0.1–75	Tap and mineral waters, sausages, salami, and cheese samples. Recovery: 98.3–102.5%	[172]
Amperometry	PANI@GO/GCE	Nitrite	0.5	0.002–44	Phosphate buffer	[173]
Amperometry	Ferrocene/rGO/SPCE *	Nitrite	0.35	2.5–1450	Spiked mineral water. Recovery: 95% and 101%	[174]
Amperometry	Ag/Cu/MWNT/GCE	Nitrite	0.2	1–1000	Lake water, Drinking water and Seawater. Recovery: 92–105%	[175]
DPV	Au Cu NCNs/GCE	Nitrite	0.2	10–4000	After storing in a refrigerator at 4 °C for 35 days, the peak current responses were still retained 98.60% of the initial values	[176]

Table 5. Cont.

Detection Principle	Electrode/Materials	Analytes	LOD ( $\mu\text{M}$ )	Dynamic Range ( $\mu\text{M}$ )	Comments	Reference
Amperometry	GO-CS-AuNPs/GCE	Nitrite	0.3	0.9–18.9	Phosphate buffer	[177]
Amperometry	AuNPs-Fe <sub>2</sub> O <sub>3</sub> /FTO	Nitrite	0.07	1–1000	Tap and rain water samples	[178]
LSV *	3D lamellar nanocomposite/AgNS*/rGO/ $\beta$ -cyclodextrin/SPCE	Nitrite	0.24	1–2000	Nitrite in spiked pickles.(RSD) = 2.35% (n = 5)	[179]
DPV	Fe <sub>3</sub> O <sub>4</sub> /GO/COOH/GCE	Nitrite	0.37	1–85 and 90–600	Phosphate buffer	[180]
SWV	LIG/f-MWCNT-AuNPs	Nitrite	0.9	10–140	Tap water	[181]
Amperometry	Co <sub>3</sub> O <sub>4</sub> -rGO/CNTs/GCE	Nitrite	0.016	8000–56,000	Recoveries: 95.7–102.2% 83.3% of initial sensitivity after one month storage	[182]
CV *	3D Au-rGO/FTO	Nitrite	-	20.99–5740	Phosphate buffer	[183]
Amperometry	Pt/Ni(OH) <sub>2</sub> /MWCNTs/GCE	Nitrite	0.13	0.4–5670	Milk Recoveries 96–104%	[184]
Amperometry	PANI/CNTs/GCE	Nitrite	1.6	-	PBS RSD 3.4% (n = 9)	[185]
Amperometry	Ni <sub>7</sub> S <sub>6</sub> /MWCNTs/GCE	Nitrite	0.3	1.0–4002	Lake later, Tape and water Pickle water	[186]
DPV	GO-MWCNT-PMA*-Au/GCE	Nitrite	0.67	2–10,000	Water RSD (n = 5) 4%	[187]
DPV	AuNPs-S-Gr/GCE	Nitrite	0.003	12.5–680.92	Water RSD (n = 3) 0.87%	[188]
Amperometry	rGO/Acr paper	Nitrite	0.12	0.40–3600	Milk and water	[189]
DPV	Self-assembled graphene CuNP/AuE	Nitrate	7.98	10–90	Lake water	[190]
Amperometry	CNT/PPy * film electrode with Nitrate reductase	Nitrate	170	440–1450	Nitrate in water	[191]
CV	Cu, Zn (SOD1 *) and nitrate reductase (NaR) coimmobilized on CNT-PPy modified Pt * electrode (NaR-SOD1-CNT-PPy-Pt)	Nitrate Nitrite	0.2 0.05	0.5–10,000 0.0001–1000	Human plasma, whole blood and saliva samples	[192]
CV	Ag-doped zeolite-expanded graphite-epoxy electrode	Nitrate	100	1000–10,000	Spiked tap water	[193]
SWV	Ag dendritic nanostructure on Au microelectrode array	Nitrate Nitrite	2	2–1000	River and lake water	[194]
CV	Cu* nanoclusters, electrodeposited on Pt microelectrode	Nitrate	-	12.5–300	Fresh water	[195]
SWV	Cu microelectrode array	Nitrate	1.8	10–1070	Mineral water	[196]
LSV	Cu nanowire array	Nitrate	1.7–3	10–400	Mineral water	[197]

Table 5. Cont.

Detection Principle	Electrode/Materials	Analytes	LOD ( $\mu\text{M}$ )	Dynamic Range ( $\mu\text{M}$ )	Comments	Reference
DPV	Cu microspheres decorated on polyaniline on microneedle	Nitrate	8	20–6000	Pre-treated river water	[198]
CV	Ag branchlike on Ag or carbon ultramicroelectrodes	Nitrate	3.2–5.1	4–1000	Synthetic aquifer	[199]

\* AgNS: Silver nanostructures, Gr: Graphene, Hb: hemoglobin, GNP: graphene nanoparticles, SPE: Screen printed electrode, PPy: polypyrrole, PMA: 1-pyrenemethylamine, MWCNT: Multi walled carbon nanotubes, NPs: Nanoparticles, RGO: Reduced graphene oxide, GO: Graphene oxide, GCE: Glassy Carbon electrode, NRs: Nanoroads, SOD1: Zinc superoxide dismutase, CV: Cyclic voltammetry, LSV: linear sweep voltammetry.

### 3.3.1. Carbon-Based Materials

Graphene is a crucial promising two-dimensional carbon nanomaterial presenting several advantages; excellent conductivity and catalytic activity [200]. Metal nanoparticles [170,201], can be functionalized together with graphene and used as a sensitive layer for the electrochemical sensor for nitrite and nitrate detection. Wang et al. [190] have developed a screen-printed electrode to detect nitrate in lake water (see Figure 6a). Combining graphene and Cu NPs can improve the sensor response, which presents a limit of detection of  $7.89 \mu\text{M}$ . Xio et al. [201] have developed graphene and chitosan (CS) nanocomposite (see Figure 6b). due to the better conductivity and absorbability of the prepared graphene-based composite. The developed sensor has good reproducibility, a limit of detection of  $0.02 \mu\text{M}$  in the linear concentration range between  $0.2\text{--}1000 \mu\text{M}$  was obtained. Since graphene has limited performance on its own, it is often combined with metamaterials in composite nanomaterials [202].

Carbon nanotubes (CNTs) also is an essential carbon-based material. Due to its superior characteristics, electrical conductivity, empty cylindrical structure, large specific surface area and good electrocatalytic activity, etc. it is considered that the blend of CNTs and metal nanomaterials, for example, the decoration of CNTs by metal nanoparticles, additionally enhances the electrochemical response in the presence of CNTs by accelerating the electron transfer on the electrode surface. Thirumalraj et al. [203] reported on an amperometric electrochemical nitrite sensor using functionalized MWCNT decorated by palladium nanoparticles (PdNPs). The PdNPs were fixed into the carbon nanotubes modified glassy carbon electrode surface by the electrodeposition method. A f-MWCNT/PdNPs composite-based sensor was applied to detect nitrite in water samples. It showed satisfactory results, a detection limit of  $22 \cdot 10^{-3} \mu\text{M}$  and a wide linear range of concentration from  $0.05\text{--}2887.6 \mu\text{M}$ . It also showed long-term stability, good selectivity toward interferences, high reproducibility, and applicability in different real water samples with high accuracy. Another sensor has been reported by Bagheri et al. [172] for the simultaneous monitoring of nitrite and nitrate in the tap and mineral waters, sausages, salami, and cheese samples. The sensor is based on copper nanoparticles decorated multiwalled carbon nanotubes–reduced graphene oxide nanocomposite modified glassy carbon electrode (Cu/MWCNT/RGO/GCE). Under optimized conditions the Cu/MWCNT/RGO/GCE shows a limit of detection of  $30 \cdot 10^{-3} \mu\text{M}$  and  $20 \cdot 10^{-3} \mu\text{M}$  for nitrite and nitrate ions, respectively, in the range from  $0.1\text{--}75 \mu\text{M}$ .

### 3.3.2. Metal Nanomaterial

Metal nanoparticles, such as gold, silver, platinum, palladium, copper, bimetallic and so on, were widely used to fabricate nitrite electrochemical sensors with increased sensitivity according to their excellent catalytic activity and conductivity unique structure and high specific surface area.

Fajerwerger et al. [204] electroreduced nitrate at the surface of a silver nanoparticle (AgNPs)-electrodeposited gold electrode. Chronoamperometry was used to generate the AgNPs. The charge (Q) used here for the electrodeposition of AgNPs is lower than the charge used for the fabrication of the silver monolayer. The proposed sensor AgNPs/gold electrode shows a low limit of detection of 10  $\mu\text{M}$  because of the interaction of two chemical reactions and electron transfer at the linear concentration range from 10–10<sup>3</sup>  $\mu\text{M}$ .

AgNPs were used as sensitive material for detecting nitrate in the investigation of Ghanbari. Silver nanoparticles dispersed in polypyrrole matrixes coated on glassy carbon electrode as a nitrate sensor [205]. The AgNPs were easily synthesized by electrodeposition onto the surface of polypyrrole (PPy) matrixes modified glassy carbon electrode (GCE). The sensor presented an excellent electrocatalytic activity for nitrate reduction, a limit of detection for nitrate of 2.0  $\mu\text{M}$  and a range of concentration from 2 to 100  $\mu\text{M}$ . Also, the sensor showed good real sample results in cheese sausage samples extracted in water and mineral water samples with excellent sensitivity, selectivity, and stability.

Xi et al. [206] reported a nitrite electrochemical sensor by depositing nanocomposites of palladium and platinum (Pd-Pt) on the surface of porous gallium nitride (PGaN). The Pd-Pt/PGaN sensor combination presents an excellent electrocatalytic activity for nitrite monitoring, with a detection limit of 0.95  $\mu\text{M}$  at two different ranges of concentration from 1 to 300  $\mu\text{M}$  and from 300 to 3000  $\mu\text{M}$ .

Mo et al. [177] developed an electrochemical sensor based on Au nanoparticle electrodeposited onto a graphene-chitosan-modified glassy carbon electrode (see Figure 6c). The prepared sensor presents 0.3  $\mu\text{M}$  as detection limit at the range from 0.9  $\mu\text{M}$ –18.9  $\mu\text{M}$ . Due to the high sensitivity of silver nanoparticles toward nitrate ions, Bonyani et al. have proposed silver nanoparticles/polymethacrylic acid nanocomposite (AgNPs/PMA) modified screen-printed electrode AgNPs/PMA/SPCEs [207]. The AgNPs/PMA/SPCEs combination based on silver dendritic structures showed a sensitivity of 130  $\mu\text{A mM}^{-1}\text{ cm}^{-2}$  at the range from 0–20  $\times 10^3$   $\mu\text{M}$ .

It can be concluded that the functionalization of the working electrode with nanostructured metallic materials plays an essential role in enhancing the electrochemical sensing performances and improving the sensor characteristics.

### 3.3.3. Conducting Polymers

Conducting polymers, such as polyacetylene, polypyrrole, polythiophene, polyaniline and their derivatives have received considerable attention for their unique metal and semiconductor-like properties compared with traditional polymers [208]. Due to their favorable mechanical, optical, electrical, and electrochemical characteristics, CPs have been widely used to fabricate sensors, biomedical and microfluidic devices, etc. Polyaniline (PANI) has been presented as a sensitive material toward nitrite and nitrate ions because of its characteristics, including conductivity, environmental stability, etc. Diariso et al. [209] synthesized a nitrite sensor using PANI. The aniline monomer was electropolymerized after the electrodeposition of 4-aminobenzenesulfonic diazonium salt (ABS) on the surface of glassy carbon electrode PANI/ABS/GCE. Furthermore, the PANI/ABS/GCE showed a 23.04  $\mu\text{A } \mu\text{M}^{-1}\text{ cm}^{-2}$  and a detection limit of 0.48  $\mu\text{M}$  at the range of nitrite concentration from 0.5 and 35  $\mu\text{M}$ , therefore good reproducibility. Yi et al. [210] functionalized a glassy carbon electrode using gold nanoparticles multilayered film of poly(3,4-ethylenedioxythiophene) (see Figure 6d). The film at the electrode surface possesses a large electroactive surface area and excellent sensitivity for nitrite detection. The proposed electrode combination PEDOT-SH/Au/GCE showed a response time of 3 s, 0.051  $\mu\text{M}$  as a detection limit at the two linear ranges from 0.15 to 1 mM and from 10<sup>3</sup> to 16  $10^3$   $\mu\text{M}$  with sensitivities 0.301  $\mu\text{A } \mu\text{M}^{-1}\text{ cm}^{-2}$  and 0.133  $\mu\text{A } \mu\text{M}^{-1}\text{ cm}^{-2}$  respectively with good selectivity, stability, and reproducibility.

Polymers can be biocompatible, stable, and conductive and can be combined with several nanomaterials, enhancing their stability and conductivity. Based on the synergetic effect of polymer and other nanomaterials, the electrocatalytic efficiency of nanocomposites

for nitrite and nitrate is improved. As a result, an increase of the concentration range for detection and the amelioration of the sensitivity and selectivity can be obtained.

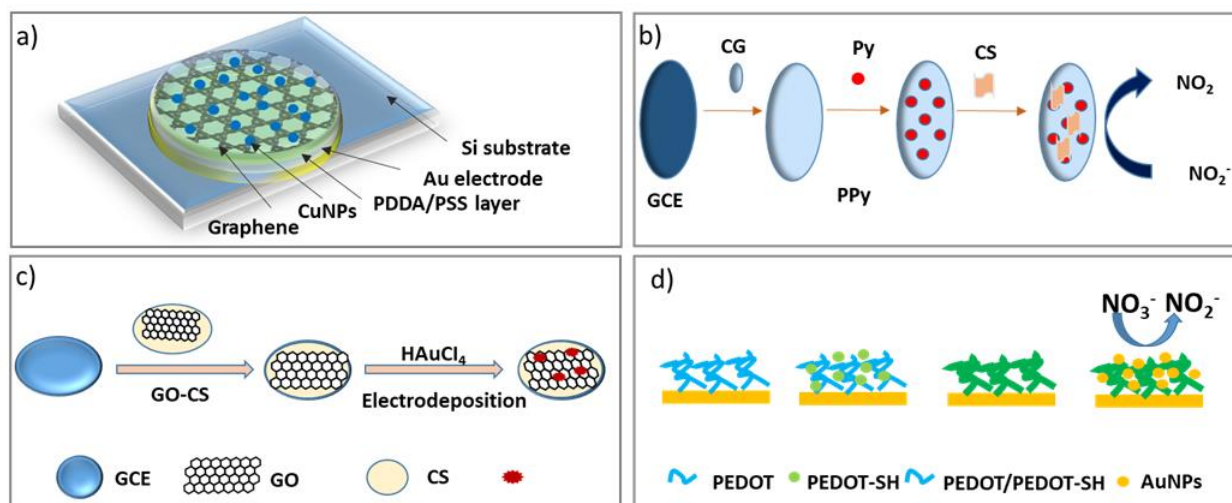


**Figure 6.** Redrawing of (a) self-assembled graphene and copper nanoparticles composite sensor structure following reference [190], (b) fabrication process of CG/PPy/CS/GCE for sensitive detection of  $\text{NO}_2^-$  following reference [201]. (c) the construction process of graphene oxide (GO)-chitosan (CS)-Au nanoparticles (AuNPs)/glassy carbon electrode (GCE) [177] and (d) Growth process of PEDOT/PEDOT-SH/Au on electrode surface [210].

### 3.4. Phosphorus Sensors

Table 6 summarizes the most recent trends in potentiometric and amperometric electrochemical sensors for phosphate detection underlining the new progress in developing nanomaterials and nanocomposites to fulfill the selectivity and sensitivity requirements.

#### 3.4.1. Polymeric Sensors

Nanomaterial-doped conducting polymers are a unique category of composite materials that combine the advantageous properties of both nanomaterials and organic conductors. They have been applied in a wide range of uses, such as electrochemical sensing [211]. In this direction, some polymers showed their excellent role in phosphorus determination. A molybdenum blue-modified poly(vinyl chloride) layer electrodeposited onto a pencil graphite electrode was developed as a novel electrochemical sensor for phosphate determination. The use of polyvinyl chloride as a coating agent for the functionalized electrodes significantly improved the stability (see Figure 7.a). The prepared sensor showed a high sensitivity for phosphate ions with a low LOD and limit of quantification [212]. Also, a chitosan-smectite biocomposite was doped as an electroactive element in a PVC membrane potentiometric sensor for the direct and selective detection of monohydrogen phosphate ions. It exhibited good merits, including high sensitivity and stability, short response time, low detection limit and a broad linear detection range [213]. A gold phosphate electrode has been coated with polyaniline film and phosphate-doped polyaniline as an ion-selective membrane. Polyaniline was chosen based on its better conductivity over other polymers (such as polypyrrole, polythiophene, PVC) because of its low impedance. It achieved an excellent linear detection range and detection limit. High sensitivity and good stability are the major practical advantages of this phosphate sensor with a response time of fewer than 10 s. The drift value of the electrical voltage during 12h of continuous observation was 0.05 mV/h, with a lifetime of over 40 days. Thus, it is appropriate for either one-time or long-term in situ surveillance of industrial water, groundwater, river water, and natural seawater [214].



**Table 6.** Overview about nanomaterials-based sensors for phosphate ion detection.

Method	Electrode/Materials	Analyte	Linear Range ( $\mu\text{M}$ )	LOD ( $\mu\text{M}$ )	Comments	Ref
Voltammetry (DPV)	molybdenum blue modified PVC*/pencil graphite electrode	$\text{K}_2\text{HPO}_4$	-	0.021	Measurement in soil sample	[212]
Potentiometry	Chitosan-clay/PVC	$\text{K}_2\text{HPO}_4$	$1\text{--}10^4$	0.6	-	[213]
Chronoamperometry	Doped PANI*/gold electrode	$\text{KH}_2\text{PO}_4$	$1\text{--}100$	1	Response time < 1 s, electrode lifetime > 40 days in solution	[214]
Potentiometry	Graphene nanocomposite/Co microelectrode	$\text{KH}_2\text{PO}_4$	$0.1\text{--}1$	0.01	Effective measurement in lake water and sediment samples for soluble phosphorus (SPR)	[215]
Chronoamperometry	Carbon black NPs-SPE	$\text{KH}_2\text{PO}_4$	$10^{-8}$	0.1	Drinking, river, aquarium, and waste water samples with satisfactory recovery values, absence of silicate interference, stable sensor (>3 months in a dry condition at RT), for online in-situ analysis.	[216]
I–V measurement	Silver/Graphene Composite/FET*	$\text{PO}_4^{3-}$	$5\text{--}6000$	0.2	Long-term stability, excellent reproducibility, and good selectivity, low-cost and applicable in real water samples	[217]
Amperometry	Paper CB-SPE*	$\text{K}_2\text{HPO}_4$	$10\text{--}300$	4	High reproducibility, long storage stability, reagentless, RSD < 6%	[218]
I–V measurement	Graphene/ionophore hybrid membrane ISFET*	$\text{PO}_4^{3-}$	-	2800	Good performance and selectivity, response time 10 s	[219]
Potentiometry	CuPc* Acrylate-Polymer/Silicon	$\text{K}_2\text{HPO}_4$	$0.001\text{--}10$	0.001	High specificity	[220]
Impedimetry	CuPc/Au electrode	$\text{Na}_2\text{HPO}_4$	$10^{-4}\text{--}1000$	0.00838	-	[221]
Potentiometry	$\text{Zn}^{2+}$ /BPMP- $\text{Cu}^{2+}$ /BPMP*	$\text{K}_2\text{HPO}_4$	$3\text{--}50$	1 0.5	Good selectivity and stability	[222]
Amperometry	Platinum/Au nanowires Arrays	Thiamine pyrophosphate (TPP)	$248\text{--}1456$	45	Good selectivity, storage in citrate buffer at $4^\circ\text{C}$ in refrigerator and measurement every three days showed good stability	[223]
Voltammetry	Silver Nanowires/SPE	$\text{Na}_2\text{HPO}_4$	$5\text{--}1000$	3	Good repeatability and recovery	[224]
Potentiometry	Cobalt NPs-RGO*/GCE*	$\text{KH}_2\text{PO}_4$	$1\text{--}10,000$	-	Measurement in tap and well water samples	[225]
Voltammetry	Graphite SPE	$\text{KH}_2\text{PO}_4$	$0.003\text{--}0.115$	0.02	Dissolved phosphorus sensing in canal water samples	[226]
Potentiometry	ZnO NRs* FET	$\text{PO}_4^{3-}$	$0.1\text{--}7000$	0.05	-	[227]
Amperometry	PyOx*/Au nanowires	$\text{KH}_2\text{PO}_4$	$12.5\text{--}1000$	0.1	Good selectivity, stability > two weeks of repeated use in water samples (recovery of $96.67 \pm 4.9\%$ )	[228]

\* PVC: Polyvinyl chloride, PANI: Polyaniline, CB-SPE: Carbon black screen printed electrodes, FET: Field-effect transistor, ISFET: Ion Sensitive Field Effect Transistor, CuPc: Copper Phthalocyanine, BPMP: 2,6-Bis[bis(2-pyridylmethyl)aminomethyl]-4-methylphenol, NPs: Nanoparticles, RGO: reduced graphene oxide, GCE: Glassy carbon electrode, NRs: Nanorods, PyOx: pyruvate oxidase.

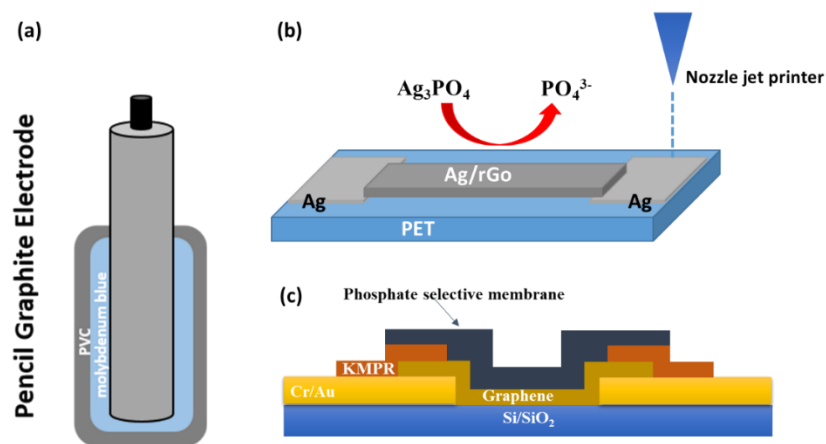


**Figure 7.** Redrawing of (a) Pencil graphite sensor coated with Molybdenum blue functionalized poly(vinyl chloride) following [212], (b) Nozzle-Jet-Printed Silver/Graphene Composite/Field-Effect Transistor Sensor following [212] and (c) ISFET structure with the phosphate selective membrane following [219].

Polymers and especially conductive polymers are therefore nowadays considered suitable sensitive materials for preparing specific, accurate and reliable sensors. Also, the nanostructuring of electrodeposited polymers, as the electrosynthesis of polymeric nanowires or nanotubes, has considerably improved detection performance [212]. In this direction, future research will likely be dedicated to the development of new biosensors based on polymeric materials.

### 3.4.2. Carbon Nanomaterials-Based Sensors

Carbon forms have been widely employed as an electrochemical sensing interface owing to their unique electrochemical properties. Graphene, carbon nanotubes, carbon nanofibers, and carbon dots are widely used in electroanalytical research for their chemical inertness, relatively wide potential window, small background current, and applicability to various types of essays. For example, other electrode materials, such as sputtered metal electrodes, have narrow potential windows and short lifetimes compared to carbon materials [229]. In the area of phosphate electrochemical sensors, carbon nanomaterials are frequently used. A cobalt-decorated graphene nanocomposite sensor has been developed for phosphate detection. The process consists of the electrodeposition of graphene oxide (GO) on a glassy carbon (GCE) electrode, then the electro-reduction to reduced graphene oxide (rGO), and finally, the electrosynthesis of cobalt nanoparticles on the GCE-RGO electrode. The potentiometric response for an acceptable detection range indicated a good linear relationship with the logarithm of the phosphate levels with a slope of  $-31.6$  mV per decade of change in concentration [225]. Moreover, a phosphate sensor was elaborated based on screen-printed electrodes functionalized with carbon black nanoparticles. Amperometric measurements were performed by electrochemical reduction of the corresponding molybdophosphate complex. Carbon black nanoparticles showed the ability of quantification of the molybdophosphate complex at a low applied voltage. Under optimized conditions, a wide linear range was achieved, with a limit of detection of  $0.1$  mM. The device was evaluated in potable water, in rivers, in aquariums and in sewage water samples providing satisfactory recovery results in accordance with a spectrophotometric reference procedure that proved the suitability of this modified carbon black screen-printed electrode coupled with the use of molybdate to measure phosphate in aqueous samples [216]. A FET sensor based on nozzle-jet-printed Ag/rGO-composite on poly(ethylene terephthalate) (PET) substrates (see Figure 7b). An Ag precursor ink and Ag/rGO hybrid ink were used for the good adhesion of printing on the FET sensor. The sensor demonstrated high sensitivity, wide detection linear range and a very low detection limit. Also, it showed long-term stability, good selectivity toward interferences, high reproducibility, and applica-

bility in different real water samples with high accuracy [217]. An ion-sensitive field-effect transistor with a hybrid graphene/ionophore membrane is fabricated (see Figure 7c). As a surrounding condition can easily alter the electrical behavior of the graphene, CVD graphene is chosen as the sensing material. Also, graphene has no selective capability for specific ions, and for that, a phosphate-selective membrane is to be used. The membrane is fabricated by a molecularly imprinted polymer (MIP). The sensor exhibited a detection limit of 1.79  $\mu\text{M}$  and a response time of 10 s [219]. Implementation progress of carbon nanomaterials for electrochemical sensors opens the possibility of reliable, fast, easy, highly sensitive, selective and cost-effective determination of specific contaminants [221].

### 3.4.3. Metal and Metal Complex-Based Sensors

Different metal-complex-based nanomaterials were used in the literature for phosphate sensing. Metallophthalocyanines (MPCs) are gaining more much interest in this direction. Due to their metal centers, MPCs are applied in chemical sensors, particularly for the detection of toxic ions [230]. An impedimetric electrochemical sensor based on new copper phthalocyanine derivative (copper phthalocyanine-C,C,C,C-tetracarboxylic acid-polyacrylamide) modified gold substrates has been elaborated. Under the optimized conditions in terms of polarization and frequency range, the developed sensor provided a large linear range with a very low LOD of  $9.48 \times 10^{-11}$  M and good sensitivity [221]. A capacitance chemical sensor-based silicon nitride substrate ( $\text{AlCu/Si-p/SiO}_2/\text{Si}_3\text{N}_4$ ) functionalized with copper C,C,C,C-tetracarboxylic phthalocyanine-acrylate polymer adduct ( $\text{Cu(II)TCPC-PAA}$ ) was developed for phosphate ions determination. It showed good performance, with a Nernstian sensitivity of 27.7 mV/decade and a low LOD. The developed sensor showed a high selectivity against several interfering ions such as chloride, sulfate, carbonate and perchlorate. Thus, it is considered very promising for sensitive and rapid detection of phosphate [220]. As well as, as phosphate receptors transition metal ions  $\text{Zn}^{2+}$  and  $\text{Cu}^{2+}$ -BPMP-doped in polymeric membranes (BPMB = 2,6-bis(bis(2-pyridylmethyl)aminomethyl)-4-methylphenol) have been also used.  $\text{Zn}^{2+}$  has high phosphate-binding stability, and  $\text{Cu}^{2+}$  has a strong anion binding behavior as their electrical configuration allows high ligand stabilization effects [222]. A properly aligned Pt/Au alloy nanowires network is synthesized and used successfully as a substrate to develop phosphate biosensors. Pyruvate oxidase was immobilized on the nanowire surface with co-factors using a cross-linking approach. As a result, the actual phosphate biosensor has high sensitivity and a wide linear range towards phosphate detection. In addition, it exhibits good selectivity and stability, promising high potential in phosphate detection applications [223].

### 3.5. Disinfectants and Byproducts

Ever since the guidelines were laid down for the DBPs by recognizing health issues, there has been a multitude of research on detecting these compounds in water. Several traditional techniques like gas, liquid and ion chromatography, mass spectroscopy and fluorescence spectroscopy have been used for their detection [231]. However, electrochemical sensors are attractive options because of the ease of use, portability, and cost-efficiency.

Based on carbon material composites, a CNT modified copper electrode with differential voltammetry measurements could detect ammonia with a linear range from 3 to 100  $\mu\text{M}$  and LOD of  $3.47 \times 10^3$   $\mu\text{M}$  [232]. A glassy carbon electrode modified with silver nanoparticles doped chitosan hydrogel film was used to detect trichloroacetic acid. The linear range of operation was 3 to 56  $\mu\text{M}$  with LOD as 1.1  $\mu\text{M}$  using Amperometry [233]. In another work, Titanate nanotubes were self-assembled onto a glassy carbon electrode modified before self-assembly with a chitosan membrane. Thionine was immobilized on the TNT/CTS/GCE surface, acting as an electrochemical probe to detect Trichloroacetic acid by cyclic voltammetry. The linear range of detection obtained was 15  $\mu\text{M}$  to  $1.5 \times 10^3$   $\mu\text{M}$  [234].

Metal-based sensors have been often used for the detection of DBPs by modifying electrodes with metallic particles because of the high catalytic nature of the particles. A pure silver-electrodes-based sensor was used for detecting three DBPs, namely trihalomethanes,

bromoform and chloroform by stripping voltammetry [235]. Detection of brominated trihaloacetic acids based on voltammetry and chemometric analysis on a gold electrode was also demonstrated [236].

A voltammetry-based detection of trichloroacetic acid has been carried out by modifying the carbon ionic liquid-based electrode with palladium-graphene composite and then immobilizing hemoglobin. The electrode response was linear in the range from  $(160 \times 10^{-5}$  to  $130 \times 10^{-5})$   $\mu\text{M}$  and LOD of 500  $\mu\text{M}$  [171]. An amperometric sensor based on a glassy carbon electrode modified with gold and silver nanorods was used for the detection of trichloroacetic acid with a linear range from 0.16  $\mu\text{M}$  to 1.7  $\mu\text{M}$  and LOD of 0.12  $\mu\text{M}$  [237].

Metal-oxide based sensors such as iron oxide ( $\text{Fe}_3\text{O}_4$ )-modified carbon paste electrodes have been utilized to detect chlorite using square wave voltammetry. The LOD achieved was 0.0086  $\mu\text{M}$  [238].  $\text{Fe}_3\text{O}_4$  was again used in another work on glassy carbon electrodes to detect trichloroacetic acid with a linear range from 70 to 205  $\mu\text{M}$  [239]. A nickel oxide modified carbon ionic liquid electrode with hemoglobin immobilized on the electrode could detect trichloroacetic acid with LOD of 500  $\mu\text{M}$  and linear range from 15,000 to  $10 \times 10^3$   $\mu\text{M}$  [240]. In a similar work, the same electrode, but modified with tin oxide, could detect trichloroacetic acid with a LOD of 0.615  $\mu\text{M}$  [241]. Myoglobin-based enzyme immobilization was demonstrated on carbon ionic liquid electrode modified with titanium oxide for the detection of trichloroacetic acid. The linear range achieved was from 5.3 to  $114.3 \times 10^3$   $\mu\text{M}$  [242]. Table 7 provides the list of sensors developed for the detection of various DBPs.

**Table 7.** Electrochemical sensor for the detection of disinfectant in water.

Method	Electrode Modification	Analyte	LOD ( $\mu\text{M}$ )	Linearity ( $\mu\text{M}$ )	Ref
CV	CILE */CTS */Hb */GR-CuS * composite	TCA *	200	$3000\text{--}64 \times 10^3$	[243]
CV	CILE/CTS/Hb/3d GR *	TCA	130	$400\text{--}26 \times 10^3$	[233]
CV	CPE */CdO	TCA	2.3	3–230	[244]
SWV	GCE */Iron pthalocyanine/ZIF-8 *	TCA	$1.89 \times 10^{-3}$		[245]
EIS	GCE/MIP *	NDMA *	0.011	0.13–3.1	[246]
CV	CILE/Nafion/Hb/borondoped graphene quatumdots	TCA, $\text{NaNO}_2$ , $\text{H}_2\text{O}_2$	53	$100\text{--}300 \times 10^3$	[247]
CV	CILE/Nafion/Hb/ZnO-CNF *	TCA and $\text{NaNO}_2$	$1.33 \times 10^3$	$4 \times 10^3\text{--}150 \times 10^3$	[248]
CV	CILE/Nafion/Hb/ $\text{Co}_3\text{O}_4$ -CNF	TCA, $\text{KBrO}_3$ and $\text{NaNO}_2$	$1.33 \times 10^3$	$40 \times 10^3\text{--}260 \times 10^3$	[249]
SWV	GCE/AgNp-Malic acid	TCA	$30 \times 10^{-3}$	01-2 & 4–100	[250]

\* CILE: Carbon ionic liquid electrode, CTS: Chitosan, GR-CuS: graphene-Copper sulfide, 3d GR:3d Graphene, GCE: Glassy carbon electrode, MIP: Molecular imprinted polymer, ZIF-8: Zinc based metal-organic framework, Hb: Haemoglobin, CNF: carbon nanofibers, TCA: Trichloroacetic acid, NDMA: N-Nitrosodimethylamine.

Even though the research on the electrochemical detection of DBPs is significant, it is primarily focused only on detecting major DBPs according to the amount present in water. However, the other DBPs though present in low quantities, is still harmful even at low concentrations. The detection is done using traditional methodologies like colorimetric [251], solid phase extraction, and gas chromatography [252]. The use of redox proteins as a catalyst for detection also has its disadvantages like high fabrication cost, denaturation of the proteins, reliability issues of the sensor. Furthermore, no papers have shown an in-situ application of the sensors. As there is a high chance of forming multiple disinfectant products simultaneously, a careful and systematic study on the selectivity of the sensors is not performed in some of the papers. Hence, there is a dire need to develop electrochemical sensors selective and sensitive to all the DBPs, which are potentially harmful to humans and the environment.

### 3.6. Emergent Contaminant Sensors

Polyphenolic compounds (PCs) have received exceptional attention due to their harmful effect on the human body and the environment. Polyphenols are omnipresent secondary

metabolites in foods [62,253]. They contain phenolic hydroxyl group(s), which are the basis of their antioxidant activity. In general, the reaction of this antioxidant takes place with the loss of one electron in order to get a non-toxic, stable composition unable to propagate the reaction [63]. Antioxidants undergo many interactions in the food matrix, like, preventing fat necrosis and reduce the harmful effects of nitrogen and active oxygen [63]. Several works have been made to introduce sensitive and straightforward methods to evaluate antioxidant capacity (AOC) and quantify polyphenols in food. Table 8 summarizes many sensors for some emergent contaminants.

### 3.6.1. Carbon-Based Materials for Phenolic Compounds Detection

Carbon materials are not only good electronic conductors, cheap, abundant and easy to work with and chemically inert, but also suitable for making composites, as can be already concluded from the previous discussion. Defects and functional groups in carbon materials, inherently present or intentionally introduced, can improve the electrochemical sensor response. Materials traditionally used for the electrochemical detection of phenolic compounds are graphene, carbon nanotubes, carbon black and carbon paste-based hybrid electrodes as an alternative strategy [62].

Undoubtedly, graphene is one of the most important discoveries of the last decade in terms of nanomaterials. This two-dimensional material opened new gates in the electrochemical sensing application. A nanocomposite of graphene/poly (3,4-ethylenedioxythiophene):poly(styrene sulfonate) electrospayed on a modified screen-printed carbon electrode (SPE-GR/PEDOT/PSS) [254]. The nanocomposite elaboration was optimized and characterized physically and electrochemically to improve the active surface area and charge transfer kinetics. The sensor has been used to quantify the antioxidant capacity of 2,2-diphenyl-1-picrylhydrazyl radical (DPPH). The developed electrochemical approach displays a LOD of 0.59  $\mu\text{M}$  at the range from 5 to 30  $\mu\text{M}$ . It was tested in real samples of herbal beverages and Thai herbs and compared with the spectrophotometric method. No variation was obtained between the two methods. A glassy carbon electrode modified with a hybrid material based on chitosan (CS), fishbone-shaped  $\text{Fe}_2\text{O}_3$  and reduced graphene oxide (GCE-GR reduced- $\text{Fe}_2\text{O}_3$ /Chit) was used to quantify gallic acid as a phenolic compound (Figure 8a) and to estimate the antioxidant capacity index of them [255]. The results show excellent linearity of the current versus the log of the concentration at a wide range from 1  $\mu\text{M}$  to 0.1 mM and a LOD of 0.15  $\mu\text{M}$ . The GCE-GR reduced- $\text{Fe}_2\text{O}_3$ /Chit electrode was used to determine polyphenols in wine as a real sample.

Several reports introduce carbon nanotubes as sensitive material for the electrochemical detection of phenolic compounds. A simple electrochemical sensor has been proposed by Lismery et al. [256] to detect gallic-acid based on carbon electrodes (GCE) modified with single-walled carbon nanotubes (SWCNTs). After modifying glassy carbon electrodes with SWCNTs, the results suggest an improvement of anodic current and electron-transfer kinetics due to its superior characteristics. After optimizing DPV measurements, a detection limit of 0.3  $\mu\text{M}$  at the concentration range from 0.5  $\mu\text{M}$  to 15  $\mu\text{M}$  of gallic acid was achieved. Based on the calibration curve of gallic acid, traces of polyphenols were estimated in wine with FC ( $R = 0.980$ ).

**Table 8.** Overview of electrochemical sensors for some emergent contaminants.

Detection Method	Eltrode/Materials	Analyte	LOD ( $\mu\text{M}$ )	Dynamic Range ( $\mu\text{M}$ )	Comments	Reference
Amperometry	GCE-MWCNTs	Gallic acid	0.19	0.66–52.8	Cognac and brandie, sample dilution not required	[257]
SWV	SPE-CB *	Catechol, gallic acid, caffeic acid, and tyrosol	0.1, 1, 0.8, and 2	1–50 1–50 10–100 10–100	Foods and beverages	[258]
DPV	Press-produced CB transducer	Tyrosol Hydroxytyrosol	20 6	10–75 10–75	Olive oil	[259]
DPV	GCE/nano-carbons-AgNPs	Gallic acid	0.063	0.5–8.5	Wine, sample dilution not required	[260]
DPV	GCE-GR/boron doped	Gallic acid	-	-	Tea infusion	[261]
DPV	GCE-GR reduced- $\text{Fe}_2\text{O}_3$ /Chitosan	Gallic acid	0.51	1–0.01	Red/white, wine, sample dilution not required	[255]
Chronoamperometry	SPE-GR/PEDOT/PSS *	Trolox	0.59	5–30	Herbs and herbal beverages	[254]
DPV	$\text{Al}_2\text{O}_3$ /AC-CPE *	Phenol	0.151	10–1000	Natural waters and olive oil	[262]
Amperometry	Nanoporous gold/Si wafer	Catechol	0.5	20–200	PBS	[263]
CV	Platinum-polytyramine composite/graphite substrate	Phenol	-	$3 \times 10^{-2}$ – $10 \times 10^{-3}$	Industrial waste waters	[264]
SWV	Tyr *-AuNPs */SPE	Phenol	1.47	1.47–441	Sensitivity of 15.7 mA ppm <sup>-1</sup> Regional water samples	[265]
Amperometry	Tyr-ZnO nanorods/ Au	Phenol	0.6	0.6–2020–50	Sensitivity of 103.08 $\mu\text{A}/\text{mM}$	[266]
Stripping voltammetry	Nafion-Modified GCE	Phenol	0.001	0.008–10	Water samples	[267]
DPV	HEX-AET *-gold nanoparticles-Glassy Carbon Elecrode	Phenolic estrogens DES DE >BPA > HEX	0.0054 0.0033 0.0043 0.0054	-	Satisfactory linear range and selectivity	[268]
DPV	DNA aptamers/ AuSPE *	17 $\beta$ -estradiol	$5 \times 10^{-7}$ in tap water/ $7 \times 10^{-7}$ in milk	$1.5 \times 10^{-6}$ – $10^{-4}$ / $10^{-4}$ –0.07	Excellent selectivity	[269]



Table 8. Cont.

Detection Method	Eltrode/Materials	Analyte	LOD ( $\mu\text{M}$ )	Dynamic Range ( $\mu\text{M}$ )	Comments	Reference
LSV	MIP */AuNPs/Au	17 $\beta$ -estradiol	$1.09 \times 10^{-9}$	$3.6 \times 10^{-9}$ – $3.6 \times 10^{-3}$	Broad linear range, high sensitivity, selectivity, and reproducibility, simple to fabricate, easy to operate.	[270]
DPV	MWCNTs/THI/AuNPs/SPWE	17 $\beta$ -estradiol	0.0002	$1.79 \times 10^{-7}$ –0.0018	Cost effective, wireless connection with smart phone	[271]
SWCASV	Polished silver solid amalgam electrode	Pyrethroid insecticide (beta-cyfluthrin ( $\beta\text{CF}$ ))	-	$1.2 \times 10^{-6}$ – $3.0 \times 10^{-5}$	Low detection limit with a high level of precision and accuracy	[272]
AdSDPV	SrTiO <sub>3</sub> /N-GNS *	Pharmaceutical compound: Diphenhydramine	0.0021	$0.038$ – $100.0 \times 10^{-6}$	Good recoveries in synthetic pharmaceutical samples and human body fluids, good candidate for real application	[273]
Voltammetry	c-MWCNTs/GCE	BPA	$5.0 \times 10^{-3}$	$(10$ – $104) \times 10^{-3}$	Recovery: 98.4–102.8%.	[274]
LSV	BSA/Anti-BPA/AuNP/MWCNT/GCE	BPA	$8.7 \times 10^{-3}$	0.01–1	Food fresh-keeping film. Recovery: 97.3–103%	[275]
Amperometry	BCNP/Tyr/Nafion/GCE	BPA	$3.18 \times 10^{-3}$	0.02–10	Water samples. Recovery: 96.67–108%.	[276]
DPV	SWCNTs/Poly-IL/GCE	BPA	$10^{-3}$	$5.0 \times 10^{-3}$ –30	Leaching from plastic drinking bottle.	[277]
DPV	Lac/Ag–ZnO/MWCNTs/CSPE	BPA	$6 \times 10^{-3}$	0.5–2.99	High level of precision and accuracy. BPA in plastic bottles.	[278]
Amperometry	Tyr-DAPPT-rGO/GCE	BPA	$3.5 \times 10^{-3}$	$1.0 \times 10^{-3}$ –38	Commercial plastic drinking bottles.	[279]
DPV	MIPPy/GQDs/GCE	BPA	0.04	0.1–50	Tap and sea water samples, with recoveries of 94.5% and 93.7%	[280]
SWV	ZnO/CNT/IL/CPE	BPA	$9 \times 10^{-3}$	0.002–700	Food samples.	[281]

Table 8. Cont.

Detection Method	Electrode/Materials	Analyte	LOD ( $\mu\text{M}$ )	Dynamic Range ( $\mu\text{M}$ )	Comments	Reference
Derivative Voltammetry	MIP/CS/Gr/ABPE	BPA	$6 \times 10^{-3}$	8.0–2.0	Plastic bottled drinking water and canned beverages.	[282]
DPV	AuNP/Gr/GCE	BPA	$5 \times 10^{-3}$	0.01–10	Milk samples with recoveries of 105%.	[283]

\* AuNPs: Gold nanoparticles, AuSPE: Gold screen printed electrode, CPE: Carbon paste electrode, MIP: Molecular imprinted polymer, CSPE: Carbon screen printed electrode, N-GNS: nano-cylindrical strontium titanate N-doped graphene, PEDOT:PSS: Poly(3,4-ethylenedioxythiophene):Polystyrene sulfonate,  $\text{Al}_2\text{O}_3/\text{AC}$ : aluminum oxide supported onto activated carbon, CB: Carbon Black, Tyr-ZnO nanorod: Tyrosinase immobilization on Zinc oxide nanorods, HEX: hexestrol, AET: 2-aminoethanethiol hydrochloride

Another sensor based on MWCNTs has been reported by Arribas et al. [284], who proposed a strategy for quantifying polyphenols in wine. GCE was modified via drop-casting of different nafen or polyethylenimine (PEI) CNTs dispersions. Then various polyphenols were evaluated (gallic acid, caffeic acid, ferulic acid, *p*-coumaric acid), resulting in an improvement of their oxidation on the surface of the MWCNTs modified electrodes. The response was linear for the four model analytes in the concentration range from 0.1  $\mu\text{M}$  to 100  $\mu\text{M}$ , and the limit of detection (LOD) using the two detection potentials was below 0.1  $\mu\text{M}$ .

Li et al. proposed a susceptible sensor to quantify the BPA involving the use of GCE functionalized with COOH-MWCNTs/GCE) [274]. The presence of COOH group at the surface of the MWCNT improves the current oxidation of COOH-MWCNT/GCE compared to the bare GCE and the MWCNT/GCE. At a pH of 7, a sharp oxidation peak was observed at 550 mV in LS voltammograms. In the concentration range from 10 to  $104 \times 10^{-3} \mu\text{M}$ , a linear and a LOD of  $5 \times 10^{-3} \mu\text{M}$  are shown. The sensor has been demonstrated to be suitable for the effective detection of BPA in real samples.

Rather et al. presented an ultrasensitive electrochemical sensor to quantify the BPA based on fullerene [285]. In comparison to GCE, the sensor shows high electrocatalytic activities, lowering anodic overpotential and creating a significant increase in the BPA anodic current, according to their analysis. Rather et al. also calculated a variety of kinetic factors, including electron transfer number ( $n$ ), electrode surface area ( $A$ ), diffusion coefficient ( $D$ ), and charge transfer coefficient ( $\alpha$ ). The oxidation peak current displayed a linear relationship in a concentration range from 0.074 to 0.23  $\mu\text{M}$ , with a LOD of  $0.37 \times 10^{-2} \mu\text{M}$ , under optimal conditions. The sensor performance was validated by detecting BPA in wastewater samples and promising analytical results for identifying BPA at trace levels were registered.

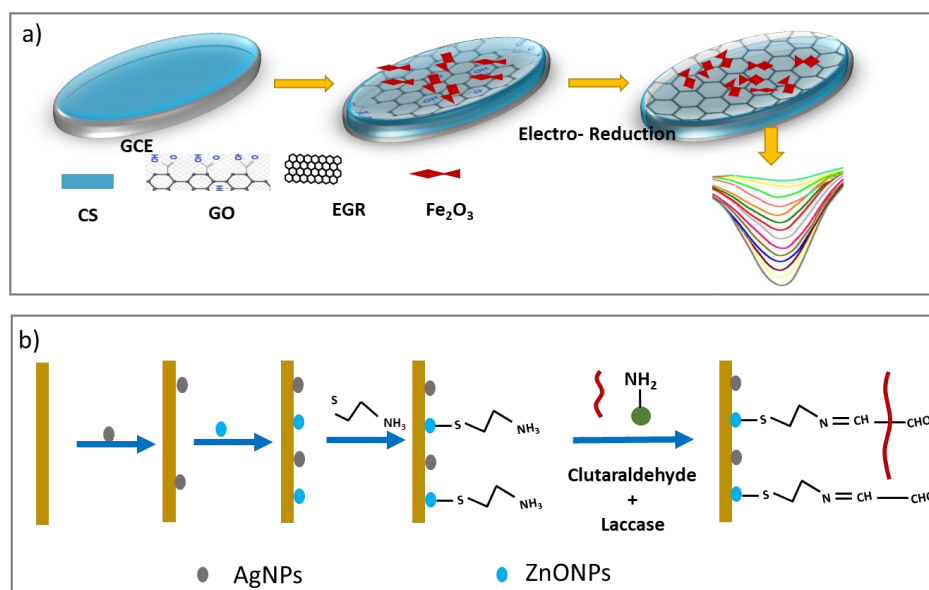


**Figure 8.** Redrawing of (a) GCE-GR reduced- $\text{Fe}_2\text{O}_3$ /Chitosan following reference [255], and (b) Chemical sequence of electro polymerization of AgNPs/ZnONPs onto Au electrode and chemical reaction of immobilization of enzyme onto modified electrode following reference [286].

### 3.6.2. Metallic Nanomaterials

As can be concluded from the previous discussion, metallic nanomaterials possess intrinsic and stable activity making them suitable for the functionalization of different electrodes as a sensitive material to quantify phenolic compounds.

An electrochemical sensor has been developed by Sheetal et al. [286] based on laccase covalently onto nanocomposite of (AgNPs) and (ZnONPs) modified gold (Au) elec-

trode surface using electrodeposition of AgNPs/ZnONPs/Au (see Figure 8b). The AgNPs/ZnONPs/Au electrode was used to detect phenolic compounds in wine samples. The amperometric measurements show a sensitivity of  $0.71 \mu\text{A } \mu\text{M}^{-1} \text{ cm}^{-2}$  for the guaiacol phenol, a limit of detection equal to  $0.05 \mu\text{M}$  and a wide linear range from  $0.1$  to  $500 \mu\text{M}$ .

Another possibility is to employ copper oxide nanoparticles (CuO NPs) as a sensitive layer for detecting phenolic compounds. Pino et al. [287] demonstrated the use of CuO NPs drop-casted onto screen-printed carbon electrodes to detect catechol, phenol, and 4-dichlorophenol with ultra-sensitivity and detection limits of  $0.047 \mu\text{M}$  to  $2.5 \mu\text{M}$  at the range from  $0.5$  to  $2.5 \mu\text{M}$ . In this approach, in the presence of phenols, the oxidation and reduction current of copper decrease due to the formation of a complex between catechol and Co-NPs.

A glassy carbon electrode (GCE) loaded with Ag nanoparticles and polyguanine has been proposed for detecting bisphenol A (BPA) (Ag-PGA) by Hong et al. [288]. The electrode, modified using a simple one-step procedure, has a considerably increased oxidation peak current corresponding to BPA due to its great adsorption capacity, resulting in a larger linear range from  $0.01$  to  $100 \mu\text{M}$ , and a low LOD of  $10^{-3} \mu\text{M}$  ( $S/N = 3$ ). The approach has been successfully validated for water samples.

In another study, Chen et al. succeeded in elaborating nano-dendrites at the surface of GCE by one-step electrodeposition in the presence of a gold precursor  $\text{AuCl}_4^-$  and L-asparagine [289]. The electrodeposited nano-dendrites were functionalized with 4-mercaptobenzoic acid (4-MBA), leading to better catalytic performance and sensitive and selective detection of BPA using DPV. The proposed sensor shows an oxidation current peak at around  $514 \text{ mV}$  BPA, which increases linearly by increasing the BPA concentrations from  $0.05$  to  $55.0 \mu\text{M}$  ( $R_2 = 0.995$ ) and a LOD of  $12 \times 10^{-2} \mu\text{M}$ . Finally, the sensor was utilized to determine trace quantities of BPA in spiked samples and has shown satisfactory results.

### 3.6.3. Polymeric Sensors

Conducting polymers have been hailed as potential electrocatalytic materials with substantial advantages for BPA electrochemical sensors [290]. Several methods have been proposed for the functionalization of the electrode with polymers, such as electrochemical polymerization solvent evaporation, dip and spin coating, radiofrequency plasma discharge, etc. Poly(3,4-ethylenedioxythiophene) (PEDOT) and polyaniline (PANI) are considered essential materials because of their regular and organized chemical structure, as well as high stability and conductivity [291].

Mazzotta et al. examined the electrochemical behavior of BPA over PEDOT-modified GCEs via CV [292]. BPA oxidation generated a BPA polymer (pBPA) with excellent redox activities, with cathodic and anodic peaks at  $0.01$  and  $0.15 \text{ V}$ , respectively. Therefore, they approximated the content of the deposited pBPA by electrochemical and spectroscopic analyses via X-ray photoelectron spectroscopy (XPS). The effects of the scan rate and pH on pBPA film oxidation behaviors have been investigated. According to the studies, the oxidation current has a linear behavior in the range from  $90$  to  $410 \mu\text{M}$ , with a LOD of  $55 \mu\text{M}$ . Consequently, the amperometric BPA determination outputs were gathered with a repetitive potential step program to give a linear response to BPA in a concentration range of  $40$  to  $410 \mu\text{M}$ , with a LOD equal to  $22 \mu\text{M}$  and sensitivity equal to  $1.57 \mu\text{M}^{-1} \text{ cm}^{-2}$ . The sensor exhibited acceptable features of reproducibility and anti-interference, showing a successful application for the detection of BPA in mineral water samples.

Poorahong, et al. proposed a simple and sensitive amperometric sensor to quantify BPA based on polyaniline nanorods and MWCNT in a pencil graphite electrodes [293]. The results show, when compared to the original pencil graphite electrode, the functionalized electrodes had higher electroactivity for BPA oxidation. The sensor shows a linear response to BPA in the  $1.0$  to  $400 \mu\text{M}$  concentration range under optimal experiments and a LOD equal to  $10 \times 10^{-2} \mu\text{M}$ . At  $100 \text{ M}$  of BPA, the modified electrode has a remarkably stable response, allowing for up to 95 injections with a relative standard deviation of  $4.2\%$ . Boiling

water spiked with BPA from four brands of baby bottles yielded recoveries ranging from 86% to 102%.

### 3.6.4. Dihydroxybenzene Isomers

Dihydroxybenzene has three isomers: hydroquinone (HQ), catechol (CC), and resorcinol (RC) (DHB). The DHB is commonly used in industrial manufacturing, and traces of these toxic compounds can be found in the environment, especially in water supplies [294]. The three DHB isomers normally coexist as toxins in environmental water samples. If DHB isomers are released into the atmosphere, they can cause severe health problems [295]. Large amounts of DHB isomers can cause illnesses including kidney failure, tachycardia, cancer, and even death. Since the bare working electrodes have a low oxidation/reduction current reaction of these DHB compounds for the electrochemical sensing methods, it isn't easy to distinguish the two or three DHB isomers. As a result, it is often important to decorate certain nanosized substances to create a new successful functioning electrode. Carbon-based nano-sized materials have been hailed as promising service materials for various applications, including sensors [296]. Table 9 provides an overview of electrochemical sensors for dihydroxybenzene isomers.

**Table 9.** Overview of electrochemical sensors for dihydroxybenzene isomers.

Detection Method	Materials	LOD ( $\mu\text{M}$ ) HQ, CC and RC	Dynamic Range ( $\mu\text{M}$ )	Comments	References
CV	CTAB-GO/MWCNTs/GCE	0.03 0.01 0.2	0.1–200 0.1–400 1–100	Tap water	[297]
DPV	WBC*/Au-850–15/GCE	0.002 0.004 -	0.008–7.0 0.01–7.0 -	Tap	[298]
DPV	MWCNTs@RGONR*/GCE	3.89 1.73 5.77	15–921 15–1101 15–1301	Tap, River	[299]
DPV	CN-F*/GCE	0.5 0.8 0.4	10–120 10–120 10–120	River	[300]
DPV	3D* CNT-Gr/AuNPs/GCE	0.8 0.95 0.1	0.0–80 0.0–80 0.0–80	Tap, River	[301]
DPV	Cu-MOF*-Gr/GCE	0.59 0.33 -	1.0–100 1.0–100 -	Tap water	[302]
DPV	UiO-66/MPC*-3/GCE	0.056 0.072 3.51	0.5–100 0.4–100 30–400	Tap-Lake	[303]
DPV	CNNS*-CNT/GCE	0.13 0.09 -	1–200 1–250 -	Tap	[304]
DPV	Chit*/MWCNTs/Ti <sub>2</sub> /GCE	0.06 0.07 0.52	0.4–276 0.4–159 3.0–657	River, Tap	[305]

\* 3D: Three-dimensional, AuNPs: Gold nanoparticle, Chit: Chitosan, CNNS: Graphitic carbon nitride nanosheets, MOF: Metal-organic framework, MPC: Mesoporous carbon, CN-F: Carbon nano-fragment, RGONR: Reduced graphene oxide nanoribbon, WBC: White myoga ginger-derived biochar.

### (a) Carbon-based hybrid nanocomposites

Experiments have shown that well-aligned hybrid structures of graphene and carbon nanotube can be formed. Their mechanical properties are easily tunable due to their highly tailorable structures hybrid structure of CNT and Gr, one of the most promising carbon derivatives. Carbon nanotubes were sandwiched between graphene sheets that served as spacers and provided diffusion paths for smooth and rapid ion conduction in the CNT-GR composite with a highly porous structure.

For the quantification of trace DHB isomers, Yang and Weikun [297] prepared hybrid MWCNTs in GO-cetyl trimethylammonium bromide (CTAB) composites adjusted GCE by Cyclic voltammetry (CV). CTAB/CNTs are negatively and positively charged, respectively, despite they are not neutral materials. As a result, there could be a close relationship between each surfactant and CNTs. CT, HQ, and RC sensor calibration curves were obtained in the range of 0.1 to 400  $\mu\text{M}$ , 0.1 to 200  $\mu\text{M}$  and 1 to 100. The detection limits were 0.01, 0.03 and 0.1  $\mu\text{M}$  for CT, HQ and RC, respectively. The CTAB-GO/MWNT sensor succeeded in detecting DHB isomers in tap water samples with promising results.

In their work, Yang et al. [299] presented a sensor based on MWCNTs coupled with RGONR modified GCE MWCNT@rGONR/GCE for simultaneous determination of HQ, CC and RC by DPV. The hydrothermal process was used to make the reduced graphene oxide nanoribbon (RGONR) composite in this analysis. For HQ, CC, and RC, the detection limit is calculated to be 0.8  $\mu\text{M}$ , 0.95  $\mu\text{M}$  and 0.1  $\mu\text{M}$  respectively, at the concentration range from 2 to 80  $\mu\text{M}$ . The findings showed that even after a month of storage, the changed electrode retained 95.1% of the original HQ current. In the end, the MWCNT@rGONR/GCE showed a satisfactory result toward the detection of HQ, CC, and RC simultaneously in water samples.

### (b) Carbon material-supported bimetallic composites

Au@Pd nanoparticles can be anchored to the surface of RGO sheets as signal amplifiers, amplifying the catalytic oxidation peak currents. Chen et al. [306] reported the simultaneous quantification of DHB isomers using Au@Pd nanoflower (PdNF)-RGO (Au@PdNF-RGO). The Au@PdNF-RGO-modified GCE produced combined RGO's specific conductivity with the Au@Pd's superior catalytic efficiency. The Au@PdNFs/RGO was deposited onto the GCE using CV in this study. The combination of Au@Pd's outstanding electrocatalytic properties and RGO's excellent conductivity produced excellent results. In contrast to AuNPs/RGO-GCE and RGO/GCE, the updated electrodes showed a high sensitivity for identifying three target isomers with good operation. The LODs of the sensor were 0.5  $\mu\text{M}$ , 0.8  $\mu\text{M}$  and 0.7  $\mu\text{M}$ , respectively for HQ, CC and RC.

Wag et al. [306] also presented a sensor based on a Au@Pd/RGO nanohybrid-modified GCE (Au@Pd/RGO/GCE) detection of HQ and CC with a LODs of 0.01  $\mu\text{M}$  and 0.1  $\mu\text{M}$ , respectively. The electrochemical activity of the Au@Pd/RGO modified electrode was observed to be higher than that of the electrochemically deposited Au@PdNF/RGO at the surface of GCE. As a result, the Au@Pd/RGO composite electrode has a broad electrochemical surface area, which results in high electrocatalytic activity. It thus has an extensive range of concentration, 0.01 to 400  $\mu\text{M}$  for HQ and 0.1 to 400  $\mu\text{M}$  for CC).

### (c) Carbon material-supported conducting polymers

The integration of conductive polymer with CNT or Gr as a composite exhibited a synergistic effect, leading to the augmentation of the electronic and mechanical characteristics of the constituent components [307].

Jiang et al. [308] investigated the electrochemical capability of the poly-tryptophan-functionalized Gr (p-Trp-Gr) toward the oxidation of HQ and CC. The results show that the involvement of Trp has an indole conjugate structure, and it assures the dispersion of Gr via the p-p interactions. Also, in PBS at pH 7.0, Trp on Gr could speed up the electron transfer rate of the isomers and provides a detection limit of 0.221 and 0.086  $\mu\text{M}$  for HQ and CC, respectively.



Song et al. [309] reported a composite based on a poly(diallyl-dimethylammonium chloride) (PDDA)/MWCNTs/Gr-PDDA/MWCNTs/Gr-modified GCE, for simultaneous detection of HQ and CC. PDDA (an ordinary and water-soluble cationic polyelectrolyte) was employed as the covalent cross-linking agent to bind MWCNTs and GR. The electrostatic activity allows the positively charged PDDA colloid to be easily coated on the negatively charged Gr or MWCNTs surfaces in this process. The results revealed that the composite MWCNTs-PDDA-GR successfully presented an enhanced electron transfer and a high electroactivity toward the HQ and CC oxidation. The proposed sensor (PDDA)/MWCNTs/Gr-PDDA/MWCNTs/Gr/GCE showed a range of concentration for both targets HQ and CC from 0.5 to 400  $\mu\text{M}$  with detection limits ( $S/N = 3$ ) of 0.02 and 0.018  $\mu\text{M}$ , respectively and a successful detection in water samples.

### 3.6.5. Further Emergent Contaminants

Most of such substances occur in the environment and are persistent to a longer extent. Common contaminants could be either described as highly persistent and do not biodegrade in the environment such as heavy metals, or persistent and slowly biodegradable, which is the case of numerous pharmaceuticals (e.g., carbamazepine). Also, persistent substances that are water-soluble can get easily into water and chemicals that may not be persistent and can be converted or removed by natural processes.

Improvements in analytical chemistry have made the detection of these pollutants possible, even at trace levels. The scope of this review is to present an overview of the most relevant electrochemical detection sensors of these contaminants, which are summarized in Table 2. An electrochemical immunosensor based on hexestrol (HEX)-2-aminoethanethiol hydrochloride (AET)-gold nanoparticles (Au NPs)-glassy carbon electrode (GCE) was developed for simultaneous determination of four different phenolic estrogens: HEX, diethylstilbestrol (DES), dienestrol (DE) and bisphenol A (BPA).  $\text{DES} > \text{DE} > \text{BPA} > \text{HEX}$  was the amperometric response sequence by differential pulse voltammetry (DPV), with detection limits of 0.0045, 0.0027, 0.0036 and 0.0045  $\mu\text{M}$ , respectively ( $S/N = 3$ ). The results show a good linear range and selectivity and satisfactory accuracy in real samples for DE detection [268].

Long-term exposure to  $17\beta$ -estradiol (E2), at even very low levels, can damage the endocrine system and cause cancer. For that reason different electrochemical sensors based on various nanomaterials have been developed. A simple aptasensor based on split DNA aptamers for E2 was used. When E2 is present, the split aptamers are bound to E2 and form the complex split1-E2-split2 on the electrode surface. The sensor recognizes E2 within 30 min with a wide linear range and detection limits of 0.5 pM and 0.7 pM in tap water and milk, respectively [269]. A label-free integrated microfluidic paper-based analytical device was also fabricated for the detection of  $17\beta$ -E2. Multi-walled carbon nanotubes/thionine/gold nanoparticles (AuNPs) nano composites were synthesized and coated on a screen-printed working electrode (SPWE) to immobilize the anti-E2. The sensor can detect  $17\beta$ -E2 as low as 10 pg/mL with a wide linear range ( $2 \times 10^{-3}$ – $1.79 \mu\text{M}$ ) [271].

For pyrethroid insecticide detection, a polished silver solid amalgam electrode (p-AgSAE) can be used. The proposed sensor was applied in natural water and tea samples and showed high robustness, good stability and sensitivity [272]. A nano-cylindrical strontium titanate/N-doped graphene ( $\text{SrTiO}_3/\text{N-GNS}$ ) hybrid composite-based sensor was reported for simultaneous detection of diphenhydramine (DPH) and bromhexine (BRO). The sensor showed a wide linear range from 0.038 to  $100 \times 10^3 \mu\text{M}$  for DPH and 0.03 to  $90 \times 10^3 \mu\text{M}$  for BRO with detection limits of 2.1 and  $1.9 \times 10^{-3} \mu\text{M}$ , respectively [273].

## 4. Conclusions and Perspectives

This review focuses on electrochemical sensors for pesticides, nitrate, nitrite, phosphate, water hardness, disinfectant, and some emergent contaminants. Within the last five years, most of the reviewed sensors show suitability for real applications from the point of view of sensitivity and interference tests. The combination of electrochemical

sensors with novel nanomaterials enables the efficient detection of several unknown and unquantified contaminants. Functionalization by nanomaterials can be in the form of a composite such as carbon nanomaterial with metallic nanoparticles. Several cases have demonstrated that nanomaterials-based label-free electrochemical sensors can realize a high sensitivity towards specific analytes with excellent selectivity. However, a plethora of research in electrochemical sensors keeps on improving sensor's sensitivity and selectivity.

Nevertheless, electrochemical sensors are generally not specific as some compounds, which can undergo electrochemical transformation within an analysis potential window, can interfere with the analyte under investigation. This could be at the same time advantageous for multiple ions/molecules detection, which can be achieved by simultaneous detection when there is a significant oxidation peak potential separation between the different species. In some cases, several compounds can be detected at the same potential, such as pesticides of the same group.

Electrochemical sensors are primarily demonstrated in a controlled lab environment. Only a few sensors available today are in actual use for on-site or in-situ measurements. This is still challenging because of different requirements of sensor properties, such as repeatability, reproducibility, and stability. The same situation occurs with sensors based on nanomaterials that not often were demonstrated for use in natural water, such as in sea water. Thus, there are a few perspectives and remaining challenges in this field, including:

- A lack of electrochemical sensors for in-situ applications [310].
- Real-time stability and reusability.
- Large-scale and inexpensive fabrication.

Developing efficient strategies to overcome these challenges is required for EC sensors to be commercially competitive for in-situ monitoring. Different types of devices were developed for pesticide detection, trying to overcome the generally poor selectivity of electrochemical methods. This issue arises from the fundamental properties of electrochemical processes. The strategy for resolving it was found in the specific interactions between the sensor and the analyte (pesticide). One of the most promising routes to enhance detection selectivity is biomimetic sensors that reach excellent sensitivity comparable to high-performance liquid chromatography and other advanced chromatographic methods. However, the problem with any sensor relying on specific guest-host interactions is that it can detect only one or a minimal number of analytes. We anticipate further developments in biomimetic sensor arrays combined with machine learning, artificial intelligence, and cloud computing. The combination of EC detection and A.I. with optical spectroscopy such as SERS will allow overcoming fundamental limitations inherent to those detection methods working alone. For example, the quantification capabilities of EC sensors with the label-free selectivity of SERS often gives complex voltammograms and spectra from real-life samples, and machine learning algorithms could help making sense of it all. Nevertheless, forecasting when small and portable solutions for routine on-field applications will become available is an exciting task that still elude us.

**Author Contributions:** Conceptualization, O.K., T.L.-P. & I.P.; writing—original draft preparation, T.L.-P., A.A.-H., S.N., M.T., A.B. & A.A.; writing—review and editing, all authors; funding acquisition, O.K., E.S., T.L.-P. & I.P. All authors have read and agreed to the published version of the manuscript.

**Funding:** This work was carried out within the projects DualSens (project no. KA 1663/13-1) funded by the Deutsche Forschungsgemeinschaft (DFG), Nitramon project (project no. 100339427) funded by the Sächsische Aufbaubank (SAB) and European Social Funds (ESF) and the Nutricon project (project no. 100403339) funded by the Sächsische Aufbaubank (SAB), the project PHOTOSENS (project no. KA 1663/12-1) funded by DFG. ES and RDR thank the Russian Science Foundation, research project number 19-75-10046. T.L.-P. and I.P. thank the Ministry of Education, Science and Technological Development of the Republic of Serbia (Grants no. 451-03-9/2021-14/200017 and 451-03-9/2021-14/200146).

**Conflicts of Interest:** The authors declare no conflict of interest.

## References

1. More Action Needed to Tackle Mixtures of Chemicals in Europe's Waters — European Environment Agency. Available online: <https://www.eea.europa.eu/highlights/more-action-needed-to-tackle> (accessed on 30 March 2021).
2. European Waters Getting Cleaner, but Big Challenges Remain — European Environment Agency. Available online: <https://www.eea.europa.eu/highlights/european-waters-getting-cleaner-but> (accessed on 30 March 2021).
3. Hernandez-Vargas, G.; Sosa-Hernández, J.; Saldarriaga-Hernandez, S.; Villalba-Rodríguez, A.; Parra-Saldivar, R.; Iqbal, H. Electrochemical Biosensors: A Solution to Pollution Detection with Reference to Environmental Contaminants. *Biosensors* **2018**, *8*, 29. [CrossRef] [PubMed]
4. García-Miranda Ferrari, A.; Carrington, P.; Rowley-Neale, S.J.; Banks, C.E. Recent Advances in Portable Heavy Metal Electrochemical Sensing Platforms. *Environ. Sci. Water Res. Technol.* **2020**, *6*, 2676–2690. [CrossRef]
5. Hernández, F.; Bakker, J.; Bijlsma, L.; de Boer, J.; Botero-Coy, A.M.; Bruinen de Bruin, Y.; Fischer, S.; Hollender, J.; Kasprzyk-Hordern, B.; Lamoree, M.; et al. The Role of Analytical Chemistry in Exposure Science: Focus on the Aquatic Environment. *Chemosphere* **2019**, *222*, 564–583. [CrossRef] [PubMed]
6. *Encyclopedia of Applied Electrochemistry*; Kreysa, G.; Ota, K.; Savinell, R.F. (Eds.) Springer: New York, NY, USA, 2014; ISBN 978-1-4419-6995-8.
7. Hanrahan, G.; Patil, D.G.; Wang, J. Electrochemical Sensors for Environmental Monitoring: Design, Development and Applications. *J. Environ. Monitor.* **2004**, *6*, 657. [CrossRef] [PubMed]
8. Kumar, H.; Kumari, N.; Sharma, R. Nanocomposites (Conducting Polymer and Nanoparticles) Based Electrochemical Biosensor for the Detection of Environment Pollutant: Its Issues and Challenges. *Environ. Impact Assess. Rev.* **2020**, *85*, 106438. [CrossRef]
9. Khanmohammadi, A.; Jalili Ghazizadeh, A.; Hashemi, P.; Afkhami, A.; Arduini, F.; Bagheri, H. An Overview to Electrochemical Biosensors and Sensors for the Detection of Environmental Contaminants. *J. Iran. Chem. Soc.* **2020**, *17*, 2429–2447. [CrossRef]
10. Jiang, C.; He, Y.; Liu, Y. Recent Advances in Sensors for Electrochemical Analysis of Nitrate in Food and Environmental Matrices. *Analyst* **2020**, *145*, 5400–5413. [CrossRef]
11. Chen, G.; Wang, X.; Wang, L. Application of Carbon Based Material for the Electrochemical Detection of Heavy Metal Ions in Water Environment. *Int. J. Electrochem. Sci.* **2020**, 4252–4263. [CrossRef]
12. Waheed, A.; Mansha, M.; Ullah, N. Nanomaterials-Based Electrochemical Detection of Heavy Metals in Water: Current Status, Challenges and Future Direction. *Trac. Trends Anal. Chem.* **2018**, *105*, 37–51. [CrossRef]
13. Ramachandran, R.; Chen, T.-W.; Chen, S.-M.; Baskar, T.; Kannan, R.; Elumalai, P.; Raja, P.; Jeyapragasam, T.; Dinakaran, K.; Gnana kumar, G. A Review of the Advanced Developments of Electrochemical Sensors for the Detection of Toxic and Bioactive Molecules. *Inorg. Chem. Front.* **2019**, *6*, 3418–3439. [CrossRef]
14. Wong, A.; Silva, T.; Caetano, F.; Bergamini, M.; Marcolino-Junior, L.; Fatibello-Filho, O.; Janegitz, B. An Overview of Pesticide Monitoring at Environmental Samples Using Carbon Nanotubes-Based Electrochemical Sensors. *C* **2017**, *3*, 8. [CrossRef]
15. Singh, M.; Bhardiya, S.R.; Verma, F.; Rai, V.K.; Rai, A. Graphene-Based Nanomaterials for Fabrication of 'Pesticide' Electrochemical Sensors. *CGS* **2020**, *3*, 26–40. [CrossRef]
16. Noori, J.S.; Mortensen, J.; Geto, A. Recent Development on the Electrochemical Detection of Selected Pesticides: A Focused Review. *Sensors* **2020**, *20*, 2221. [CrossRef]
17. European Waters—Assessment of Status and Pressures 2018—European Environment Agency. Available online: <https://www.eea.europa.eu/publications/state-of-water> (accessed on 30 March 2021).
18. MULHERN, G. Updated Surface Water Watch List Adopted by the Commission. Available online: <https://ec.europa.eu/jrc/en/science-update/updated-surface-water-watch-list-adopted-commission> (accessed on 30 March 2021).
19. EUR-Lex - 32020L2184 - EN - EUR-Lex. Available online: <https://eur-lex.europa.eu/eli/dir/2020/2184/oj> (accessed on 30 March 2021).
20. Guidelines for Drinking-Water Quality, 4th Edition, Incorporating the 1st Addendum. Available online: <https://www.who.int/publications-detail-redirect/9789241549950> (accessed on 30 March 2021).
21. National Primary Drinking Water Regulations | Ground Water and Drinking Water | US EPA. Available online: <https://www.epa.gov/ground-water-and-drinking-water/national-primary-drinking-water-regulations> (accessed on 9 June 2021).
22. Shao, Y.; Chen, Z.; Hollert, H.; Zhou, S.; Deutschmann, B.; Seiler, T.-B. Toxicity of 10 Organic Micropollutants and Their Mixture: Implications for Aquatic Risk Assessment. *Sci. Total Environ.* **2019**, *666*, 1273–1282. [CrossRef]
23. Quesada, H.B.; Baptista, A.T.A.; Cusioli, L.F.; Seibert, D.; de Oliveira Bezerra, C.; Bergamasco, R. Surface Water Pollution by Pharmaceuticals and an Alternative of Removal by Low-Cost Adsorbents: A Review. *Chemosphere* **2019**, *222*, 766–780. [CrossRef]
24. Gruden, R.; Buchholz, A.; Kanoun, O. Electrochemical Analysis of Water and Suds by Impedance Spectroscopy and Cyclic Voltammetry. *J. Sens. Sens. Syst.* **2014**, *3*, 133–140. [CrossRef]
25. Hossain, S.M.Z.; Mansour, N. Biosensors for On-Line Water Quality Monitoring – a Review. *Arab J. Basic Appl. Sci.* **2019**, *26*, 502–518. [CrossRef]
26. Harrison, V.; Mackenzie Ross, S. Anxiety and Depression Following Cumulative Low-Level Exposure to Organophosphate Pesticides. *Environ. Res.* **2016**, *151*, 528–536. [CrossRef]
27. Suarez-Lopez, J.R.; Nguyen, A.; Klas, J.; Gahagan, S.; Checkoway, H.; Lopez-Paredes, D.; Jacobs, D.R.; Noble, M. Associations of Acetylcholinesterase Inhibition Between Pesticide Spray Seasons with Depression and Anxiety Symptoms in Adolescents, and the Role of Sex and Adrenal Hormones on Gender Moderation. *Expo. Health* **2021**, *13*, 51–64. [CrossRef]

28. Panjan, P.; Ohtonen, E.; Tervo, P.; Virtanen, V.; Sesay, A.M. Shelf Life of Enzymatic Electrochemical Sensors. *Procedia Technol.* **2017**, *27*, 306–308. [\[CrossRef\]](#)
29. Panjan, P.; Virtanen, V.; Sesay, A.M. Determination of Stability Characteristics for Electrochemical Biosensors via Thermally Accelerated Ageing. *Talanta* **2017**, *170*, 331–336. [\[CrossRef\]](#) [\[PubMed\]](#)
30. Shinwari, M.W.; Zhitomirsky, D.; Deen, I.A.; Selvaganapathy, P.R.; Deen, M.J.; Landheer, D. Microfabricated Reference Electrodes and Their Biosensing Applications. *Sensors* **2010**, *10*, 1679–1715. [\[CrossRef\]](#) [\[PubMed\]](#)
31. Liu, N.; Xu, Z.; Morrin, A.; Luo, X. Low Fouling Strategies for Electrochemical Biosensors Targeting Disease Biomarkers. *Anal. Methods* **2019**, *11*, 702–711. [\[CrossRef\]](#)
32. Ayyalusamy, S.; Mishra, S.; Suryanarayanan, V. Promising Post-Consumer PET-Derived Activated Carbon Electrode Material for Non-Enzymatic Electrochemical Determination of Carbofuran Hydrolysate. *Sci. Rep.* **2018**, *8*, 13151. [\[CrossRef\]](#)
33. Hord, N.G.; Tang, Y.; Bryan, N.S. Food Sources of Nitrates and Nitrites: The Physiologic Context for Potential Health Benefits. *Am. J. Clin. Nutr.* **2009**, *90*, 1–10. [\[CrossRef\]](#)
34. Swann, P.F. Environmental Carcinogenesis: Contributions of Basic Research: Carcinogenic Risk from Nitrite, Nitrate and N-Nitrosamines in Food. *Proc. R. Soc. Med.* **1977**, *70*, 113–115. [\[CrossRef\]](#)
35. Nasraoui, S.; Al-Hamry, A.; Anurag, A.; Teixeira, P.R.; Ameer, S.; Paterno, L.G.; Ben Ali, M.; Kanoun, O. Investigation of Laser Induced Graphene Electrodes Modified by MWNT/AuNPs for Detection of Nitrite. In Proceedings of the 2019 16th International Multi-Conference on Systems, Signals & Devices (SSD), Istanbul, Turkey, 21–24 March 2019; pp. 615–620.
36. Walters, C.L. The Exposure of Humans to Nitrite. *Oncology* **1980**, *37*, 289–296. [\[CrossRef\]](#)
37. Yue, M.; Wang, R.; Cheng, N.; Cong, R.; Gao, W.; Yang, T. ZnCr2S4: Highly Effective Photocatalyst Converting Nitrate into N<sub>2</sub> without over-Reduction under Both UV and Pure Visible Light. *Sci. Rep.* **2016**, *6*, 30992. [\[CrossRef\]](#)
38. Li, G.; Xia, Y.; Tian, Y.; Wu, Y.; Liu, J.; He, Q.; Chen, D. Review—Recent Developments on Graphene-Based Electrochemical Sensors toward Nitrite. *J. Electrochem. Soc.* **2019**, *166*, B881–B895. [\[CrossRef\]](#)
39. Ryu, H.; Thompson, D.; Huang, Y.; Li, B.; Lei, Y. Electrochemical Sensors for Nitrogen Species: A Review. *Sens. Actuators Rep.* **2020**, *2*, 100022. [\[CrossRef\]](#)
40. Islam, T.; Hasan, M.M.; Awal, A.; Nurunnabi, M.; Ahammad, A.J.S. Metal Nanoparticles for Electrochemical Sensing: Progress and Challenges in the Clinical Transition of Point-of-Care Testing. *Molecules* **2020**, *25*, 5787. [\[CrossRef\]](#)
41. Sarwar, M.; Lechner, J.; Naja, G.M.; Li, C.-Z. Smart-Phone, Paper-Based Fluorescent Sensor for Ultra-Low Inorganic Phosphate Detection in Environmental Samples. *Microsyst. Nanoeng.* **2019**, *5*, 56. [\[CrossRef\]](#)
42. Nag, A.; Alahi, M.E.E.; Feng, S.; Mukhopadhyay, S.C. IoT-Based Sensing System for Phosphate Detection Using Graphite/PDMS Sensors. *Sens. Actuators A Phys.* **2019**, *286*, 43–50. [\[CrossRef\]](#)
43. Richardson, C.J.; King, R.S.; Qian, S.S.; Vaithyanathan, P.; Qualls, R.G.; Stow, C.A. Estimating Ecological Thresholds for Phosphorus in the Everglades. *Environ. Sci. Technol.* **2007**, *41*, 8084–8091. [\[CrossRef\]](#)
44. *Clinical Aspects of Natural and Added Phosphorus in Foods*; Gutiérrez, O.M.; Kalantar-Zadeh, K.; Mehrotra, R. (Eds.) Springer: New York, NY, USA, 2017; ISBN 978-1-4939-6564-9.
45. Forano, C.; Farhat, H.; Mousty, C. Recent Trends in Electrochemical Detection of Phosphate in Actual Waters. *Curr. Opin. Electrochem.* **2018**, *11*, 55–61. [\[CrossRef\]](#)
46. Lerga, T.M.; O'Sullivan, C.K. Rapid Determination of Total Hardness in Water Using Fluorescent Molecular Aptamer Beacon. *Anal. Chim. Acta* **2008**, *610*, 105–111. [\[CrossRef\]](#)
47. Hardness in Drinking-Water: Background Document for Development of WHO Guidelines for Drinking-Water Quality. Available online: <https://apps.who.int/iris/handle/10665/70168> (accessed on 31 March 2021).
48. Zhang, W.; Wang, L.; Yang, Y.; Gaskin, P.; Teng, K.S. Recent Advances on Electrochemical Sensors for the Detection of Organic Disinfection Byproducts in Water. *ACS Sens.* **2019**, *4*, 1138–1150. [\[CrossRef\]](#)
49. Richardson, S.D.; Postigo, C. Drinking Water Disinfection By-products. In *Emerging Organic Contaminants and Human Health*; Barceló, D., Ed.; The Handbook of Environmental Chemistry; Springer: Berlin/Heidelberg, Germany, 2011; Volume 20, pp. 93–137, ISBN 978-3-642-28131-0.
50. Ghernaout, D.; Ghernaout, B. From Chemical Disinfection to Electrod disinfection: The Obligatory Itinerary? *Desalination Water Treat.* **2010**, *16*, 156–175. [\[CrossRef\]](#)
51. Roberts, M.G.; Singer, P.C.; Obolensky, A. Comparing Total HAA and Total THM Concentrations using ICR Data. *J. Am. Water Work. Assoc.* **2002**, *94*, 103–114. [\[CrossRef\]](#)
52. Dai, N.; Zeng, T.; Mitch, W.A. Predicting N-Nitrosamines: N-Nitrosodiethanolamine as a Significant Component of Total N-Nitrosamines in Recycled Wastewater. *Environ. Sci. Technol. Lett.* **2015**, *2*, 54–58. [\[CrossRef\]](#)
53. Parvez, S.; Rivera-Núñez, Z.; Meyer, A.; Wright, J.M. Temporal Variability in Trihalomethane and Haloacetic Acid Concentrations in Massachusetts Public Drinking Water Systems. *Environ. Res.* **2011**, *111*, 499–509. [\[CrossRef\]](#) [\[PubMed\]](#)
54. Emerging Pollutants in Water and Wastewater. Available online: <https://en.unesco.org/emergingpollutantsinwaterandwastewater> (accessed on 9 June 2021).
55. Rasheed, T.; Bilal, M.; Nabeel, F.; Adeel, M.; Iqbal, H.M.N. Environmentally-Related Contaminants of High Concern: Potential Sources and Analytical Modalities for Detection, Quantification, and Treatment. *Environ. Int.* **2019**, *122*, 52–66. [\[CrossRef\]](#)
56. Gogoi, A.; Mazumder, P.; Tyagi, V.K.; Tushara Chaminda, G.G.; An, A.K.; Kumar, M. Occurrence and Fate of Emerging Contaminants in Water Environment: A Review. *Groundw. Sustain. Dev.* **2018**, *6*, 169–180. [\[CrossRef\]](#)



57. Im, J.; Rizzo, C.B.; de Barros, F.P.J. Resilience of Groundwater Systems in the Presence of Bisphenol A under Uncertainty. *Sci. Total Environ.* **2020**, *727*, 138363. [\[CrossRef\]](#)
58. Ana, K.M.S.; Espino, M.P. Occurrence and Distribution of Hormones and Bisphenol A in Laguna Lake, Philippines. *Chemosphere* **2020**, *256*, 127122. [\[CrossRef\]](#)
59. Fonseca, V.F.; Reis-Santos, P.; Duarte, B.; Cabral, H.N.; Caçador, M.I.; Vaz, N.; Dias, J.M.; Pais, M.P. Roving Pharmacies: Modelling the Dispersion of Pharmaceutical Contamination in Estuaries. *Ecol. Indic.* **2020**, *115*, 106437. [\[CrossRef\]](#)
60. Lecomte, S.; Habauzit, D.; Charlier, T.; Pakdel, F. Emerging Estrogenic Pollutants in the Aquatic Environment and Breast Cancer. *Genes* **2017**, *8*, 229. [\[CrossRef\]](#)
61. Lapworth, D.J.; Baran, N.; Stuart, M.E.; Ward, R.S. Emerging Organic Contaminants in Groundwater: A Review of Sources, Fate and Occurrence. *Environ. Pollut.* **2012**, *163*, 287–303. [\[CrossRef\]](#)
62. Flavio Della Pelle; Dario Compagnone Nanomaterial-Based Sensing and Biosensing of Phenolic Compounds and Related Antioxidant Capacity in Food. *Sensors* **2018**, *18*, 462. [\[CrossRef\]](#)
63. Pisoschi, A.M.; Cimpanu, C.; Predoi, G. Electrochemical Methods for Total Antioxidant Capacity and Its Main Contributors Determination: A Review. *Open Chem.* **2015**, *13*. [\[CrossRef\]](#)
64. Yao, D.; Cheng, L.; Wu, Q.; Zhang, G.; Wu, B.; He, Y. Assessment and Prediction of Fishery Water Quality Using Electrochemical Sensor Array Carried by UAV. In Proceedings of the 2019 IEEE International Symposium on Olfaction and Electronic Nose (ISOEN), Fukuoka, Japan, 26–29 May 2019; pp. 1–4.
65. Lezi, N.; Economou, A. Voltammetric Determination of Neonicotinoid Pesticides at Disposable Screen-Printed Sensors Featuring a Sputtered Bismuth Electrode. *Electroanalysis* **2015**, *27*, 2313–2321. [\[CrossRef\]](#)
66. Al-Qasbi, N.; Hameed, A.; Khan, A.N.; Aslam, M.; Ismail, I.M.I.; Soomro, M.T. Mercury Meniscus on Solid Silver Amalgam Electrode as a Sensitive Electrochemical Sensor for Tetrachlorvinphos. *J. Saudi Chem. Soc.* **2018**, *22*, 496–507. [\[CrossRef\]](#)
67. Gajdár, J.; Barek, J.; Fischer, J. Electrochemical Microcell Based on Silver Solid Amalgam Electrode for Voltammetric Determination of Pesticide Difenzoquat. *Sens. Actuators B Chem.* **2019**, *299*, 126931. [\[CrossRef\]](#)
68. Noori, J.; Dimaki, M.; Mortensen, J.; Svendsen, W. Detection of Glyphosate in Drinking Water: A Fast and Direct Detection Method without Sample Pretreatment. *Sensors* **2018**, *18*, 2961. [\[CrossRef\]](#)
69. Balasubramanian, P.; Balamurugan, T.S.T.; Chen, S.-M.; Chen, T.-W.; Sharmila, G.; Yu, M.-C. One-Step Green Synthesis of Colloidal Gold Nano Particles: A Potential Electrocatalyst towards High Sensitive Electrochemical Detection of Methyl Parathion in Food Samples. *J. Taiwan Inst. Chem. Eng.* **2018**, *87*, 83–90. [\[CrossRef\]](#)
70. Gao, X.; Gao, Y.; Bian, C.; Ma, H.; Liu, H. Electroactive Nanoporous Gold Driven Electrochemical Sensor for the Simultaneous Detection of Carbendazim and Methyl Parathion. *Electrochim. Acta* **2019**, *310*, 78–85. [\[CrossRef\]](#)
71. Shams, N.; Lim, H.N.; Hajian, R.; Yusof, N.A.; Abdullah, J.; Sulaiman, Y.; Ibrahim, I.; Huang, N.M. Electrochemical Sensor Based on Gold Nanoparticles/Ethylenediamine-Reduced Graphene Oxide for Trace Determination of Fenitrothion in Water. *RSC Adv.* **2016**, *6*, 89430–89439. [\[CrossRef\]](#)
72. Shams, N.; Lim, H.N.; Hajian, R.; Yusof, N.A.; Abdullah, J.; Sulaiman, Y.; Ibrahim, I.; Huang, N.M.; Pandikumar, A. A Promising Electrochemical Sensor Based on Au Nanoparticles Decorated Reduced Graphene Oxide for Selective Detection of Herbicide Diuron in Natural Waters. *J. Appl. Electrochem.* **2016**, *46*, 655–666. [\[CrossRef\]](#)
73. Rahmani, T.; Bagheri, H.; Behbahani, M.; Hajian, A.; Afkhami, A. Modified 3D Graphene-Au as a Novel Sensing Layer for Direct and Sensitive Electrochemical Determination of Carbaryl Pesticide in Fruit, Vegetable, and Water Samples. *Food Anal. Methods* **2018**, *11*, 3005–3014. [\[CrossRef\]](#)
74. Hou, X.; Liu, X.; Li, Z.; Zhang, J.; Du, G.; Ran, X.; Yang, L. Electrochemical Determination of Methyl Parathion Based on Pillar[5]Arene@AuNPs@reduced Graphene Oxide Hybrid Nanomaterials. *New J. Chem.* **2019**, *43*, 13048–13057. [\[CrossRef\]](#)
75. Mojtaba, N.J.; Tayadon, F.; Bagheri, H. A New Electrochemical Sensor Based on an Au-Pd/Reduced Graphene Oxide Nanocomposite for Determination of Parathion. *Int. J. Environ. Anal. Chem.* **2020**, *100*, 1101–1117. [\[CrossRef\]](#)
76. Dong, J.; Wang, X.; Qiao, F.; Liu, P.; Ai, S. Highly Sensitive Electrochemical Stripping Analysis of Methyl Parathion at MWCNTs–CeO<sub>2</sub>–Au Nanocomposite Modified Electrode. *Sens. Actuators B Chem.* **2013**, *186*, 774–780. [\[CrossRef\]](#)
77. Fu, X.-C.; Zhang, J.; Tao, Y.-Y.; Wu, J.; Xie, C.-G.; Kong, L.-T. Three-Dimensional Mono-6-Thio- $\beta$ -Cyclodextrin Covalently Functionalized Gold Nanoparticle/Single-Wall Carbon Nanotube Hybrids for Highly Sensitive and Selective Electrochemical Determination of Methyl Parathion. *Electrochim. Acta* **2015**, *153*, 12–18. [\[CrossRef\]](#)
78. Abbaci, A.; Azzouz, N.; Bouznit, Y. Development and Validation of a New Sensor for Methomyl Detection. *Anal. Methods* **2013**, *5*, 3663. [\[CrossRef\]](#)
79. Rathnakumar, S.S.; Noluthando, K.; Kulandaiswamy, A.J.; Rayappan, J.B.B.; Kasinathan, K.; Kennedy, J.; Maaza, M. Stalling Behaviour of Chloride Ions: A Non-Enzymatic Electrochemical Detection of  $\alpha$ -Endosulfan Using CuO Interface. *Sens. Actuators B Chem.* **2019**, *293*, 100–106. [\[CrossRef\]](#)
80. Ghodsi, J.; Rafati, A.A. A Voltammetric Sensor for Diazinon Pesticide Based on Electrode Modified with TiO<sub>2</sub> Nanoparticles Covered Multi Walled Carbon Nanotube Nanocomposite. *J. Electroanal. Chem.* **2017**, *807*, 1–9. [\[CrossRef\]](#)
81. Tian, X.; Liu, L.; Li, Y.; Yang, C.; Zhou, Z.; Nie, Y.; Wang, Y. Nonenzymatic Electrochemical Sensor Based on CuO-TiO<sub>2</sub> for Sensitive and Selective Detection of Methyl Parathion Pesticide in Ground Water. *Sens. Actuators B Chem.* **2018**, *256*, 135–142. [\[CrossRef\]](#)

82. Khairy, M.; Ayoub, H.A.; Banks, C.E. Non-Enzymatic Electrochemical Platform for Parathion Pesticide Sensing Based on Nanometer-Sized Nickel Oxide Modified Screen-Printed Electrodes. *Food Chem.* **2018**, *255*, 104–111. [\[CrossRef\]](#)
83. Ensafi, A.A.; Noroozi, R.; Zandi—Atashbar, N.; Rezaei, B. Cerium(IV) Oxide Decorated on Reduced Graphene Oxide, a Selective and Sensitive Electrochemical Sensor for Fenitrothion Determination. *Sens. Actuators B Chem.* **2017**, *245*, 980–987. [\[CrossRef\]](#)
84. Sahoo, D.; Mandal, A.; Mitra, T.; Chakraborty, K.; Bardhan, M.; Dasgupta, A.K. Nanosensing of Pesticides by Zinc Oxide Quantum Dot: An Optical and Electrochemical Approach for the Detection of Pesticides in Water. *J. Agric. Food Chem.* **2018**, *66*, 414–423. [\[CrossRef\]](#)
85. Karthik, R.; Kumar, J.V.; Chen, S.-M.; Kokulnathan, T.; Chen, T.-W.; Sakthinathan, S.; Chiu, T.-W.; Muthuraj, V. Development of Novel 3D Flower-like Praseodymium Molybdate Decorated Reduced Graphene Oxide: An Efficient and Selective Electrocatalyst for the Detection of Acetylcholinesterase Inhibitor Methyl Parathion. *Sens. Actuators B Chem.* **2018**, *270*, 353–361. [\[CrossRef\]](#)
86. Yue, Y.; Jiang, L.; Li, Z.; Yuan, J.; Shi, H.; Feng, S. A Glassy Carbon Electrode Modified with a Monolayer of Zirconium(IV) Phosphonate for Sensing of Methyl-Parathion by Square Wave Voltammetry. *Microchim. Acta* **2019**, *186*, 433. [\[CrossRef\]](#) [\[PubMed\]](#)
87. de Oliveira, R.C.; Sousa, C.P.; Freire, T.M.; Freire, R.M.; Denardin, J.C.; Fehine, P.B.A.; Becker, H.; Morais, S.; de Lima-Neto, P.; Correia, A.N. Chitosan-Magnetite Nanocomposite as a Sensing Platform to Bendiocarb Determination. *Anal. Bioanal. Chem.* **2018**, *410*, 7229–7238. [\[CrossRef\]](#) [\[PubMed\]](#)
88. Li, Q.; Xia, Y.; Wan, X.; Yang, S.; Cai, Z.; Ye, Y.; Li, G. Morphology-Dependent MnO<sub>2</sub>/Nitrogen-Doped Graphene Nanocomposites for Simultaneous Detection of Trace Dopamine and Uric Acid. *Mater. Sci. Eng. C* **2020**, *109*, 110615. [\[CrossRef\]](#)
89. Cozzarini, L.; Bertolini, G.; Šuran-Brunelli, S.T.; Radivo, A.; Bracamonte, M.V.; Tavagnacco, C.; Goldoni, A. Metal Decorated Carbon Nanotubes for Electrocatalytic Water Splitting. *Int. J. Hydrog. Energy* **2017**, *42*, 18763–18773. [\[CrossRef\]](#)
90. Pedrosa, V.A.; Miwa, D.; Machado, S.A.S.; Avaca, L.A. On the Utilization of Boron Doped Diamond Electrode as a Sensor for Parathion and as an Anode for Electrochemical Combustion of Parathion. *Electroanalysis* **2006**, *18*, 1590–1597. [\[CrossRef\]](#)
91. Švorc, L.; Rievaj, M.; Bustin, D. Green Electrochemical Sensor for Environmental Monitoring of Pesticides: Determination of Atrazine in River Waters Using a Boron-Doped Diamond Electrode. *Sens. Actuators B Chem.* **2013**, *181*, 294–300. [\[CrossRef\]](#)
92. Costa, D.J.E.; Santos, J.C.S.; Sanches-Brandão, F.A.C.; Ribeiro, W.F.; Salazar-Banda, G.R.; Araujo, M.C.U. Boron-Doped Diamond Electrode Acting as a Voltammetric Sensor for the Detection of Methomyl Pesticide. *J. Electroanal. Chem.* **2017**, *789*, 100–107. [\[CrossRef\]](#)
93. Majidi, M.R.; Asadpour-Zeynali, K.; Nazarpur, M. Determination of Fenitrothion in River Water and Commercial Formulations by Adsorptive Stripping Voltammetry with a Carbon Ceramic Electrode. *J. AOAC Int.* **2009**, *92*, 548–554. [\[CrossRef\]](#)
94. Okumura, L.L.; Saczk, A.A.; de Oliveira, M.F.; de Fulgêncio, A.C.C.; Torrezani, L.; Gomes, P.E.N.; Peixoto, R.M. Electrochemical Feasibility Study of Methyl Parathion Determination on Graphite-Modified Basal Plane Pyrolytic Graphite Electrode. *J. Braz. Chem. Soc.* **2011**, *22*, 652–659. [\[CrossRef\]](#)
95. Amare, M.; Abicho, S.; Admassie, S. Determination of Fenitrothion in Water Using a Voltammetric Sensor Based on a Polymer-Modified Glassy Carbon Electrode. *J. AOAC Int.* **2014**, *97*, 580–585. [\[CrossRef\]](#)
96. Deroco, P.B.; Lourencao, B.C.; Fatibello-Filho, O. The Use of Modified Electrode with Carbon Black as Sensor to the Electrochemical Studies and Voltammetric Determination of Pesticide Mesotrione. *Microchem. J.* **2017**, *133*, 188–194. [\[CrossRef\]](#)
97. Bolat, G.; Abaci, S.; Vural, T.; Bozdogan, B.; Denkbaz, E.B. Sensitive Electrochemical Detection of Fenitrothion Pesticide Based on Self-Assembled Peptide-Nanotubes Modified Disposable Pencil Graphite Electrode. *J. Electroanal. Chem.* **2018**, *809*, 88–95. [\[CrossRef\]](#)
98. Itkes, M.P.M.; de Oliveira, G.G.; Silva, T.A.; Fatibello-Filho, O.; Janegitz, B.C. Voltammetric Sensing of Fenitrothion in Natural Water and Orange Juice Samples Using a Single-Walled Carbon Nanohorns and Zein Modified Sensor. *J. Electroanal. Chem.* **2019**, *840*, 21–26. [\[CrossRef\]](#)
99. Geto, A.; Noori, J.S.; Mortensen, J.; Svendsen, W.E.; Dimaki, M. Electrochemical Determination of Bentazone Using Simple Screen-Printed Carbon Electrodes. *Environ. Int.* **2019**, *129*, 400–407. [\[CrossRef\]](#)
100. Zeng, Y.; Yu, D.; Yu, Y.; Zhou, T.; Shi, G. Differential Pulse Voltammetric Determination of Methyl Parathion Based on Multiwalled Carbon Nanotubes–Poly(Acrylamide) Nanocomposite Film Modified Electrode. *J. Hazard. Mater.* **2012**, *217–218*, 315–322. [\[CrossRef\]](#)
101. Noyrod, P.; Chailapakul, O.; Wonsawat, W.; Chuanuwatanakul, S. The Simultaneous Determination of Isoproturon and Carben-dazim Pesticides by Single Drop Analysis Using a Graphene-Based Electrochemical Sensor. *J. Electroanal. Chem.* **2014**, *719*, 54–59. [\[CrossRef\]](#)
102. Dong, J.; Hou, J.; Jiang, J.; Ai, S. Innovative Approach for the Electrochemical Detection of Non-Electroactive Organophosphorus Pesticides Using Oxime as Electroactive Probe. *Anal. Chim. Acta* **2015**, *885*, 92–97. [\[CrossRef\]](#)
103. Ma, H.; Wang, L.; Liu, Z.; Guo, Y. Ionic Liquid–Graphene Hybrid Nanosheets-Based Electrochemical Sensor for Sensitive Detection of Methyl Parathion. *Int. J. Environ. Anal. Chem.* **2016**, *96*, 161–172. [\[CrossRef\]](#)
104. Wei, P.; Gan, T.; Wu, K. N-Methyl-2-Pyrrolidone Exfoliated Graphene as Highly Sensitive Analytical Platform for Carbendazim. *Sens. Actuators B Chem.* **2018**, *274*, 551–559. [\[CrossRef\]](#)
105. Tan, X.; Liu, Y.; Zhang, T.; Luo, S.; Liu, X.; Tian, H.; Yang, Y.; Chen, C. Ultrasensitive Electrochemical Detection of Methyl Parathion Pesticide Based on Cationic Water-Soluble Pillar[5]Arene and Reduced Graphene Nanocomposite. *RSC Adv.* **2019**, *9*, 345–353. [\[CrossRef\]](#)



106. Velusamy, V.; Palanisamy, S.; Chen, S.-W.; Balu, S.; Yang, T.C.K.; Banks, C.E. Novel Electrochemical Synthesis of Cellulose Microfiber Entrapped Reduced Graphene Oxide: A Sensitive Electrochemical Assay for Detection of Fenitrothion Organophosphorus Pesticide. *Talanta* **2019**, *192*, 471–477. [[CrossRef](#)] [[PubMed](#)]
107. Masibi, K.K.; Fayemi, O.E.; Adekunle, A.S.; Al-Mohaimeed, A.M.; Fahim, A.M.; Mamba, B.B.; Ebenso, E.E. Electrochemical Detection of Endosulfan Using an AONP-PANI-SWCNT Modified Glassy Carbon Electrode. *Materials* **2021**, *14*, 723. [[CrossRef](#)] [[PubMed](#)]
108. Sun, G.; Wang, P.; Ge, S.; Ge, L.; Yu, J.; Yan, M. Photoelectrochemical Sensor for Pentachlorophenol on Microfluidic Paper-Based Analytical Device Based on the Molecular Imprinting Technique. *Biosens. Bioelectron.* **2014**, *56*, 97–103. [[CrossRef](#)]
109. Xie, C.; Gao, S.; Guo, Q.; Xu, K. Electrochemical Sensor for 2,4-Dichlorophenoxy Acetic Acid Using Molecularly Imprinted Polypyrrole Membrane as Recognition Element. *Microchim. Acta* **2010**, *169*, 145–152. [[CrossRef](#)]
110. Shi, H.; Zhao, G.; Liu, M.; Zhu, Z. A Novel Photoelectrochemical Sensor Based on Molecularly Imprinted Polymer Modified TiO<sub>2</sub> Nanotubes and Its Highly Selective Detection of 2,4-Dichlorophenoxyacetic Acid. *Electrochem. Commun.* **2011**, *13*, 1404–1407. [[CrossRef](#)]
111. Li, H.; Wang, Z.; Wu, B.; Liu, X.; Xue, Z.; Lu, X. Rapid and Sensitive Detection of Methyl-Parathion Pesticide with an Electropolymerized, Molecularly Imprinted Polymer Capacitive Sensor. *Electrochim. Acta* **2012**, *62*, 319–326. [[CrossRef](#)]
112. Bakas, I.; Hayat, A.; Piletsky, S.; Piletska, E.; Chehimi, M.M.; Noguer, T.; Rouillon, R. Electrochemical Impedimetric Sensor Based on Molecularly Imprinted Polymers/Sol–Gel Chemistry for Methidathion Organophosphorous Insecticide Recognition. *Talanta* **2014**, *130*, 294–298. [[CrossRef](#)]
113. Motaharian, A.; Motaharian, F.; Abnous, K.; Hosseini, M.R.M.; Hassanzadeh-Khayyat, M. Molecularly Imprinted Polymer Nanoparticles-Based Electrochemical Sensor for Determination of Diazinon Pesticide in Well Water and Apple Fruit Samples. *Anal. Bioanal. Chem.* **2016**, *408*, 6769–6779. [[CrossRef](#)]
114. Bow, Y.; Sutriyono, E.; Nasir, S.; Iskandar, I. Molecularly Imprinted Polymers (MIP) Based Electrochemical Sensor for Detection of Endosulfan Pesticide. *Int. J. Adv. Sci. Eng. Inf. Technol.* **2017**, *7*, 662–668. [[CrossRef](#)]
115. Khadem, M.; Faridbod, F.; Norouzi, P.; Rahimi Foroushani, A.; Ganjali, M.R.; Shahtaheri, S.J.; Yarahmadi, R. Modification of Carbon Paste Electrode Based on Molecularly Imprinted Polymer for Electrochemical Determination of Diazinon in Biological and Environmental Samples. *Electroanalysis* **2017**, *29*, 708–715. [[CrossRef](#)]
116. Shahtaheri, S.J.; Faridbod, F.; Khadem, M. Highly Selective Voltammetric Sensor Based on Molecularly Imprinted Polymer and Carbon Nanotubes to Determine the Dicloran Pesticide in Biological and Environmental Samples. *Procedia Technol.* **2017**, *27*, 96–97. [[CrossRef](#)]
117. Ahmad, A.L.; Lah, N.F.C.; Low, S.C. Configuration of Molecular Imprinted Polymer for Electrochemical Atrazine Detection. *J. Polym. Res.* **2018**, *25*, 243. [[CrossRef](#)]
118. Khalifa, M.E.; Abdallah, A.B. Molecular Imprinted Polymer Based Sensor for Recognition and Determination of Profenofos Organophosphorous Insecticide. *Biosens. Bioelectron. X* **2019**, *2*, 100027. [[CrossRef](#)]
119. Aghoutane, Y.; Diouf, A.; Österlund, L.; Bouchikhi, B.; El Bari, N. Development of a Molecularly Imprinted Polymer Electrochemical Sensor and Its Application for Sensitive Detection and Determination of Malathion in Olive Fruits and Oils. *Bioelectrochemistry* **2020**, *132*, 107404. [[CrossRef](#)]
120. Durand, P.; Thomas, D. Use of Immobilized Enzyme Coupled with an Electrochemical Sensor for the Detection of Organophosphates and Carbamates Pesticides. *J. Environ. Pathol. Toxicol. Oncol.* **1984**, *5*, 51–57.
121. Palleschi, G.; Bernabei, M.; Cremisini, C.; Mascini, M. Determination of Organophosphorus Insecticides with a Choline Electrochemical Biosensor. *Sens. Actuators B Chem.* **1992**, *7*, 513–517. [[CrossRef](#)]
122. Hassani, S.; Momtaz, S.; Vakhshiteh, F.; Maghsoudi, A.S.; Ganjali, M.R.; Norouzi, P.; Abdollahi, M. Biosensors and Their Applications in Detection of Organophosphorus Pesticides in the Environment. *Arch. Toxicol.* **2017**, *91*, 109–130. [[CrossRef](#)]
123. Chauhan, N.; Pundir, C.S. An Amperometric Acetylcholinesterase Sensor Based on Fe<sub>3</sub>O<sub>4</sub> Nanoparticle/Multi-Walled Carbon Nanotube-Modified ITO-Coated Glass Plate for the Detection of Pesticides. *Electrochim. Acta* **2012**, *67*, 79–86. [[CrossRef](#)]
124. Kaur, B.; Srivastava, R.; Satpati, B. Nanocrystalline Titanosilicate-Acetylcholinesterase Electrochemical Biosensor for the Ultra-Trace Detection of Toxic Organophosphate Pesticides. *ChemElectroChem* **2015**, *2*, 1164–1173. [[CrossRef](#)]
125. Chauhan, N.; Narang, J.; Jain, U. Amperometric Acetylcholinesterase Biosensor for Pesticides Monitoring Utilising Iron Oxide Nanoparticles and Poly(Indole-5-Carboxylic Acid). *J. Exp. Nanosci.* **2016**, *11*, 111–122. [[CrossRef](#)]
126. Dong, P.; Jiang, B.; Zheng, J. A Novel Acetylcholinesterase Biosensor Based on Gold Nanoparticles Obtained by Electroless Plating on Three-Dimensional Graphene for Detecting Organophosphorus Pesticides in Water and Vegetable Samples. *Anal. Methods* **2019**, *11*, 2428–2434. [[CrossRef](#)]
127. Gangadhara Reddy, K.; Madhavi, G.; Kumara Swamy, B.E. Mobilized Lipase Enzymatic Biosensor for the Determination of Chlorfenvinphos and Malathion in Contaminated Water Samples: A Voltammetric Study. *J. Mol. Liq.* **2014**, *198*, 181–186. [[CrossRef](#)]
128. Alves, M. de F.; Corrêa, R.A.M. de S.; da Cruz, F.S.; Franco, D.L.; Ferreira, L.F. Electrochemical Enzymatic Fenitrothion Sensor Based on a Tyrosinase/Poly(2-Hydroxybenzamide)-Modified Graphite Electrode. *Anal. Biochem.* **2018**, *553*, 15–23. [[CrossRef](#)]
129. Malvano, F.; Albanese, D.; Pilloton, R.; Di Matteo, M.; Crescitelli, A. A New Label-Free Impedimetric Affinity Sensor Based on Cholinesterases for Detection of Organophosphorous and Carbamic Pesticides in Food Samples: Impedimetric Versus Amperometric Detection. *Food Bioprocess. Technol.* **2017**, *10*, 1834–1843. [[CrossRef](#)]

130. Mulchandani, A.; Mulchandani, P.; Chen, W.; Wang, J.; Chen, L. Amperometric Thick-Film Strip Electrodes for Monitoring Organophosphate Nerve Agents Based on Immobilized Organophosphorus Hydrolase. *Anal. Chem.* **1999**, *71*, 2246–2249. [\[CrossRef\]](#)
131. Crew, A.; Lonsdale, D.; Byrd, N.; Pittson, R.; Hart, J.P. A Screen-Printed, Amperometric Biosensor Array Incorporated into a Novel Automated System for the Simultaneous Determination of Organophosphate Pesticides. *Biosens. Bioelectron.* **2011**, *26*, 2847–2851. [\[CrossRef\]](#) [\[PubMed\]](#)
132. Laothanachareon, T.; Champreda, V.; Sritongkham, P.; Somasundrum, M.; Surareungchai, W. Cross-Linked Enzyme Crystals of Organophosphate Hydrolase for Electrochemical Detection of Organophosphorus Compounds. *World J. Microbiol. Biotechnol.* **2008**, *24*, 3049–3055. [\[CrossRef\]](#)
133. Beleno Cabarcas, M.T.; Stoytcheva, M.; Zlatev, R.; Montero, G.; Velkova, Z.; Gochev, V. Chitosan Nanocomposite Modified OPH-Based Amperometric Sensor for Organophosphorus Pesticides Determination. *CAC* **2018**, *14*. [\[CrossRef\]](#)
134. Deng, A.-P.; Yang, H. A Multichannel Electrochemical Detector Coupled with an ELISA Microtiter Plate for the Immunoassay of 2,4-Dichlorophenoxyacetic Acid. *Sens. Actuators B Chem.* **2007**, *124*, 202–208. [\[CrossRef\]](#)
135. Bauer, C.G.; Eremenko, A.V.; Ehrentreich-Förster, E.; Bier, F.F.; Makower, A.; Halsall, H.B.; Heineman, W.R.; Scheller, F.W. Zeptomole-Detecting Biosensor for Alkaline Phosphatase in an Electrochemical Immunoassay for 2,4-Dichlorophenoxyacetic Acid. *Anal. Chem.* **1996**, *68*, 2453–2458. [\[CrossRef\]](#) [\[PubMed\]](#)
136. Dzantiev, B.B.; Zherdev, A.V.; Yulaev, M.F.; Sittikov, R.A.; Dmitrieva, N.M.; Moreva, I.Y. Electrochemical Immunosensors for Determination of the Pesticides 2,4-Dichlorophenoxyacetic and 2,4,5-Trichlorophenoxyacetic Acids. *Biosens. Bioelectron.* **1996**, *11*, 179–185. [\[CrossRef\]](#)
137. Hleli, S.; Martelet, C.; Abdelghani, A.; Burais, N.; Jaffrezic-Renault, N. Atrazine Analysis Using an Impedimetric Immunosensor Based on Mixed Biotinylated Self-Assembled Monolayer. *Sens. Actuators B Chem.* **2006**, *113*, 711–717. [\[CrossRef\]](#)
138. Bhardwaj, S.K.; Sharma, A.L.; Kim, K.-H.; Deep, A. Antibody Conjugated Glycine Doped Polyaniline Nanofilms as Efficient Biosensor for Atrazine. *Mater. Res. Express* **2017**, *4*, 125022. [\[CrossRef\]](#)
139. Mehta, J.; Vinayak, P.; Tuteja, S.K.; Chhabra, V.A.; Bhardwaj, N.; Paul, A.K.; Kim, K.-H.; Deep, A. Graphene Modified Screen Printed Immunosensor for Highly Sensitive Detection of Parathion. *Biosens. Bioelectron.* **2016**, *83*, 339–346. [\[CrossRef\]](#)
140. Mehta, J.; Bhardwaj, N.; Bhardwaj, S.K.; Tuteja, S.K.; Vinayak, P.; Paul, A.K.; Kim, K.-H.; Deep, A. Graphene Quantum Dot Modified Screen Printed Immunosensor for the Determination of Parathion. *Anal. Biochem.* **2017**, *523*, 1–9. [\[CrossRef\]](#)
141. Supraja, P.; Tripathy, S.; Krishna Vanjari, S.R.; Singh, V.; Singh, S.G. Label Free, Electrochemical Detection of Atrazine Using Electrospun Mn<sub>2</sub>O<sub>3</sub> Nanofibers: Towards Ultrasensitive Small Molecule Detection. *Sens. Actuators B Chem.* **2019**, *285*, 317–325. [\[CrossRef\]](#)
142. Qian, J.; Li, J.; Fang, D.; Yu, Y.; Zhi, J. A Disposable Biofilm-Modified Amperometric Biosensor for the Sensitive Determination of Pesticide Biototoxicity in Water. *RSC Adv.* **2014**, *4*, 55473–55482. [\[CrossRef\]](#)
143. Abu-Ali, H.; Nabok, A.; Smith, T.J.; Al-Shanawa, M. Development of a Novel Electrochemical Inhibition Sensor Array Based on Bacteria Immobilized on Modified Screen-Printed Gold Electrodes for Water Pollution Detection. *Bionanoscience* **2019**, *9*, 345–355. [\[CrossRef\]](#)
144. Abu-Ali, H.; Nabok, A.; Smith, T.J. Electrochemical Inhibition Bacterial Sensor Array for Detection of Water Pollutants: Artificial Neural Network (ANN) Approach. *Anal. Bioanal. Chem.* **2019**, *411*, 7659–7668. [\[CrossRef\]](#)
145. Fei, A.; Liu, Q.; Huan, J.; Qian, J.; Dong, X.; Qiu, B.; Mao, H.; Wang, K. Label-Free Impedimetric Aptasensor for Detection of Femtomole Level Acetamiprid Using Gold Nanoparticles Decorated Multiwalled Carbon Nanotube-Reduced Graphene Oxide Nanoribbon Composites. *Biosens. Bioelectron.* **2015**, *70*, 122–129. [\[CrossRef\]](#)
146. Liu, M.; Khan, A.; Wang, Z.; Liu, Y.; Yang, G.; Deng, Y.; He, N. Aptasensors for Pesticide Detection. *Biosens. Bioelectron.* **2019**, *130*, 174–184. [\[CrossRef\]](#)
147. Fu, J.; Dong, H.; Zhao, Q.; Cheng, S.; Guo, Y.; Sun, X. Fabrication of Refreshable Aptasensor Based on Hydrophobic Screen-Printed Carbon Electrode Interface. *Sci. Total Environ.* **2020**, *712*, 136410. [\[CrossRef\]](#)
148. Sgobbi, L.F.; Machado, S.A.S. Functionalized Polyacrylamide as an Acetylcholinesterase-Inspired Biomimetic Device for Electrochemical Sensing of Organophosphorus Pesticides. *Biosens. Bioelectron.* **2018**, *100*, 290–297. [\[CrossRef\]](#)
149. Karimian, N.; Fakhri, H.; Amidi, S.; Hajian, A.; Arduini, F.; Bagheri, H. A Novel Sensing Layer Based on Metal–Organic Framework UiO-66 Modified with TiO<sub>2</sub>–Graphene Oxide: Application to Rapid, Sensitive and Simultaneous Determination of Paraoxon and Chlorpyrifos. *New J. Chem.* **2019**, *43*, 2600–2609. [\[CrossRef\]](#)
150. Aghaie, A.; Khanmohammadi, A.; Hajian, A.; Schmid, U.; Bagheri, H. Nonenzymatic Electrochemical Determination of Paraoxon Ethyl in Water and Fruits by Graphene-Based NiFe Bimetallic Phosphosulfide Nanocomposite as a Superior Sensing Layer. *Food Anal. Methods* **2019**, *12*, 1545–1555. [\[CrossRef\]](#)
151. Cinti, S.; Neagu, D.; Carbone, M.; Cacciotti, I.; Moscone, D.; Arduini, F. Novel Carbon Black-Cobalt Phthalocyanine Nanocomposite as Sensing Platform to Detect Organophosphorus Pollutants at Screen-Printed Electrode. *Electrochim. Acta* **2016**, *188*, 574–581. [\[CrossRef\]](#)
152. Yola, M.L. Electrochemical Activity Enhancement of Monodisperse Boron Nitride Quantum Dots on Graphene Oxide: Its Application for Simultaneous Detection of Organophosphate Pesticides in Real Samples. *J. Mol. Liq.* **2019**, *277*, 50–57. [\[CrossRef\]](#)
153. Zheng, A.; Shen, C.; Tang, Q.; Gong, C.; Chow, C. Catalytic Chemosensing Assay for Selective Detection of Methyl Parathion Organophosphate Pesticide. *Chem. Eur. J.* **2019**, *25*, 9643–9649. [\[CrossRef\]](#)

154. Xiang, H.; Cai, Q.; Li, Y.; Zhang, Z.; Cao, L.; Li, K.; Yang, H. Sensors Applied for the Detection of Pesticides and Heavy Metals in Freshwaters. *J. Sens.* **2020**, *2020*, 1–22. [\[CrossRef\]](#)
155. Opekar, F.; Tůma, P. Dual-Channel Capillary Electrophoresis for Simultaneous Determination of Cations and Anions. *J. Chromatogr. A* **2016**, *1446*, 158–163. [\[CrossRef\]](#) [\[PubMed\]](#)
156. Saurina, J.; López-Aviles, E.; Le Moal, A.; Hernández-Cassou, S. Determination of Calcium and Total Hardness in Natural Waters Using a Potentiometric Sensor Array. *Anal. Chim. Acta* **2002**, *464*, 89–98. [\[CrossRef\]](#)
157. Cuartero, M.; Pankratova, N.; Cherubini, T.; Crespo, G.A.; Massa, F.; Confalonieri, F.; Bakker, E. In Situ Detection of Species Relevant to the Carbon Cycle in Seawater with Submersible Potentiometric Probes. *Environ. Sci. Technol. Lett.* **2017**, *4*, 410–415. [\[CrossRef\]](#)
158. Stoodley, R.; Rodriguez Nuñez, J.R.; Bartz, T. Field and In-Lab Determination of  $\text{Ca}^{2+}$  in Seawater. *J. Chem. Educ.* **2014**, *91*, 1954–1957. [\[CrossRef\]](#)
159. Li, M.; Li, Y.-T.; Li, D.-W.; Long, Y.-T. Recent Developments and Applications of Screen-Printed Electrodes in Environmental Assays—A Review. *Anal. Chim. Acta* **2012**, *734*, 31–44. [\[CrossRef\]](#)
160. Yin, T.; Yu, H.; Ding, J.; Qin, W. An Integrated Screen-Printed Potentiometric Strip for Determination of  $\text{Ca}^{2+}$  in Seawater. *J. Electrochem. Soc.* **2019**, *166*, B589–B593. [\[CrossRef\]](#)
161. Schwarz, J.; Trommer, K.; Gerlach, F.; Mertig, M. All-Solid-State Screen-Printed Sensors for Potentiometric Calcium(II) Determinations in Environmental Samples. *Am. J. Anal. Chem.* **2018**, *9*, 113–123. [\[CrossRef\]](#)
162. Liu, Y.; Liu, Y.; Yan, R.; Gao, Y.; Wang, P. Bimetallic AuCu Nanoparticles Coupled with Multi-Walled Carbon Nanotubes as Ion-to-Electron Transducers in Solid-Contact Potentiometric Sensors. *Electrochim. Acta* **2020**, *331*, 135370. [\[CrossRef\]](#)
163. Yin, T.; Li, J.; Qin, W. An All-Solid-State Polymeric Membrane  $\text{Ca}^{2+}$ -Selective Electrode Based on Hydrophobic Alkyl-Chain-Functionalized Graphene Oxide. *Electroanalysis* **2017**, *29*, 821–827. [\[CrossRef\]](#)
164. Akhter, F.; Nag, A.; Alahi, M.E.E.; Liu, H.; Mukhopadhyay, S.C. Electrochemical Detection of Calcium and Magnesium in Water Bodies. *Sens. Actuators A Phys.* **2020**, *305*, 111949. [\[CrossRef\]](#)
165. Levin, M.B.; Khripoun, G.A.; Korneev, S.M.; Mikhelson, K.N. Water Hardness Electrodes with Ionophores Containing Oxy- and Ester-Groups. *Russ. J. Electrochem.* **2018**, *54*, 391–399. [\[CrossRef\]](#)
166. Wang, N.; Kanhere, E.; Tao, K.; Wu, J.; Miao, J.; Triantafyllou, M.S. Water Hardness Determination Using Disposable MEMS-Based Electrochemical Sensor. In Proceedings of the 2018 IEEE 8th International Nanoelectronics Conferences (INEC), Kuala Lumpur, Malaysia, 3–5 January 2018; pp. 43–44.
167. He Zhang; Rongyan Chuai; Xin Li; Bing Zhang Design, Preparation and Performance Study of On-Chip Flow-Through Amperometric Sensors with an Integrated Ag/AgCl Reference Electrode. *Micromachines* **2018**, *9*, 114. [\[CrossRef\]](#)
168. Haldorai, Y.; Kim, J.Y.; Vilian, A.T.E.; Heo, N.S.; Huh, Y.S.; Han, Y.-K. An Enzyme-Free Electrochemical Sensor Based on Reduced Graphene Oxide/Co<sub>3</sub>O<sub>4</sub> Nanospindle Composite for Sensitive Detection of Nitrite. *Sens. Actuators B Chem.* **2016**, *227*, 92–99. [\[CrossRef\]](#)
169. Tian, F.; Li, H.; Li, M.; Li, C.; Lei, Y.; Yang, B. Synthesis of One-Dimensional Poly(3,4-Ethylenedioxythiophene)-Graphene Composites for the Simultaneous Detection of Hydroquinone, Catechol, Resorcinol, and Nitrite. *Synth. Met.* **2017**, *226*, 148–156. [\[CrossRef\]](#)
170. Wang, P.; Wang, M.; Zhou, F.; Yang, G.; Qu, L.; Miao, X. Development of a Paper-Based, Inexpensive, and Disposable Electrochemical Sensing Platform for Nitrite Detection. *Electrochem. Commun.* **2017**, *81*, 74–78. [\[CrossRef\]](#)
171. Chen, W.; Niu, X.; Li, X.; Li, X.; Li, G.; He, B.; Li, Q.; Sun, W. Investigation on Direct Electrochemical and Electrocatalytic Behavior of Hemoglobin on Palladium-Graphene Modified Electrode. *Mater. Sci. Eng. C Mater. Biol. Appl.* **2017**, *80*, 135–140. [\[CrossRef\]](#)
172. Bagheri, H.; Hajian, A.; Rezaei, M.; Shirzadmehr, A. Composite of Cu Metal Nanoparticles-Multiwall Carbon Nanotubes-Reduced Graphene Oxide as a Novel and High Performance Platform of the Electrochemical Sensor for Simultaneous Determination of Nitrite and Nitrate. *J. Hazard. Mater.* **2017**, *324*, 762–772. [\[CrossRef\]](#)
173. Sivakumar, M. An Electrochemical Selective Detection of Nitrite Sensor for Polyaniline Doped Graphene Oxide Modified Electrode. *Int. J. Electrochem. Sci.* **2017**, *14*, 4835–4846. [\[CrossRef\]](#)
174. Rabti, A.; Ben Aoun, S.; Raouafi, N. A Sensitive Nitrite Sensor Using an Electrode Consisting of Reduced Graphene Oxide Functionalized with Ferrocene. *Microchim. Acta* **2016**, *183*, 3111–3117. [\[CrossRef\]](#)
175. Zhang, Y.; Nie, J.; Wei, H.; Xu, H.; Wang, Q.; Cong, Y.; Tao, J.; Zhang, Y.; Chu, L.; Zhou, Y.; et al. Electrochemical Detection of Nitrite Ions Using Ag/Cu/MWNT Nanoclusters Electrodeposited on a Glassy Carbon Electrode. *Sens. Actuators B Chem.* **2018**, *258*, 1107–1116. [\[CrossRef\]](#)
176. Huang, S.-S.; Liu, L.; Mei, L.-P.; Zhou, J.-Y.; Guo, F.-Y.; Wang, A.-J.; Feng, J.-J. Electrochemical Sensor for Nitrite Using a Glassy Carbon Electrode Modified with Gold-Copper Nanochain Networks. *Microchim. Acta* **2016**, *183*, 791–797. [\[CrossRef\]](#)
177. Mo, R.; Wang, X.; Yuan, Q.; Yan, X.; Su, T.; Feng, Y.; Lv, L.; Zhou, C.; Hong, P.; Sun, S.; et al. Electrochemical Determination of Nitrite by Au Nanoparticle/Graphene-Chitosan Modified Electrode. *Sensors* **2018**, *18*, 1986. [\[CrossRef\]](#) [\[PubMed\]](#)
178. Kang, S.; Zhang, H.; Wang, G.; Zhang, Y.; Zhao, H.; Zhou, H.; Cai, W. Highly Sensitive Detection of Nitrite by Using Gold Nanoparticle-Decorated  $\alpha\text{-Fe}_2\text{O}_3$  Nanorod Arrays as Self-Supporting Photo-Electrodes. *Inorg. Chem. Front.* **2019**, *6*, 1432–1441. [\[CrossRef\]](#)



179. Zhe, T.; Sun, X.; Wang, Q.; Liu, Y.; Li, R.; Li, F.; Wang, L. A Screen Printed Carbon Electrode Modified with a Lamellar Nanocomposite Containing Dendritic Silver Nanostructures, Reduced Graphene Oxide, and  $\beta$ -Cyclodextrin for Voltammetric Sensing of Nitrite. *Microchim. Acta* **2019**, *186*, 319. [\[CrossRef\]](#)
180. Rostami, M.; Abdi, G.; Kazemi, S.H.; Alizadeh, A. Nanocomposite of Magnetic Nanoparticles/Graphene Oxide Decorated with Acetic Acid Moieties on Glassy Carbon Electrode: A Facile Method to Detect Nitrite Concentration. *J. Electroanal. Chem.* **2019**, *847*, 113239. [\[CrossRef\]](#)
181. Nasraoui, S.; Al-Hamry, A.; Teixeira, P.R.; Ameer, S.; Paterno, L.G.; Ben Ali, M.; Kanoun, O. Electrochemical Sensor for Nitrite Detection in Water Samples Using Flexible Laser-Induced Graphene Electrodes Functionalized by CNT Decorated by Au Nanoparticles. *J. Electroanal. Chem.* **2021**, *880*, 114893. [\[CrossRef\]](#)
182. Zhao, Z.; Zhang, J.; Wang, W.; Sun, Y.; Li, P.; Hu, J.; Chen, L.; Gong, W. Synthesis and Electrochemical Properties of Co<sub>3</sub>O<sub>4</sub>-RGO/CNTs Composites towards Highly Sensitive Nitrite Detection. *Appl. Surf. Sci.* **2019**, *485*, 274–282. [\[CrossRef\]](#)
183. Li, C.; Chen, D.; Wang, Y.; Lai, X.; Peng, J.; Wang, X.; Zhang, K.; Cao, Y. Simultaneous Electrochemical Detection of Nitrite and Hydrogen Peroxide Based on 3D Au-RGO/FTO Obtained Through a One-Step Synthesis. *Sensors* **2019**, *19*, 1304. [\[CrossRef\]](#)
184. Sheng, Q.; Liu, D.; Zheng, J. A Nonenzymatic Electrochemical Nitrite Sensor Based on Pt Nanoparticles Loaded Ni(OH)<sub>2</sub>/Multi-Walled Carbon Nanotubes Nanocomposites. *J. Electroanal. Chem.* **2017**, *796*, 9–16. [\[CrossRef\]](#)
185. Hui, N.; Chai, F.; Lin, P.; Song, Z.; Sun, X.; Li, Y.; Niu, S.; Luo, X. Electrodeposited Conducting Polyaniline Nanowire Arrays Aligned on Carbon Nanotubes Network for High Performance Supercapacitors and Sensors. *Electrochim. Acta* **2016**, *199*, 234–241. [\[CrossRef\]](#)
186. Wu, W.; Li, Y.; Jin, J.; Wu, H.; Wang, S.; Ding, Y.; Ou, J. Sensing Nitrite with a Glassy Carbon Electrode Modified with a Three-Dimensional Network Consisting of Ni<sub>7</sub>S<sub>6</sub> and Multi-Walled Carbon Nanotubes. *Microchim. Acta* **2016**, *183*, 3159–3166. [\[CrossRef\]](#)
187. Rao, D.; Sheng, Q.; Zheng, J. Self-Assembly Preparation of Gold Nanoparticle Decorated 1-Pyrenemethylamine Functionalized Graphene Oxide–Carbon Nanotube Composites for Highly Sensitive Detection of Nitrite. *Anal. Methods* **2016**, *8*, 4926–4933. [\[CrossRef\]](#)
188. Bhat, S.A.; Pandit, S.A.; Rather, M.A.; Rather, G.M.; Rashid, N.; Ingole, P.P.; Bhat, M.A. Self-Assembled AuNPs on Sulphur-Doped Graphene: A Dual and Highly Efficient Electrochemical Sensor for Nitrite (NO<sub>2</sub><sup>−</sup>) and Nitric Oxide (NO). *New J. Chem.* **2017**, *41*, 8347–8358. [\[CrossRef\]](#)
189. Aksu, Z.; Alanyalıoğlu, M. Fabrication of Free-Standing Reduced Graphene Oxide Composite Papers Doped with Different Dyes and Comparison of Their Electrochemical Performance for Electrocatalytic Oxidation of Nitrite. *Electrochim. Acta* **2017**, *258*, 1376–1386. [\[CrossRef\]](#)
190. Wang, L.; Kim, J.; Cui, T. Self-Assembled Graphene and Copper Nanoparticles Composite Sensor for Nitrate Determination. *Microsyst. Technol.* **2018**, *24*, 3623–3630. [\[CrossRef\]](#)
191. Can, F.; Korkut Ozoner, S.; Ergenekon, P.; Erhan, E. Amperometric Nitrate Biosensor Based on Carbon Nanotube/Polypyrrole/Nitrate Reductase Biofilm Electrode. *Mater. Sci. Eng. C* **2012**, *32*, 18–23. [\[CrossRef\]](#)
192. Madasamy, T.; Pandiaraj, M.; Balamurugan, M.; Bhargava, K.; Sathy, N.K.; Karunakaran, C. Copper, Zinc Superoxide Dismutase and Nitrate Reductase Coimmobilized Bionzymatic Biosensor for the Simultaneous Determination of Nitrite and Nitrate. *Biosens. Bioelectron.* **2014**, *52*, 209–215. [\[CrossRef\]](#)
193. Manea, F.; Remes, A.; Radovan, C.; Pode, R.; Picken, S.; Schoonman, J. Simultaneous Electrochemical Determination of Nitrate and Nitrite in Aqueous Solution Using Ag-Doped Zeolite-Expanded Graphite-Epoxy Electrode. *Talanta* **2010**, *83*, 66–71. [\[CrossRef\]](#)
194. Hu, J.; Sun, J.; Bian, C.; Tong, J.; Shanhong, X. 3D Dendritic Nanostructure of Silver-Array: Preparation, Growth Mechanism and Application in Nitrate Sensor. *Electroanalysis* **2013**, *25*, 546–556. [\[CrossRef\]](#)
195. Li, Y.; Sun, J.; Bian, C.; Tong, J.; Xia, S. Electrodeposition of Copper Nano-Clusters at a Platinum Microelectrode for Trace Nitrate Determination. *Procedia Eng.* **2010**, *5*, 339–342. [\[CrossRef\]](#)
196. da Silva, I.S.; de Araujo, W.R.; Paixão, T.R.L.C.; Angnes, L. Direct Nitrate Sensing in Water Using an Array of Copper-Microelectrodes from Flat Flexible Cables. *Sens. Actuators B Chem.* **2013**, *188*, 94–98. [\[CrossRef\]](#)
197. Stortini, A.M.; Moretto, L.M.; Mardegan, A.; Ongaro, M.; Ugo, P. Arrays of Copper Nanowire Electrodes: Preparation, Characterization and Application as Nitrate Sensor. *Sens. Actuators B Chem.* **2015**, *207*, 186–192. [\[CrossRef\]](#)
198. Li, Y.; Han, H.; Pan, D.; Zhang, P. Fabrication of a Micro-Needle Sensor Based on Copper Microspheres and Polyaniline Film for Nitrate Determination in Coastal River Waters. *J. Electrochem. Soc.* **2019**, *166*, B1038–B1043. [\[CrossRef\]](#)
199. Lotfi Zadeh Zhad, H.R.; Lai, R.Y. Comparison of Nanostructured Silver-Modified Silver and Carbon Ultramicroelectrodes for Electrochemical Detection of Nitrate. *Anal. Chim. Acta* **2015**, *892*, 153–159. [\[CrossRef\]](#)
200. Yang, H.; Cui, H.; Tang, W.; Li, Z.; Han, N.; Xing, F. A Critical Review on Research Progress of Graphene/Cement Based Composites. *Compos. Part A Appl. Sci. Manuf.* **2017**, *102*, 273–296. [\[CrossRef\]](#)
201. Xiao, Q.; Feng, M.; Liu, Y.; Lu, S.; He, Y.; Huang, S. The Graphene/Polypyrrole/Chitosan-Modified Glassy Carbon Electrode for Electrochemical Nitrite Detection. *Ionics* **2018**, *24*, 845–859. [\[CrossRef\]](#)
202. Yao, Y.; Ping, J. Recent Advances in Graphene-Based Freestanding Paper-like Materials for Sensing Applications. *TrAC Trends Anal. Chem.* **2018**, *105*, 75–88. [\[CrossRef\]](#)

203. Thirumalraj, B.; Palanisamy, S.; Chen, S.-M.; Zhao, D.-H. Amperometric Detection of Nitrite in Water Samples by Use of Electrodes Consisting of Palladium-Nanoparticle-Functionalized Multi-Walled Carbon Nanotubes. *J. Colloid Interface Sci.* **2016**, *478*, 413–420. [\[CrossRef\]](#)
204. Fajerwerg, K.; Ynam, V.; Chaudret, B.; Garçon, V.; Thouron, D.; Comtat, M. An Original Nitrate Sensor Based on Silver Nanoparticles Electrodeposited on a Gold Electrode. *Electrochem. Commun.* **2010**, *12*, 1439–1441. [\[CrossRef\]](#)
205. Ghanbari, K. Silver Nanoparticles Dispersed in Polypyrrole Matrixes Coated on Glassy Carbon Electrode as a Nitrate Sensor. *Anal. Bioanal. Electrochem.* **2013**, *5*, 46–58.
206. Xi, R.; Zhang, S.-H.; Zhang, L.; Wang, C.; Wang, L.-J.; Yan, J.-H.; Pan, G.-B. Electrodeposition of Pd-Pt Nanocomposites on Porous GaN for Electrochemical Nitrite Sensing. *Sensors* **2019**, *19*, 606. [\[CrossRef\]](#)
207. Bonyani, M.; Mirzaei, A.; Leonardi, S.G.; Neri, G. Silver Nanoparticles/Polymethacrylic Acid (AgNPs/PMA) Hybrid Nanocomposites-Modified Electrodes for the Electrochemical Detection of Nitrate Ions. *Measurement* **2016**, *84*, 83–90. [\[CrossRef\]](#)
208. Runsewe, D.; Betancourt, T.; Irvin, J.A. Biomedical Application of Electroactive Polymers in Electrochemical Sensors: A Review. *Materials* **2019**, *12*, 2629. [\[CrossRef\]](#)
209. Roldán-Carmona, C.; Malinkiewicz, O.; Soriano, A.; Mínguez Espallargas, G.; Garcia, A.; Reinecke, P.; Kroyer, T.; Dar, M.I.; Nazeeruddin, M.K.; Bolink, H.J. Flexible High Efficiency Perovskite Solar Cells. *Energy Environ. Sci.* **2014**, *7*, 994. [\[CrossRef\]](#)
210. Ge, Y.; Jamal, R.; Zhang, R.; Zhang, W.; Yu, Z.; Yan, Y.; Liu, Y.; Abdiryim, T. Electrochemical Synthesis of Multilayered PEDOT/PEDOT-SH/Au Nanocomposites for Electrochemical Sensing of Nitrite. *Microchim. Acta* **2020**, *187*, 248. [\[CrossRef\]](#)
211. Wang, G.; Morrin, A.; Li, M.; Liu, N.; Luo, X. Nanomaterial-Doped Conducting Polymers for Electrochemical Sensors and Biosensors. *J. Mater. Chem. B* **2018**, *6*, 4173–4190. [\[CrossRef\]](#)
212. Arvas, M.B.; Gorduk, O.; Gencten, M.; Sahin, Y. Preparation of a Novel Electrochemical Sensor for Phosphate Detection Based on a Molybdenum Blue Modified Poly(Vinyl Chloride) Coated Pencil Graphite Electrode. *Anal. Methods* **2019**, *11*, 3874–3881. [\[CrossRef\]](#)
213. Topcu, C.; Caglar, B.; Onder, A.; Coldur, F.; Caglar, S.; Guner, E.K.; Cubuk, O.; Tabak, A. Structural Characterization of Chitosan-Smectite Nanocomposite and Its Application in the Development of a Novel Potentiometric Monohydrogen Phosphate-Selective Sensor. *Mater. Res. Bull.* **2018**, *98*, 288–299. [\[CrossRef\]](#)
214. Haung, Y.; Ye, Y.; Zhao, G.; Wu, X.; Kan, Y.; Mur, L.; Han, J.; Qin, H. An All-Solid-State Phosphate Electrode with H<sub>3</sub>PO<sub>4</sub> Doped Polyaniline as the Sensitive Layer. *Int. J. Electrochem. Sci.* **2017**, *12*, 4677–4691. [\[CrossRef\]](#)
215. Ding, X.; Behbahani, M.; Gruden, C.; Seo, Y. Characterization and Evaluation of Phosphate Microsensors to Monitor Internal Phosphorus Loading in Lake Erie Sediments. *J. Environ. Manag.* **2015**, *160*, 193–200. [\[CrossRef\]](#)
216. Talarico, D.; Arduini, F.; Amine, A.; Moscone, D.; Palleschi, G. Screen-Printed Electrode Modified with Carbon Black Nanoparticles for Phosphate Detection by Measuring the Electroactive Phosphomolybdate Complex. *Talanta* **2015**, *141*, 267–272. [\[CrossRef\]](#) [\[PubMed\]](#)
217. Bhat, K.S.; Nakate, U.T.; Yoo, J.-Y.; Wang, Y.; Mahmoudi, T.; Hahn, Y.-B. Nozzle-Jet-Printed Silver/Graphene Composite-Based Field-Effect Transistor Sensor for Phosphate Ion Detection. *ACS Omega* **2019**, *4*, 8373–8380. [\[CrossRef\]](#) [\[PubMed\]](#)
218. Cinti, S.; Talarico, D.; Palleschi, G.; Moscone, D.; Arduini, F. Novel Reagentless Paper-Based Screen-Printed Electrochemical Sensor to Detect Phosphate. *Anal. Chim. Acta* **2016**, *919*, 78–84. [\[CrossRef\]](#) [\[PubMed\]](#)
219. Kim, J.; Wang, L.; Bourouina, T.; Cui, T. Ion Sensitive Field Effect Transistor Based on Graphene and Ionophore Hybrid Membrane for Phosphate Detection. *Microsyst. Technol.* **2019**, *25*, 3357–3364. [\[CrossRef\]](#)
220. Barhoumi, L.; Baraket, A.; Nooredeen, N.M.; Ali, M.B.; Abbas, M.N.; Bausells, J.; Errachid, A. Silicon Nitride Capacitive Chemical Sensor for Phosphate Ion Detection Based on Copper Phthalocyanine - Acrylate-Polymer. *Electroanalysis* **2017**, *29*, 1586–1595. [\[CrossRef\]](#)
221. Zina, F.; Nooredeen, N.M.; Azzouzi, S.; Ali, M.B.; Abbas, M.N.; Errachid, A. Novel Sensitive Impedimetric Microsensor for Phosphate Detection Based on a Novel Copper Phthalocyanine Derivative. *Anal. Lett.* **2018**, *51*, 371–386. [\[CrossRef\]](#)
222. Li, L.; Shang, G.; Qin, W. Potentiometric Sensing of Aqueous Phosphate by Competition Assays Using Ion-Exchanger Doped-Polymeric Membrane Electrodes as Transducers. *Analyst* **2016**, *141*, 4573–4577. [\[CrossRef\]](#)
223. Cui, J.; Ogabiela, E.E.; Hui, J.; Wang, Y.; Zhang, Y.; Tong, L.; Zhang, J.; Adeloju, S.B.; Zhang, X.; Wu, Y. Electrochemical Biosensor Based on Pt/Au Alloy Nanowire Arrays for Phosphate Detection. *J. Electrochem. Soc.* **2015**, *162*, B62–B67. [\[CrossRef\]](#)
224. Kabir, M.F.; Rahman, M.T.; Gurung, A.; Qiao, Q. Electrochemical Phosphate Sensors Using Silver Nanowires Treated Screen Printed Electrodes. *IEEE Sens. J.* **2018**, *18*, 3480–3485. [\[CrossRef\]](#)
225. Kazem, K.; Payam, H.; Hamid, A.S. Cobalt-Graphene Nanocomposite Electrode for Phosphate Sensing. *Anal. Bioanal. Electrochem.* **2017**, *9*, 521–534.
226. Kolliopoulos, A.V.; Kampouris, D.K.; Banks, C.E. Rapid and Portable Electrochemical Quantification of Phosphorus. *Anal. Chem.* **2015**, *87*, 4269–4274. [\[CrossRef\]](#)
227. Ahmad, R.; Ahn, M.-S.; Hahn, Y.-B. ZnO Nanorods Array Based Field-Effect Transistor Biosensor for Phosphate Detection. *J. Colloid Interface Sci.* **2017**, *498*, 292–297. [\[CrossRef\]](#)
228. Ogabiela, E.; Adeloju, S.B.; Cui, J.; Wu, Y.; Chen, W. A Novel Ultrasensitive Phosphate Amperometric Nanobiosensor Based on the Integration of Pyruvate Oxidase with Highly Ordered Gold Nanowires Array. *Biosens. Bioelectron.* **2015**, *71*, 278–285. [\[CrossRef\]](#)
229. Power, A.C.; Gorey, B.; Chandra, S.; Chapman, J. Carbon Nanomaterials and Their Application to Electrochemical Sensors: A Review. *Nanotechnol. Rev.* **2018**, *7*, 19–41. [\[CrossRef\]](#)

230. Talbi, M.; Al-Hamry, A.; Ali, M.B.; Kanoun, O. Carbon Screen Printed Electrodes Functionalized with Cu(II)Pc for Phosphate Detection. In Proceedings of the 2020 17th International Multi-Conference on Systems, Signals Devices (SSD), Monastir, Tunisia, 20–23 July 2020; pp. 869–872.
231. Hariganesh, S.; Vadivel, S.; Maruthamani, D.; Rangabhashiyam, S. Disinfection by-products in drinking water: Detection and treatment methods. In *Disinfection By-products in Drinking Water*; Butterworth-Heinemann: Oxford, UK, 2020; pp. 279–304, ISBN 978-0-08-102977-0.
232. Valentini, F.; Biagiotti, V.; Lete, C.; Palleschi, G.; Wang, J. The Electrochemical Detection of Ammonia in Drinking Water Based on Multi-Walled Carbon Nanotube/Copper Nanoparticle Composite Paste Electrodes. *Sens. Actuators B Chem.* **2007**, *128*, 326–333. [[CrossRef](#)]
233. Sun, W.; Hou, F.; Gong, S.; Han, L.; Wang, W.; Shi, F.; Xi, J.; Wang, X.; Li, G. Direct Electrochemistry and Electrocatalysis of Hemoglobin on Three-Dimensional Graphene Modified Carbon Ionic Liquid Electrode. *Sens. Actuators B Chem.* **2015**, *219*, 331–337. [[CrossRef](#)]
234. Dai, H.; Xu, H.; Wu, X.; Lin, Y.; Wei, M.; Chen, G. Electrochemical Behavior of Thionine at Titanate Nanotubes-Based Modified Electrode: A Sensing Platform for the Detection of Trichloroacetic Acid. *Talanta* **2010**, *81*, 1461–1466. [[CrossRef](#)]
235. Peverly, A.A.; Peters, D.G. Electrochemical Determination of Trihalomethanes in Water by Means of Stripping Analysis. *Anal. Chem.* **2012**, *84*, 6110–6115. [[CrossRef](#)]
236. Cetó, X.; Saint, C.; Chow, C.W.K.; Voelcker, N.H.; Prieto-Simón, B. Electrochemical Fingerprints of Brominated Trihaloacetic Acids (HAA3) Mixtures in Water. *Sens. Actuators B Chem.* **2017**, *247*, 70–77. [[CrossRef](#)]
237. Qian, D.; Li, W.; Chen, F.; Huang, Y.; Bao, N.; Gu, H.; Yu, C. Voltammetric Sensor for Trichloroacetic Acid Using a Glassy Carbon Electrode Modified with Au@Ag Nanorods and Hemoglobin. *Microchim. Acta* **2017**, *184*, 1977–1985. [[CrossRef](#)]
238. Al-Zahrani, E.; Soomro, M.T.; Bashami, R.M.; Rehman, A.U.; Danish, E.; Ismail, I.M.I.; Aslam, M.; Hameed, A. Fabrication and Performance of Magnetite (Fe<sub>3</sub>O<sub>4</sub>) Modified Carbon Paste Electrode for the Electrochemical Detection of Chlorite Ions in Aqueous Medium. *J. Environ. Chem. Eng.* **2016**, *4*, 4330–4341. [[CrossRef](#)]
239. Wang, Y.-H.; Yu, C.-M.; Gu, H.-Y.; Tu, Y.-F. The Hemoglobin-Modified Electrode with Chitosan/Fe<sub>3</sub>O<sub>4</sub> Nanocomposite for the Detection of Trichloroacetic Acid. *J. Solid State Electrochem.* **2016**, *20*, 1337–1344. [[CrossRef](#)]
240. Zhao, W.; Li, X.; Wen, Z.; Niu, X.; Shen, Q.; Sun, Z.; Dong, R.; Sun, W. Application of Ionic Liquid-Graphene-NiO Hollowsphere Composite Modified Electrode for Electrochemical Investigation on Hemoglobin and Electrocatalysis to Trichloroacetic Acid. *Int. J. Electrochem. Sci.* **2017**, *12*, 2025–2034. [[CrossRef](#)]
241. Kong, L.; Du, Z.; Xie, Z.; Chen, R.; Jia, S.; Dong, R.; Sun, Z.; Sun, W. Electrochemistry of Hemoglobin-Ionic Liquid-Graphene-SnO<sub>2</sub> Nanosheet Composite Modified Electrode and Electrocatalysis. *Int. J. Electrochem. Sci.* **2017**, *12*, 2297–2305. [[CrossRef](#)]
242. Yan, H.; Chen, X.; Shi, Z.; Feng, Y.; Li, J.; Lin, Q.; Wang, X.; Sun, W. Direct Electrochemistry of Myoglobin on TiO<sub>2</sub> and Alginate Composite Modified Carbon Ionic Liquid Electrode via the Electrodeposition Method. *J. Solid State Electrochem.* **2016**, *20*, 1783–1792. [[CrossRef](#)]
243. Shi, F.; Zheng, W.; Wang, W.; Hou, F.; Lei, B.; Sun, Z.; Sun, W. Application of Graphene–Copper Sulfide Nanocomposite Modified Electrode for Electrochemistry and Electrocatalysis of Hemoglobin. *Biosens. Bioelectron.* **2015**, *64*, 131–137. [[CrossRef](#)]
244. Najafi, M.; Darabi, S.; Tadjarodi, A.; Imani, M. Determination of Trichloroacetic Acid (TCAA) Using CdO Nanoparticles Modified Carbon Paste Electrode. *Electroanalysis* **2013**, *25*, 487–492. [[CrossRef](#)]
245. Zeng, Z.; Fang, X.; Miao, W.; Liu, Y.; Maiyalagan, T.; Mao, S. Electrochemically Sensing of Trichloroacetic Acid with Iron(II) Phthalocyanine and Zn-Based Metal Organic Framework Nanocomposites. *ACS Sens.* **2019**, *4*, 1934–1941. [[CrossRef](#)]
246. Cetó, X.; Saint, C.P.; Chow, C.W.K.; Voelcker, N.H.; Prieto-Simón, B. Electrochemical Detection of N-nitrosodimethylamine Using a Molecular Imprinted Polymer. *Sens. Actuators B Chem.* **2016**, *237*, 613–620. [[CrossRef](#)]
247. Chen, W.; Weng, W.; Niu, X.; Li, X.; Men, Y.; Sun, W.; Li, G.; Dong, L. Boron-Doped Graphene Quantum Dots Modified Electrode for Electrochemistry and Electrocatalysis of Hemoglobin. *J. Electroanal. Chem.* **2018**, *823*, 137–145. [[CrossRef](#)]
248. Zhu, L.; Li, X.; Deng, Y.; Zou, R.; Shao, B.; Yan, L.; Ruan, C.; Sun, W. Construction and Electrochemical Behavior of Hemoglobin Sensor Based on ZnO Doped Carbon Nanofiber Modified Electrode. *J. Iran. Chem. Soc.* **2020**. [[CrossRef](#)]
249. Xie, H.; Luo, G.; Niu, Y.; Weng, W.; Zhao, Y.; Ling, Z.; Ruan, C.; Li, G.; Sun, W. Synthesis and Utilization of Co<sub>3</sub>O<sub>4</sub> Doped Carbon Nanofiber for Fabrication of Hemoglobin-Based Electrochemical Sensor. *Mater. Sci. Eng. C* **2020**, *107*, 110209. [[CrossRef](#)] [[PubMed](#)]
250. Bashami, R.M.; Soomro, M.T.; Khan, A.N.; Aazam, E.S.; Ismail, I.M.I.; El-Shahawi, M.S. A Highly Conductive Thin Film Composite Based on Silver Nanoparticles and Malic Acid for Selective Electrochemical Sensing of Trichloroacetic Acid. *Anal. Chim. Acta* **2018**, *1036*, 33–48. [[CrossRef](#)] [[PubMed](#)]
251. Nguyen, T.-H.; Mugherli, L.; Rivron, C.; Tran-Thi, T.-H. Innovative Colorimetric Sensors for the Selective Detection of Monochloramine in Air and in Water. *Sens. Actuators B Chem.* **2015**, *208*, 622–627. [[CrossRef](#)]
252. Serrano, M.; Silva, M.; Gallego, M. Determination of 14 Haloketones in Treated Water Using Solid-Phase Microextraction and Gas Chromatography–Mass Spectrometry. *J. Chromatogr. A* **2015**, *1407*, 208–215. [[CrossRef](#)]
253. Nasraoui, S.; Al-Hamry, A.; Ameer, S.; Ben Ali, M.; Kanoun, O. Graphene Induced Using 405 Nm Laser as Electrode Material for the Electrochemical Sensing Application. In Proceedings of the 2019 5th International Conference on Nanotechnology for Instrumentation and Measurement (NanofIM), Sfax, Tunisia, 30 October 2019; pp. 1–5.



254. Tirawattanakoson, R.; Rattanasarat, P.; Ngamrojanavanich, N.; Rodthongkum, N.; Chailapakul, O. Free Radical Scavenger Screening of Total Antioxidant Capacity in Herb and Beverage Using Graphene/PEDOT: PSS-Modified Electrochemical Sensor. *J. Electroanal. Chem.* **2016**, *767*, 68–75. [\[CrossRef\]](#)
255. Gao, F.; Zheng, D.; Tanaka, H.; Zhan, F.; Yuan, X.; Gao, F.; Wang, Q. An Electrochemical Sensor for Gallic Acid Based on Fe<sub>2</sub>O<sub>3</sub>/Electro-Reduced Graphene Oxide Composite: Estimation for the Antioxidant Capacity Index of Wines. *Mater. Sci. Eng. C* **2015**, *57*, 279–287. [\[CrossRef\]](#)
256. Souza, L.P.; Calegari, F.; Zarbin, A.J.G.; Marcolino-Júnior, L.H.; Bergamini, M.F. Voltammetric Determination of the Antioxidant Capacity in Wine Samples Using a Carbon Nanotube Modified Electrode. *J. Agric. Food Chem.* **2011**, *59*, 7620–7625. [\[CrossRef\]](#)
257. Ziyatdinova, G.; Salikhova, I.; Budnikov, H. Chronoamperometric Estimation of Cognac and Brandy Antioxidant Capacity Using MWNT Modified Glassy Carbon Electrode. *Talanta* **2014**, *125*, 378–384. [\[CrossRef\]](#)
258. Talarico, D.; Arduini, F.; Constantino, A.; Del Carlo, M.; Compagnone, D.; Moscone, D.; Palleschi, G. Carbon Black as Successful Screen-Printed Electrode Modifier for Phenolic Compound Detection. *Electrochem. Commun.* **2015**, *60*, 78–82. [\[CrossRef\]](#)
259. Della Pelle, F.; Di Battista, R.; Vázquez, L.; Palomares, F.J.; Del Carlo, M.; Sergi, M.; Compagnone, D.; Escarpa, A. Press-Transferred Carbon Black Nanoparticles for Class-Selective Antioxidant Electrochemical Detection. *Appl. Mater. Today* **2017**, *9*, 29–36. [\[CrossRef\]](#)
260. Raymundo-Pereira, P.A.; Campos, A.M.; Prado, T.M.; Furini, L.N.; Boas, N.V.; Calegari, M.L.; Machado, S.A.S. Synergy between Printex Nano-Carbons and Silver Nanoparticles for Sensitive Estimation of Antioxidant Activity. *Anal. Chim. Acta* **2016**, *926*, 88–98. [\[CrossRef\]](#)
261. Hui, K.H.; Ambrosi, A.; Pumera, M.; Bonanni, A. Improving the Analytical Performance of Graphene Oxide towards the Assessment of Polyphenols. *Chem. Eur. J.* **2016**, *22*, 3830–3834. [\[CrossRef\]](#)
262. Hammani, H.; Boumya, W.; Laghrib, F.; Farahi, A.; Lahrich, S.; Aboulkas, A.; El Mhammedi, M.A. Electro-Catalytic Effect of Al<sub>2</sub>O<sub>3</sub> Supported onto Activated Carbon in Oxidizing Phenol at Graphite Electrode. *Mater. Today Chem.* **2017**, *3*, 27–36. [\[CrossRef\]](#)
263. Quynh, B.T.P.; Byun, J.Y.; Kim, S.H. Non-Enzymatic Amperometric Detection of Phenol and Catechol Using Nanoporous Gold. *Sens. Actuators B Chem.* **2015**, *221*, 191–200. [\[CrossRef\]](#)
264. Spătaru, T.; Spătaru, N. Voltammetric Detection of Phenol at Platinum–Polytyramine Composite Electrodes in Acidic Media. *J. Hazard. Mater.* **2010**, *180*, 777–780. [\[CrossRef\]](#)
265. Nurul Karim, M.; Lee, H.J. Amperometric Phenol Biosensor Based on Covalent Immobilization of Tyrosinase on Au Nanoparticle Modified Screen Printed Carbon Electrodes. *Talanta* **2013**, *116*, 991–996. [\[CrossRef\]](#)
266. Gu, B.X.; Xu, C.X.; Zhu, G.P.; Liu, S.Q.; Chen, L.Y.; Li, X.S. Tyrosinase Immobilization on ZnO Nanorods for Phenol Detection. *J. Phys. Chem. B* **2009**, *113*, 377–381. [\[CrossRef\]](#)
267. Yi, H. Adsorption Stripping Voltammetry of Phenol at Nafion-Modified Glassy Carbon Electrode in the Presence of Surfactants. *Talanta* **2001**, *55*, 1205–1210. [\[CrossRef\]](#)
268. Pan, G.; Zhao, G.; Wei, M.; Wang, Y.; Zhao, B. Design of Nanogold Electrochemical Immunosensor for Detection of Four Phenolic Estrogens. *Chem. Phys. Lett.* **2019**, *732*, 136657. [\[CrossRef\]](#)
269. Nameghi, M.A.; Danesh, N.M.; Ramezani, M.; Aliboland, M.; Abnous, K.; Taghdisi, S.M. An Ultrasensitive Electrochemical Sensor for 17 $\beta$ -Estradiol Using Split Aptamers. *Anal. Chim. Acta* **2019**, *1065*, 107–112. [\[CrossRef\]](#) [\[PubMed\]](#)
270. Florea, A.; Cristea, C.; Vocanson, F.; Săndulescu, R.; Jaffrezic-Renault, N. Electrochemical Sensor for the Detection of Estradiol Based on Electropolymerized Molecularly Imprinted Polythioaniline Film with Signal Amplification Using Gold Nanoparticles. *Electrochem. Commun.* **2015**, *59*, 36–39. [\[CrossRef\]](#)
271. Wang, Y.; Luo, J.; Liu, J.; Li, X.; Kong, Z.; Jin, H.; Cai, X. Electrochemical Integrated Paper-Based Immunosensor Modified with Multi-Walled Carbon Nanotubes Nanocomposites for Point-of-Care Testing of 17 $\beta$ -Estradiol. *Biosens. Bioelectron.* **2018**, *107*, 47–53. [\[CrossRef\]](#) [\[PubMed\]](#)
272. Silva, C.C.G.; Silva, L.M.; e Silva, B.C.; Garrido, S.S.; Boldrin, M.V.; De Souza, D. Cathodic Stripping Voltammetric Determination of  $\beta$ -Cyfluthrin, a Pyrethroid Insecticide, Using Polished Silver Solid Amalgam Electrode. *J. Solid State Electrochem.* **2020**, *24*, 1819–1826. [\[CrossRef\]](#)
273. Punde, N.S.; Rajpurohit, A.S.; Srivastava, A.K. Sensitive Electrochemical Platform Based on Nano-Cylindrical Strontium Titanate/N-Doped Graphene Hybrid Composite for Simultaneous Detection of Diphenhydramine and Bromhexine. *Electrochim. Acta* **2019**, *319*, 727–739. [\[CrossRef\]](#)
274. Li, J.; Kuang, D.; Feng, Y.; Zhang, F.; Liu, M. Voltammetric Determination of Bisphenol A in Food Package by a Glassy Carbon Electrode Modified with Carboxylated Multi-Walled Carbon Nanotubes. *Microchim. Acta* **2011**, *172*, 379–386. [\[CrossRef\]](#)
275. Huang, Y.; Li, X.; Zheng, S. A Novel and Label-Free Immunosensor for Bisphenol A Using Rutin as the Redox Probe. *Talanta* **2016**, *160*, 241–246. [\[CrossRef\]](#)
276. Liu, Y.; Yao, L.; He, L.; Liu, N.; Piao, Y. Electrochemical Enzyme Biosensor Bearing Biochar Nanoparticle as Signal Enhancer for Bisphenol A Detection in Water. *Sensors* **2019**, *19*, 1619. [\[CrossRef\]](#)
277. Chen, X.; Ren, T.; Ma, M.; Wang, Z.; Zhan, G.; Li, C. Voltammetric Sensing of Bisphenol A Based on a Single-Walled Carbon Nanotubes/Poly[3-Butyl-1-[3-(N-Pyrrolyl)Propyl] Imidazolium Ionic Liquid] Composite Film Modified Electrode. *Electrochim. Acta* **2013**, *111*, 49–56. [\[CrossRef\]](#)

278. Kunene, K.; Sabela, M.; Kanchi, S.; Bisetty, K. High Performance Electrochemical Biosensor for Bisphenol A using Screen Printed Electrodes Modified with Multiwalled Carbon Nanotubes Functionalized with Silver-Doped Zinc Oxide. *Waste Biomass Valori.* **2020**, *11*, 1085–1096. [[CrossRef](#)]
279. Li, R.; Wang, Y.; Deng, Y.; Liu, G.; Hou, X.; Huang, Y.; Li, C. Enhanced Biosensing of Bisphenol A Using a Nanointerface Based on Tyrosinase/Reduced Graphene Oxides Functionalized with Ionic Liquid. *Electroanalysis* **2016**, *28*, 96–102. [[CrossRef](#)]
280. Tan, F.; Cong, L.; Li, X.; Zhao, Q.; Zhao, H.; Quan, X.; Chen, J. An Electrochemical Sensor Based on Molecularly Imprinted Polypyrrole/Graphene Quantum Dots Composite for Detection of Bisphenol A in Water Samples. *Sens. Actuators B Chem.* **2016**, *233*, 599–606. [[CrossRef](#)]
281. Najafi, M.; Khalilzadeh, M.A.; Karimi-Maleh, H. A New Strategy for Determination of Bisphenol A in the Presence of Sudan I Using a ZnO/CNTs/Ionic Liquid Paste Electrode in Food Samples. *Food Chem.* **2014**, *158*, 125–131. [[CrossRef](#)]
282. Deng, P.; Xu, Z.; Kuang, Y. Electrochemical Determination of Bisphenol A in Plastic Bottled Drinking Water and Canned Beverages Using a Molecularly Imprinted Chitosan–Graphene Composite Film Modified Electrode. *Food Chem.* **2014**, *157*, 490–497. [[CrossRef](#)]
283. Zhou, L.; Wang, J.; Li, D.; Li, Y. An Electrochemical Aptasensor Based on Gold Nanoparticles Dotted Graphene Modified Glassy Carbon Electrode for Label-Free Detection of Bisphenol A in Milk Samples. *Food Chem.* **2014**, *162*, 34–40. [[CrossRef](#)]
284. Supraja, P.; Tripathy, S.; Krishna Vanjari, S.R.; Singh, V.; Singh, S.G. Electrospun Tin (IV) Oxide Nanofiber Based Electrochemical Sensor for Ultra-Sensitive and Selective Detection of Atrazine in Water at Trace Levels. *Biosens. Bioelectron.* **2019**, *141*, 111441. [[CrossRef](#)]
285. Rather, J.A.; De Wael, K. Fullerene-C60 Sensor for Ultra-High Sensitive Detection of Bisphenol-A and Its Treatment by Green Technology. *Sens. Actuators B Chem.* **2013**, *176*, 110–117. [[CrossRef](#)]
286. Chawla, S.; Rawal, R.; Kumar, D.; Pundir, C.S. Amperometric Determination of Total Phenolic Content in Wine by Laccase Immobilized onto Silver Nanoparticles/Zinc Oxide Nanoparticles Modified Gold Electrode. *Anal. Biochem.* **2012**, *430*, 16–23. [[CrossRef](#)]
287. Pino, F.; Mayorga-Martinez, C.C.; Merkoçi, A. High-Performance Sensor Based on Copper Oxide Nanoparticles for Dual Detection of Phenolic Compounds and a Pesticide. *Electrochem. Commun.* **2016**, *71*, 33–37. [[CrossRef](#)]
288. Li, H.-Y.; Wang, X.-L.; Wang, Z.-X.; Jiang, W. Sensitive Determination of Bisphenol A Based on Ag Nanoparticles/Polyguanine Modified Electrode. *Russ. J. Electrochem.* **2017**, *53*, 132–139. [[CrossRef](#)]
289. Chen, W.-Y.; Mei, L.-P.; Feng, J.-J.; Yuan, T.; Wang, A.-J.; Yu, H. Electrochemical Determination of Bisphenol A with a Glassy Carbon Electrode Modified with Gold Nanodendrites. *Microchim. Acta* **2015**, *182*, 703–709. [[CrossRef](#)]
290. Tajik, S.; Beitollahi, H.; Nejad, F.G.; Shoaie, I.S.; Khalilzadeh, M.A.; Asl, M.S.; Van Le, Q.; Zhang, K.; Jang, H.W.; Shokouhimehr, M. Recent Developments in Conducting Polymers: Applications for Electrochemistry. *RSC Adv.* **2020**, *10*, 37834–37856. [[CrossRef](#)]
291. Zhang, J.; Ellis, H.; Yang, L.; Johansson, E.M.J.; Boschloo, G.; Vlachopoulos, N.; Hagfeldt, A.; Bergquist, J.; Shevchenko, D. Matrix-Assisted Laser Desorption/Ionization Mass Spectrometric Analysis of Poly(3,4-Ethylenedioxythiophene) in Solid-State Dye-Sensitized Solar Cells: Comparison of *In Situ* Photoelectrochemical Polymerization in Aqueous Micellar and Organic Media. *Anal. Chem.* **2015**, *87*, 3942–3948. [[CrossRef](#)] [[PubMed](#)]
292. Mazzotta, E.; Malitesta, C.; Margapoti, E. Direct Electrochemical Detection of Bisphenol A at PEDOT-Modified Glassy Carbon Electrodes. *Anal. Bioanal. Chem.* **2013**, *405*, 3587–3592. [[CrossRef](#)]
293. Poorahong, S.; Thammakhet, C.; Thavarungkul, P.; Limbut, W.; Numnuam, A.; Kanatharana, P. Amperometric Sensor for Detection of Bisphenol A Using a Pencil Graphite Electrode Modified with Polyaniline Nanorods and Multiwalled Carbon Nanotubes. *Microchim. Acta* **2012**, *176*, 91–99. [[CrossRef](#)]
294. Suresh, S.; Srivastava, V.C.; Mishra, I.M. Adsorption of Catechol, Resorcinol, Hydroquinone, and Their Derivatives: A Review. *Int. J. Energy Environ. Eng.* **2012**, *3*, 32. [[CrossRef](#)]
295. Bieniek, G. Simultaneous Determination of Phenol, Cresol, Xylenol Isomers and Napthols in Urine by Capillary Gas Chromatography. *J. Chromatogr. B Biomed. Sci. Appl.* **1996**, *682*, 167–172. [[CrossRef](#)]
296. Li, J.; Xu, Z.; Liu, M.; Deng, P.; Tang, S.; Jiang, J.; Feng, H.; Qian, D.; He, L. Ag/N-Doped Reduced Graphene Oxide Incorporated with Molecularly Imprinted Polymer: An Advanced Electrochemical Sensing Platform for Salbutamol Determination. *Biosens. Bioelectron.* **2017**, *90*, 210–216. [[CrossRef](#)]
297. Yang, Y.J.; Weikun, L. Simultaneous Determination of Catechol, Hydroquinone, and Resorcinol on CTAB Functionalized Graphene Oxide/Multiwalled Carbon Nanotube Modified Electrode. *Fuller. Nanotub. Carbon Nanostructures* **2015**, *23*, 410–417. [[CrossRef](#)]
298. Wang, J.; Yang, J.; Xu, P.; Liu, H.; Zhang, L.; Zhang, S.; Tian, L. Gold Nanoparticles Decorated Biochar Modified Electrode for the High-Performance Simultaneous Determination of Hydroquinone and Catechol. *Sens. Actuators B Chem.* **2020**, *306*, 127590. [[CrossRef](#)]
299. Yang, S.; Yang, M.; Liu, Q.; Wang, X.; Fa, H.; Wang, Y.; Hou, C. An Ultrasensitive Electrochemical Sensor Based on Multiwalled Carbon Nanotube@Reduced Graphene Oxide Nanoribbon Composite for Simultaneous Determination of Hydroquinone, Catechol and Resorcinol. *J. Electrochem. Soc.* **2019**, *166*, B547–B553. [[CrossRef](#)]
300. Liu, L.; Ma, Z.; Zhu, X.; Zeng, R.; Tie, S.; Nan, J. Electrochemical Behavior and Simultaneous Determination of Catechol, Resorcinol, and Hydroquinone Using Thermally Reduced Carbon Nano-Fragment Modified Glassy Carbon Electrode. *Anal. Methods* **2016**, *8*, 605–613. [[CrossRef](#)]

301. Chen, T.W.; Yu, X.N.; Li, S.J. Simultaneous Determination of Dihydroxybenzene Isomers Using Glass Carbon Electrode Modified with 3D CNT-Graphene Decorated with Au Nanoparticles. *Int. J. Electrochem. Sci.* **2019**, *14*, 7037–7046. [[CrossRef](#)]
302. Li, J.; Xia, J.; Zhang, F.; Wang, Z.; Liu, Q. An Electrochemical Sensor Based on Copper-Based Metal-Organic Frameworks-Graphene Composites for Determination of Dihydroxybenzene Isomers in Water. *Talanta* **2018**, *181*, 80–86. [[CrossRef](#)]
303. Deng, M.; Lin, S.; Bo, X.; Guo, L. Simultaneous and Sensitive Electrochemical Detection of Dihydroxybenzene Isomers with UiO-66 Metal-Organic Framework/Mesoporous Carbon. *Talanta* **2017**, *174*, 527–538. [[CrossRef](#)]
304. Zhang, H.; Huang, Y.; Hu, S.; Huang, Q.; Wei, C.; Zhang, W.; Yang, W.; Dong, P.; Hao, A. Self-Assembly of Graphitic Carbon Nitride Nanosheets–Carbon Nanotube Composite for Electrochemical Simultaneous Determination of Catechol and Hydroquinone. *Electrochim. Acta* **2015**, *176*, 28–35. [[CrossRef](#)]
305. Fotouhi, L.; Dorraji, P.S.; Keshmiri, Y.S.S.; Hamtak, M. Electrochemical Sensor Based on Nanocomposite of Multi-Walled Carbon Nanotubes/TiO<sub>2</sub> Nanoparticles in Chitosan Matrix for Simultaneous and Separate Determination of Dihydroxybenzene Isomers. *J. Electrochem. Soc.* **2018**, *165*, B202–B211. [[CrossRef](#)]
306. Wang, H.; Zhang, S.; Li, S.; Qu, J. Simultaneous Determination of Hydroquinone and Catechol Using a Glassy Carbon Electrode Modified with Au@Pd Loaded on Reduced Graphene Oxide. *Anal. Methods* **2018**, *10*, 1331–1338. [[CrossRef](#)]
307. Singh, P. Composites Based on Conducting Polymers and Carbon Nanotubes for Supercapacitors. In *Conducting Polymer Hybrids*; Kumar, V., Kalia, S., Swart, H.C., Eds.; Springer Series on Polymer and Composite Materials; Springer International Publishing: Cham, Switzerland, 2017; pp. 305–336, ISBN 978-3-319-46456-5.
308. Jiang, H.; Zhang, D.; He, Z.; Lian, Q.; Xue, Z.; Zhou, X.; Lu, X. A Novel Sensitive Electrochemical Sensor for the Simultaneous Determination of Hydroquinone and Catechol Using Tryptophan-Functionalized Graphene. *Anal. Lett.* **2015**, *48*, 1426–1436. [[CrossRef](#)]
309. Song, D.; Xia, J.; Zhang, F.; Bi, S.; Xiang, W.; Wang, Z.; Xia, L.; Xia, Y.; Li, Y.; Xia, L. Multiwall Carbon Nanotubes-Poly(Diallyldimethylammonium Chloride)-Graphene Hybrid Composite Film for Simultaneous Determination of Catechol and Hydroquinone. *Sens. Actuators B Chem.* **2015**, *206*, 111–118. [[CrossRef](#)]
310. Cuartero, M. Electrochemical Sensors for In-Situ Measurement of Ions in Seawater. *Sens. Actuators B Chem.* **2021**, *334*, 129635. [[CrossRef](#)]